Faculty of Engineering and the Build Environment

Department of Chemical Engineering

Developing a Relationship between Ore Feed Grade and Flotation Performance

Mahlogonolo Nkadimeng

A thesis submitted to the Faculty of Engineering and the Built Environment, University of Cape Town, in fulfilment of the requirements for the degree of Master of Science in Engineering in Chemical Engineering

“Nothing in life is to be feared, it is only to be understood. Now is the time to understand more, so that we may fear less” – Marie Curie.

Plagiarism Declaration

I know the meaning of plagiarism and declare that all the work in the document, save for that which is properly acknowledged, is my own. This thesis has been submitted to the Turnitin module and I confirm that my supervisors have seen my report and any concerns revealed by such have been resolved with my supervisors.

Signed by Candidate.

Mahlogonolo Nkadimeng

18 July 2024.

On this date

Publications and Presentations

M. Nkadimeng, M. S. Manono, K. C. Corin, 2023. Investigating the impact of varying ore feed on entrainment, froth stability and flotation performance under varying water qualities. *Presented at the 11th International Flotation Conference (Flotation '23), held on 6-9 November 2023*. Cape Town, South Africa.

M. Nkadimeng, M. S. Manono, K. C. Corin, 2023. Developing a relationship between ore feed grade and flotation performance. *Presented at the 2nd International Electronic Conference on Processes: Process Engineering—Current State and Future Trends (ECP 2023)*. 17-31 May 2023.

M. Nkadimeng, M. S. Manono, K. C. Corin, 2023. Investigating the impact of varying ore feed grade on entrainment, froth stability and flotation performance under varying water qualities. *Presented at the SAIMM Minerals Research Showcase 2023 Conference*. 13-14 November 2023. Cape Town, South Africa

FUNDING ACKNOWLEDGEMENT

This work is based on the research supported in part by the National Research Foundation of South Africa (Grant Numbers: 123591 and 138294). Any opinions, findings, conclusions or recommendations expressed in any publication generated by NRF supported research is that of the authors and the NRF accepts no liability.

AECI Mining Chemicals for the contribution of reagents.

Axis House for providing access to run samples on their XRF instrument.

The University of Cape Town for providing funding assistance to support this research.

Acknowledgements

I would like to take this moment to extend my sincerest gratitude to the following people, all of whom have provided me with unwavering faith and support, and made this journey enjoyable, fulfilling and worth embarking:

- A/Prof. Kirsten Corin and A/Prof Malibongwe Manono, for their remarkable supervision, guidance, patience, humour and open-door policy which made all this work much more exciting, intriguing and awesome. Your overwhelming care, understanding, technical support and investment into nurturing my growth as a researcher made all difference in the world for me, especially in moments of when I doubted myself. Thank you for opening your door for me and enabling me to explore my capabilities and curiosity as a knowledge seeker. Thank you for all the opportunities and entrusting me to fulfil this work. You are the best supervisors I could have ever asked for; words will never be enough to express my gratitude for all that you have done for me. You provided such a beautiful and healthy working environment for me, and this has immensely enabled me to experience a well-rounded and fulfilling academic experience.

- To my parents, Senyanyathi Patricia and Ikalafeng Lesley, thank you for always believing in me and allowing me to shoot for the stars through a career path of my choosing. You have shown me the greatest love and support through thick and thin, instilled confidence and faith in me from a young age. You raised and nurtured me to be my authentic self in all that I do. I am eternally grateful for your presence in my life and don't take any of your efforts for granted. I hope to make you proud in all that I do on this planet as God is my witness, I will never be able to express my gratitude in words for all that you are to me.

- To my grandmother Mamasegare Josephina Nkadimeng, this work is specially dedicated to you. Thank you for your unwavering love, care and faith in me throughout my existence on this planet. Thank you for all the lessons and wisdom you taught me. Thank you for always showing up for me when I needed you the most and ululating all sorts of praises for me at primary school awards, talent shows etc. Thank you for gifting me the graduation gown. I will treasure it as an invaluable piece of artwork and wear it with pride during my graduation(s). I miss you so much and wish God had given you more time to at least attend one of my graduations and see how good I look in your gown. I feel your absence deeply and will treasure all the memories we shared in your time on this planet. I will remain eternally grateful for having experienced a grandmother's love through you. I hope you are resting in eternal peace and are proud of all that I have and will continue to achieve in this lifetime. Until we meet again, love.

- To all my peers at the CMR: Floyd, Matimba, Avuyile, Thabang, Thabiso, Sancho, Kabeli, Rešoketšwe (Shoki), Noluthando, Morina, Liseka, Sibulele, Ivana and Refilwe. It was truly fascinating to engage with you all in the labs, on campus or our so called *"parliamentary space"* and all over Cape Town. Thank you all for the wonderful chats we had, both trivial and academic. I hope that we will all make an impact to this world.

- To the laboratory staff at the Centre for Minerals Research: Refilwe Moalosi, Kenneth Maseko, Shireen Govender, Monde Bekaphi, Lorraine Nkemba. Gary Groenmeyer, A'isha Gierdien and Jawaad Gamieldien, thank you for ensuring that I conduct my experiments in one of the best

flotation research laboratory in the world, and I never ran out of reagents, water or anything I needed.

- To Heather Sundstrom, thank you for your impeccable administrative prowess and making sure that I was settled not only in the department and CMR, but also with funding and ensuring that my living expenses were running smoothly throughout this journey. You and Kirsten really made life easier for me. Thank you.

- To Nonhlanhla Ndovela, David Chikochi and Bernard Oostendorp at Axis House Group, thank you so much for allowing us to use your facilities and the XRF instrument to aid with the mineral assays of this work during a time when our XRF instrument was in for maintenance. The successful completion of this work as well as my presentation at the *11th International Flotation Conference (Flotation '23),* would have not been possible without your assistance. Your hospitality and kindness is highly appreciated.

- To Refilwe Moalosi, thank you so much for inducting me in the process of doing milling, batch floats and column work. Your selflessness, kindness and willingness into helping others is immensely appreciated. You are one of the main reasons I found ease and joy into doing this work. Your technical knowledge and dedication to your work is truly admirable. I shall cherish all the wonderful chats and great humour we had in lab 4.15, 2B and everywhere else on campus, as well as at all the CMR events. May you continue doing for others what you have done for me.

- To my friend Isaac Sihlangu, I have lost count of the many times you have pulled me up when I was at my lowest. Your unwavering support, advice, kindness and selflessness is greatly appreciated. You have wished me well throughout my academic career and continue to do so to an extent where you even envision me wearing a Red Gown. Thank you for your friendship and taking the time to have a read at my thesis.

- To my friend Jonathan Da Luz, thank you for your kindness, friendship and taking the time to read my thesis.

- To Mr Shongwe, thank you for seeing potential in me and making me believe that I could also go to university and get an education. You have instilled a hard-working mentality in me and I am forever grateful for your contribution and to have had a teacher of your calibre.

- To my little sister, Keamogetswe Nkadimeng, you are not so little anymore but thank you for your continued faith in me and for taking care of our parents while I was in university all these years.

- To my ancestors and guardian angels, thank you for the protection and guidance: my story continues.

- And finally, to God almighty, thank you for ensuring that I am where I am today.

Synopsis

Flotation systems are complex, multifaceted and water-intensive. Prevalent water restrictions globally have made it a necessity for mining operations to recycle onsite process water. This recycling leads to increased ionic strength and may introduce deleterious ions dissolved in solution which affect reagent action, mineral surface properties and pulp chemistry. This may change the water quality over time and may in turn impact plant performance. The depletion of high-grade ore deposits has posed the mining industry with the challenge of processing much more complex, low-grade ores to meet the growing demand of metal production for our technologically driven future. A fundamental understanding of mineral processing is therefore critical for the optimisation of valuable mineral recoveries from such ores. The mineralogy of an ore determines its flotation performance and is thus important to consider. Although evidently critical, ore feed and water quality are in most cases not controlled, therefore rarely investigated. This study seeks to understand the impact of varying ore feed grade(s) on froth stability, gangue recovery and flotation performance using different water qualities. Ionic strength of plant water is defined as water quality in this study.

As a means to better understand the impact of varying ore feed grade and water quality, this study considered two synthetic ores; pyrite-based and galena-based synthetic ores. Pyrite and galena were chosen because they are widely studied in the flotation of sulphide ores. Each synthetic ore was analysed in isolation using the same experimental approach to better understand the behaviour(s) of pyrite and galena-based ores with varying feed grades and in a complex water matrix that mimics onsite process water. The experimental approach consisted of batch flotation and froth column tests. Talc, a froth stabilising mineral, was maintained as a constant throughout. The batch flotation tests were carried out to evaluate the effect of varying ore feed grade, water quality and depressant dosage on the overall flotation performance. Froth column tests showed how froth stability, as measured by the froth height and dynamic froth stability, was affected by the changes in ore feed sulphide grade and ionic strength of plant water. In addition, the 3-phase column findings were used to validate the froth stability results obtained from the batch flotation tests.

To better understand the effects of depleting ore feed grades and water recycling in flotation, three different ore feed sulphide grades, namely 3, 6 and 12% were considered with a polysaccharide depressant, carboxymethyl cellulose (CMC) at dosages of 0, 100 and 500 g/t, in a complex water matrix consisting of two synthetic plant water types, 3SPW and 10SPW. The simultaneous effects of these variables on solids and water recovery, concentrate iron (Fe) and lead (Pb) grades, froth stability, as well as total gangue recovery in the flotation of the sulphide bearing synthetic ores were investigated.

The findings of the pyrite-based synthetic ore showed that the amount of solids and water reporting to the concentrate increased with pyrite feed grade at all depressant dosages and ionic strength of synthetic plant water types. Higher ionic strength of plant water led to higher solids and water recoveries at all depressant dosages and pyrite feed grades, indicating an increase in froth stability owing to a reduction in bubble size and the inhibition of bubble coalescence at high ionic strength of plant water. The 2-phase column findings complemented literature studies and showed that foam height and foam stability increased with the ionic strength of plant water, indicating an enhancement in foam stability by the increased amount of inorganic electrolytes dissolved in the aqueous solution. The 3-phase column findings showed that increasing the ionic strength of synthetic plant water from 3SPW to 10SPW led to an increase in froth height and froth stability at all pyrite feed grades. Furthermore, a simultaneous increase in pyrite feed grade and ionic strength of plant water led to an increase in froth height and froth stability, thereby complementing the froth stability results obtained from batch flotation tests.

The introduction of a depressant led to a decrease in the amount of solids and water reporting to the concentrate at all ionic strengths of synthetic plant water and pyrite feed grades. Fe grades increased with pyrite feed grade at all depressant dosages and ionic strength of synthetic plant water. Fe grades also increased concurrently with depressant dosage at all pyrite feed grades and ionic strength of synthetic plant water, with the highest Fe grade generally attained at 500 g/t CMC depressant dosage. Increasing the ionic strength of synthetic plant water led to an increase in Fe grades with pyrite feed grade at all depressant dosages. Furthermore, this work showed that simultaneously increasing pyrite feed grade and ionic strength of synthetic plant water generally had no apparent effect on the Fe recoveries; however, Fe grades increased at all depressant dosages.

Galena is a highly hydrophobic sulphide mineral and a major source of commercial lead. The findings of the galena-based synthetic ore showed that the amount of solids reporting to the concentrate increased with increasing galena feed grade at all depressant dosages and ionic strength of synthetic plant water type, while the opposite was true with water recovery, i.e. the amount of water reporting to the concentrate decreased with increasing galena feed grade at all depressant dosages and ionic strength of synthetic plant water. This decrease in water recovery with an increase in galena feed grade was thought to have been owing to the highly hydrophobic mineral component in the feed as the galena feed grade was increased. Solids and water recovery increased as the ionic strength of plant water was increased at all galena feed grades and depressant dosages. The froth column findings showed that froth height and froth stability increased as the ionic strength of plant water type was increased at all galena feed grades. These findings complemented the batch flotation results by further showing that froth height and dynamic froth stability decreased with an increase in galena feed grade at each ionic strength of plant water type.

The introduction of a depressant to the galena system led to a decrease in solids and water reporting to the concentrate at all galena feed grades and ionic strength of synthetic plant water types. Pb grades increased with galena feed grade at all depressant dosages and ionic strength of synthetic plant water types. A concurrent increase in Pb grades with depressant dosage was seen at all galena feed grades and ionic strength of plant water. Increasing the ionic strength of synthetic plant water led to an increase in concentrate Pb grades with galena feed grade at all depressant dosages. Simultaneously increasing the galena feed grade and ionic strength of synthetic plant water led to an increase in Pb grades at all depressant dosages, however the Pb recoveries were generally unaffected.

This work has demonstrated the need to evaluate the depletion of ore feed sulphide grades in complex water matrices and has shown a relationship between ore feed grade and flotation performance. The knowledge contribution of this study may be key for the mining industry in the quest to addressing environmental degradation and water scarcity issues. Mineral processing plants in which pyrite is a non-valuable mineral may need to implement early mitigation strategies for managing the recovery of pyrite in future as this work has shown there is a greater chance of recovering this mineral as the ores deplete with time. This work has shown that there would still be a greater chance of recovering lead from ores in which lead is the major commercial component mined even at lower feed grades, as such, this kind of knowledge contribution may be a positive for Pb based mining operations. Furthermore, this work has highlighted the use of synthetic ores as proxies for flotation performance under varying ionic strengths of plant water; plant water of higher ionic strengths showed no detrimental effect on flotation performance. Although this may not necessarily represent real industrial conditions, knowledge contributions from this study are a step in the right direction towards developing an understanding into depletion of ore feed grades and degrading water quality on sulphides flotation performance. Findings of this work should be considered for future work and by mineral processing plants which have incorporated a closed-circuit water system in their operations.

Nomenclature and Abbreviations

BMS	Base metal sulphide
C1	first concentrate (with C2 being the second, C3 being the third, etc.)
CCC	critical coalescence concentration
cm	centimetres
CMC	carboxymethyl cellulose
CMR	Centre for Minerals Research
DO	Dissolved oxygen
DOW200	DOW froth 200
DS	Degree of substitution
DTC	Dithiocarbonate
DTP	Dithiophosphates
EC	Electrical Conductivity
EDTA	ethylene diamine tetraacetic acid
Eh	pulp/redox potential
Fe	Iron
g	grams
g/mol	grams per mole
g/t	grams per ton
HG	high grade
IS	ionic strength
kg	kilograms
L	litres
L/mol.cm	litres per mole per centimetres
L/min	litres per minute
min	minutes
mg/l	milligrams per litres
mm	millimetres
mL	millilitres
NFG	Naturally Floatable Gangue
UG2	Upper Group Chromite No.2
Pb	lead
PGE	platinum group element
PGM	platinum group minerals
ppm	parts per million

rpm	revolutions per minute
SDG	Sustainable development goals
SIBX	sodium isobutyl xanthate
SPW	synthetic plant water
TDS	total dissolved solids
UCT	University of Cape Town
µm	micrometres
wt.	weight
XRD	X-ray powder diffraction
XRF	X-ray fluorescence

Table of Contents

List of Figures

List of Tables

Chapter 1. Introduction

1.1 Background

Mining is a key sector central to economic growth and future technological development. However, it has a poor reputation with respect to past environmental degradation and water usage, owing to irresponsible usage of water. This sector is complex, multifaceted and water-intensive, and cannot operate without safe and continuous access to water, the majority of which is utilised by mineral processing and dust suppression (Gunson et al., 2012, Northey et al., 2016). Stringent water restrictions and regulations have made it a necessity for mines to find alternative sources of water that meet the water demands required for operation, hence, recycling of onsite process water has become a norm for many operations (Bester and Vermeulen, 2010, Mhlongo et al., 2018, Naicker et al., 2003). This recycling changes the water quality over time and may compromise the flotation process; by affecting the rate of mineral recovery, mineral pulp chemistry, froth stability and flotation performance. Furthermore, the efficiency of the chemical reagents involved may also be affected (Bester and Vermeulen, 2010). These changes in water chemistry adds complexity to the flotation process and hence a fundamental understanding of mineral processing is critical.

The depletion of high-feed grade ore deposits to more complex, low-grade ores has posed processing challenges for mineral processing operations, owing to the growing demand to increase metal production for our technologically driven future. The depletion of high feed grade ores further adds to environmental degradation as it has forced mining operations to dig deeper into ore bodies in search of valuable minerals. Ore feed grade is evidently critical in processing, however, it is in most cases not controlled and hence rarely explored in literature. There is a need to understand the impact of depleting ore feed grades not only for meeting metal production demands, but also for ensuring that alternative processing methods are explored and considered, and that environmental degradation issues are mitigated. A fundamental understanding of the impact of these depleting ore feed grades is a necessity for mineral processing.

There are two primary stages in mineral processing, namely, comminution and separation (Craig et al., 1981). Comminution is essential for achieving the desired liberation of valuable minerals from unwanted gangue for effective separation. Flotation is the most common separation process. The process utilizes the differences in surface properties of mineral particles to separate valuable minerals from unwanted gangue (Wills and Finch, 2015). A considerable amount of continuous water input is required for froth flotation, thus making water quality an important factor for achieving high process performance and enrichment of valuable minerals (Cisternas and Gálvez, 2018). Numerous physical and chemical factors are involved in the recovery of valuable minerals during the flotation process. The chemistry of the system can be manipulated to improve performance; however, the system is limited by the mineralogy of the incoming ore as well as the quality of the process water, which in most cases is not controlled.

The mineralogy of an ore is one of the determining factors to its flotation performance. Knowledge of an ore's mineralogy is thus critical for mineral processing. An ore's feed grade can be defined as the concentration of valuable minerals within an ore body. This variable is important as it determines how much valuable and non-valuable minerals can be recovered from an ore body. An understanding of the effects this variable may have on the flotation process is thus critical and necessary to aid the mining industry in addressing the challenge of depleting ores. Different ores bear different minerals and thus behave differently in the presence of chemical reagents; this makes it difficult to isolate and quantify

individual reagent interaction with minerals in the ore (Dzingai et al., 2020, Bradshaw and O'Connor, 1998). Although limited by surface liberation, a synthetic ore allows for the isolation of distinct mineral behaviour and can be used to mimic a real ore. This study aims to investigate the impact of varying ore feed sulphide grades on froth stability, total gangue recovery and flotation performance, under varying water qualities.

1.2 Scope and Limitations

This study recognises that the depletion of high-feed grade ore deposits to more complex, low-grade ores has posed a serious processing challenge for the mining industry and that there is limited or no exploration of such a topic in literature. The study further recognises water scarcity as a global threat and that this threat has brought about stringent water regulations and restrictions, such that mineral processing operations are forced to recycle onsite process water in search of alternative sources of water. As such, the study aims to infer these challenges by investigating the impact of changing ore sulphide feed grades under varying water qualities on flotation performance. These two variables, ore feed grades and water quality may be critical for mineral beneficiation, however, they are in most cases not controlled or controllable and hence rarely investigated.

Although limited by liberation, a synthetic ore mimics a real ore and can thus be used as a proxy to investigate complex topics such as the depletion of ore feed grades. As such, the study made use of two synthetic ores, namely, pyrite-based and galena-based synthetic ores. The synthetic ores consisted of fully liberated minerals and only two gangue mineral components; quartz and talc.

By carefully controlling the feed and water quality, the effects of varying ore feed grade on froth stability, gangue recovery and flotation performance under varying water qualities, were investigated. The flotation performance of the ores was evaluated by analysing solids and water recoveries, valuable mineral recovery and concentrate grade. A non-continuous column was used to measure froth stability using two proxies, maximum froth height and dynamic froth stability. These tests were used to validate the froth stability results from batch flotation tests. Illustrated in Figure 1- 1 is a schematic representation of the overall summary of the study's scope.

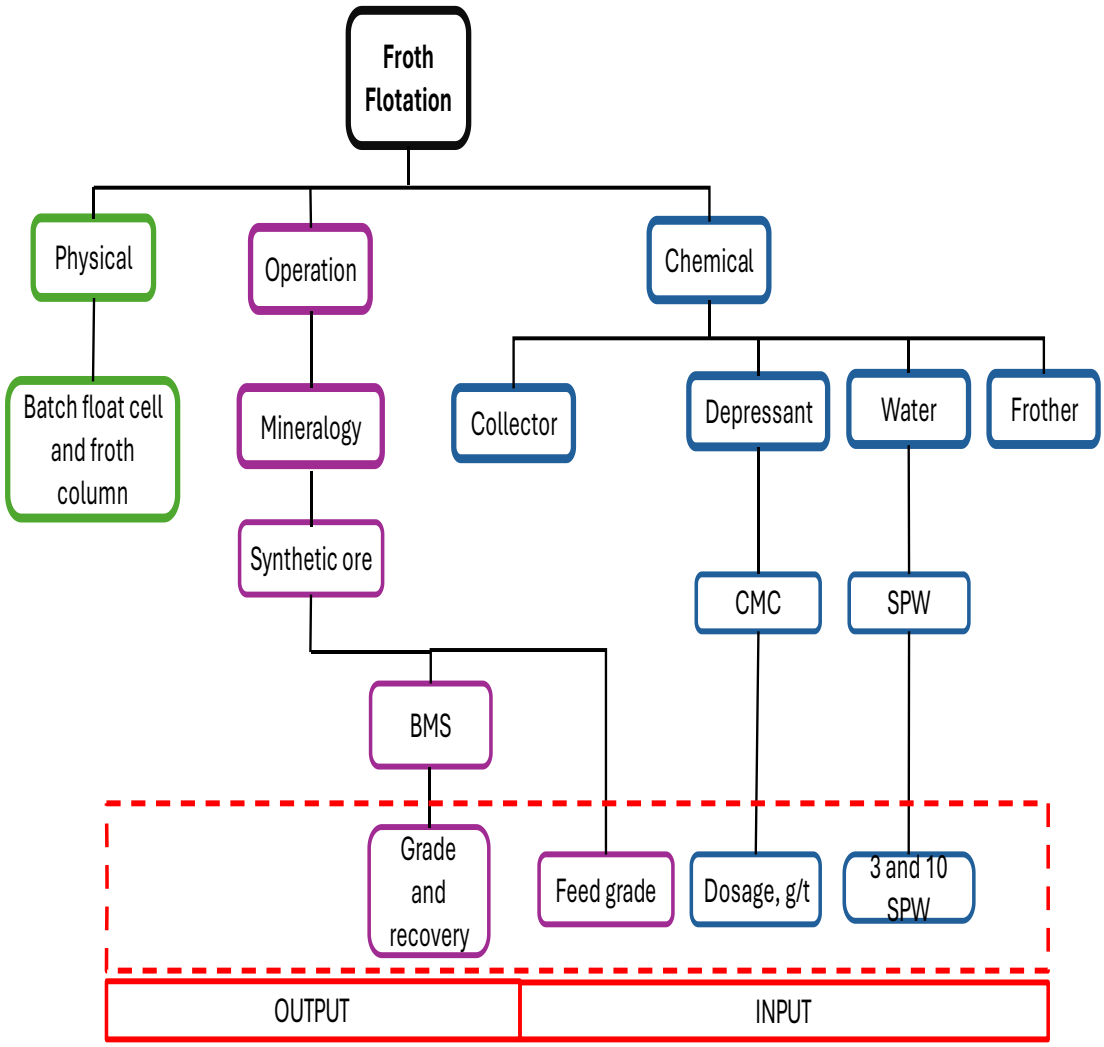

Figure 1- 1: Schematic representation of the overall summary of the study.

Chapter 2. Literature Review

2.1 Froth Flotation

Flotation is a selective physico-chemical separation process which utilises the differences in surface properties of valuable minerals and unwanted gangue minerals (Wills and Finch, 2015). The process is extensively used in mineral processing for separating minerals to concentrate them for economic beneficiation. It was discovered in the 18th century and has become a vital process for the recovery of sulphide minerals from sulphide ores (Tolley et al., 1996). Figure 2- 1 shows a simplified diagram of a typical flotation cell. The froth flotation process consists of two distinct phases, namely, the pulp phase, where mineral recovery occurs, and the froth phase, in which concentrated valuable minerals are separated from the bulk (Goodall, 1993).

Suspended particles in the flotation pulp may report to the concentrate through three distinct mechanisms, namely, true flotation, entrainment and entrapment (Laskowski and Woodburn, 1998, Klimpel and Isherwood, 1991, Trahar, 1984b). True flotation is a selective process responsible for the recovery of valuable hydrophobic minerals, while entrainment is a non-selective process, and together with entrapment this mechanism is responsible for the collection of both valuable and unwanted hydrophilic gangue reporting to the concentrate. Entrapment refers to hydrophilic gangue mineral particles sandwiched within the hydrophobic mineral particles and transported to the mineral concentrate.

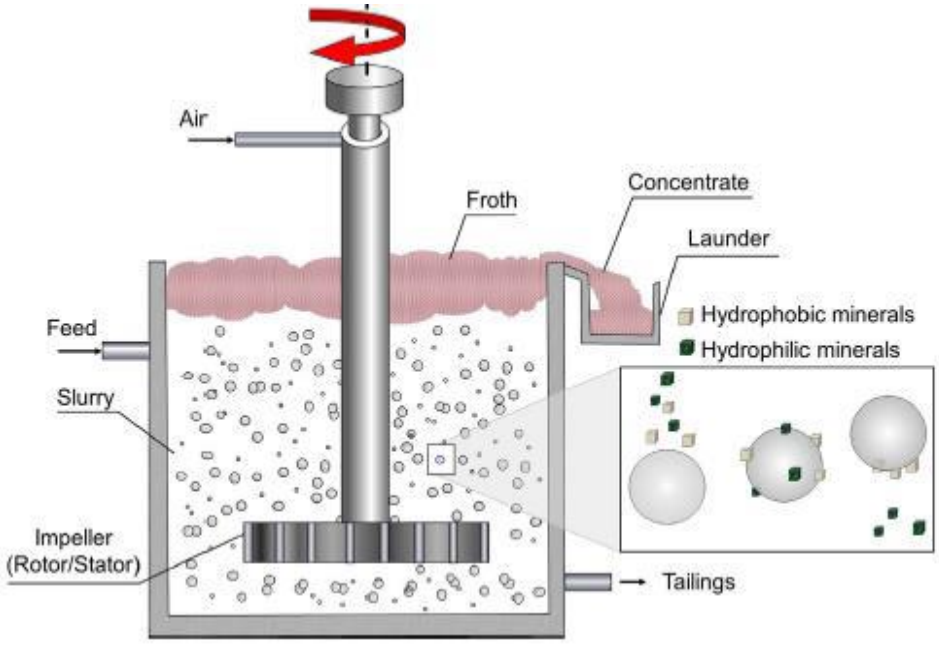

Figure 2- 1: Schematic illustration a typical flotation cell (Wills and Finch, 2015).

2.1.1 Flotation Fundamentals

Froth flotation is a process which takes advantage of particle surface properties to selectively separate hydrophobic from hydrophilic particles. The term hydrophobic refers to particles which repel water, such molecules are non-polar in nature. On the other hand, particles which have an affinity for water are termed hydrophilic, and such molecules are polar in nature. Minerals are classified as polar and non-polar based on their surface properties (Wills and Finch, 2015, Wiese et al., 2008). Polar minerals are bonded by strong covalent or ionic bonding at their surfaces and exhibit high free surface energies.

Surface hydration for these minerals is rapid owing to their strong reaction with water molecules, and hence these minerals are hydrophilic in nature.

Non-polar mineral molecules are bonded by weak Van der Waals forces. Surface hydration for these minerals is difficult and hence such minerals are hydrophobic in nature. Talc, graphite, diamond, coal, and sulphur are examples of naturally floatable minerals (NFG). Ores containing naturally hydrophobic minerals usually require the addition of non-specific collectors to their mineral pulp to aid the floatable fraction to be floatable (Fuerstenau, 1982b). On the other hand, ores containing hydrophilic mineral species require surface modifiers to render them amenable to flotation.

2.1.1.1 Pulp Phase

There are three distinct mechanisms through which mineral recovery in the froth phase can occur, namely, true flotation, entrainment and entrapment (Wills and Finch, 2015). True flotation is a selective process responsible for the collection of valuable hydrophobic minerals into the concentrate grade. Entrainment is a non-selective mechanical mass transfer process responsible for the recovery of both valuable and unwanted gangue minerals reporting to the concentrate (WAng et al., 2015). Entrapment occurs when particle aggregates physically trap other particles in between them, resulting in these particles reporting to the froth phase (Yianatos et al., 1988). Entrainment and entrapment are thus responsible for the collection both valuable and unwanted gangue minerals reporting to the concentrate.

2.1.1.2 Froth Phase

The role of the froth phase is to provide an environment to manage the separation of valuable mineral particles from unwanted gangue and allow for the drainage of entrained material back into the flotation pulp (Harris, 1982). The froth phase therefore contains two types of particles; particles attached to the bubble lamella, and unattached particles which unselectively move freely through the plateau borders due to entrainment. To attain an optimum flotation performance, it is critical for flotation systems to exhibit optimum froth stability (Wiese et al., 2011). Froth stability can be defined as the ability of air bubbles to resist bursting or coalescence. When the froth is unstable, bubbles continuously break before collection, owing to liquid drainage from entrained material back into the flotation pulp (Harris, 1982); and when the froth is too stable, not enough liquid drainage occurs and as a result, high water and gangue recoveries are achieved. In the froth phase, valuable minerals are concentrated and separated from the bulk to undergo further processing (Goodall, 1993).

2.1.2 Flotation Mechanisms

2.1.2.1 True Flotation

During the flotation process, generated air bubbles pass through the pulp phase and emerge into the froth phase with a thin liquid film surrounding them. When there are at least three bubbles clustering, a plateau border containing a liquid film forms, and when there is continuous clustering of bubbles, polyhedra are typically formed (Ventura-Medina and Cilliers, 2002). In the case of a two-phase system (air and water), this is referred to as foam, while in the case of a three-phase system containing solid particles, it is known as froth. True flotation is a selective process whereby hydrophobic particles selectively attach to the air bubbles and are collected in the froth phase as concentrate. True flotation is the dominant mechanism for the recovery of valuable hydrophobic minerals. This mechanism is directly affected by chemical changes such the addition of a collector, depressant or frother to the flotation system.

2.1.2.2 Entrainment

Entrainment is a non-selective process responsible for the recovery of both valuable and unwanted gangue mineral particles reporting to the concentrate. This process is a two-step process which occurs when mineral particles from the flotation pulp enters the froth phase. In the first step of the process, suspended mineral particles are transported upwards to the froth phase, and in the second step, these mineral particles are collected along with water in a concentrate launder (Wang et al., 2016). Only particles smaller than 45 μm are expected to be recovered by this mechanism (Wills and Napier-Munn, 2005, Smith and Warren, 1989). The amount of entrained material is related to the water recovered (Boylu and Laskowski, 2007, Yang and Aldrich, 2006, Ekmekçi et al., 2003), drainage in the froth phase, and the state of the suspended solid particles in the pulp phase.

Entrainment is thus largely dependent on particle size and particle density. Other major factors affecting entrainment include, particle shape, froth structure and froth residence time (Savassi et al., 1998, Smith and Warren, 1989). Entrainment is not directly affected by reagent addition or chemical changes, but rather by the changes in froth stability brought upon by chemical changes (Wiese, 2009). Entrainment is directly proportional to the amount of water recovered from the froth phase (Neethling and Cilliers, 2009, Zheng et al., 2006, Neethling and Cilliers, 2002, Engelbrecht and Woodburn, 1975). The non-selective recovery of gangue minerals in the concentrate is one of the mechanisms responsible for the reduction in concentrate grade (Wiese, 2009). The degree of entrainment or entrainability can be measured using the recovery of the non-floating gangue (NFG) component in correlation to water, in ratio terms (Savassi et al., 1998). Entrainability is a strong determining factor of the flotation separation efficiency between valuable minerals and unwanted gangue minerals (Zheng et al., 2006).

Entrainment is a mechanical phenomenon (Wiese, 2009); it is not directly affected by changes in physical properties, but rather by particle properties. Entrainment of gangue minerals is strongly related to the amount of water recovered, which in turn is related to the froth behaviour (Neethling and Cilliers, 2009, Neethling and Cilliers, 2002). Entrainment of material is directly proportional to the amount of water recovered from the froth phase (Zheng et al., 2006, Neethling and Cilliers, 2002, Engelbrecht and Woodburn, 1975). The dominant mechanism for the recovery valuable minerals to the concentrate is true flotation, however, the rising air bubbles may result in unwanted gangue mineral particles unselectively reporting to the concentrate via entrainment. It is important to minimise the contribution by entrainment and maximise on the recovery by true flotation. Since entrainment is proportional to water recovery, reducing water recovery decreases entrainment and increases the valuable mineral grade in the concentrate. The structure of the froth allows for drainage of water and thereby minimizes entrainment.

2.1.3 Factors Affecting Flotation

Numerous factors affect the flotation process, both directly and indirectly. Froth flotation can be affected by up to 25 clearly identifiable parameters, though over 100 variables can be used to fully describe it (Crozier, 1992, Klimpel, 1984). Klimpel (1984) divided the major variables affecting flotation systems into three interactive groups, namely, the operation components (e.g., temperature, feed rate, mineralogy and particle size), the equipment components (e.g., air flow and agitation/turbulence, cell design and solids suspension), and the chemistry components (e.g., collectors, pH, mineral dissolution, activators, and depressants) as shown in Figure 2- 2 These variables determine the kinetics or dynamic response associated with the flotation process (Xu, 2000). This study falls within the chemistry and operation components, with primary variables of focus being ore feed grade and ionic strength of plant water.

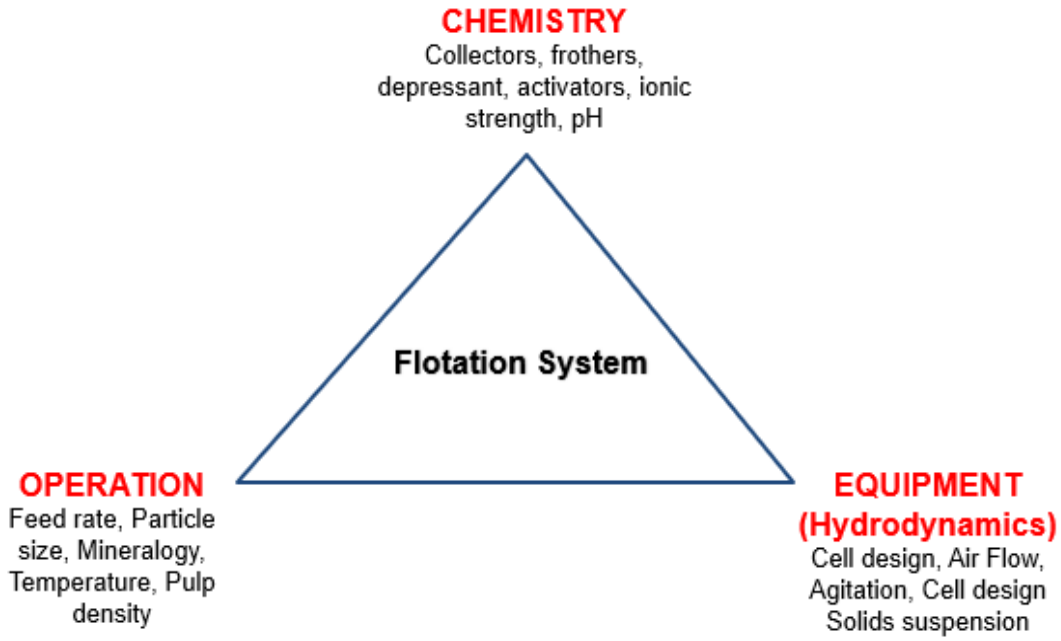

Figure 2- 2: A summary of the variables in the flotation system (Klimpel, 1984).

2.1.4 Flotation Kinetics

The froth flotation process occurs in time and is affected by various factors as outlined in Section 2.1.3. Brożek and Młynarczykowska (2006) noted that the value of the kinetic energy of a particle and the bubble-particle collision are of random character. Collision is required for a particle to attach to a bubble, and the kinetic energy involved in the attachment process needs to be high enough to overcome the particle-bubble interaction barrier and low enough to ensure that this interaction is stable. Kinetic models for the flotation process invoke the analogy of a chemical reactor and consider flotation as a reaction between particles and bubbles. These models have been broadly based on the analogy of homogenous chemical kinetics in which the concentration in a batch reactor follows the first order differential equation (Equation 1);

$$\frac{dy}{dx} = -k.C^n \qquad \text{Equation 1}$$

where C is the concentration of the valuable mineral, k is the flotation rate constant, n is the kinetic order. When $n = 1$, the first order differential equation is transformed into Equation 2 for the recovery of a mineral as a function of time.

$$R = R_{max}\left(1 - e^{-kt}\right) \qquad \text{Equation 2}$$

where R is the recovery of the mineral and a measure of the flotation performance, R_{max} (%) is the maximum possible recovery of the mineral, given infinite time, k is the first order flotation rate constant (min^{-1}), and t is the flotation time (min).

According to Hernáinz and Calero (2001), the flotation rate constant can be evaluated using first order, second order or non-integral order equations. True flotation conditions do not consider particles recovered by entrainment, and only consider overflowing particles which were successfully attached to the bubbles in the froth phase, and thus collected into the concentrate launder.

Equation 2 is the classical first-order kinetic expression for the flotation process and is sometimes referred to as "the unique rate constant" model. This model describes the flotation kinetics of particles which have homogenous surface properties (Brożek and Młynarczykowska, 2006). The model is a special case and does not account for the broad range of conditions in flotation systems (e.g., particle shapes and size distributions, surface property differences, bubble size distributions etc.) (Polat and Chander, 2000). The classical first-order model assumes that at constant bubble concentration, the rate of particle-bubble collision is first-order with respect to the number of particles (Polat and Chander, 2000). Furthermore, this model represents a single stage (in the froth phase) in batch flotation cells and assumes 100% mineral recovery within the froth phase. This model is not the only flotation rate distribution model that has been used to describe first-order batch flotation processes; other models which have been extensively used include the rectangular model (Klimpel, 1980) and Gamma distribution (Yianatos et al., 2010, Woodburn and Loveday, 1965). All these models keep a low number of factors or parameters and have shown acceptable performance in their applications for describing first order batch flotation process.

2.2 Flotation Reagents

Flotation reagents aid with facilitating hydrophobicity between gangue and desired minerals (Bradshaw and O'Connor, 1998). Reagents are added to a milled ore slurry to manipulate the physiochemical nature of the minerals present, and therefore facilitate separation within the ore (Cho and Laskowski, 2002, Melo and Laskowski, 2006). Their addition to an ore enhances the difference in surface properties between minerals. A typical reagent suite consists of collectors, depressants, frothers and sometimes activators (Davis et al., 1975, Wiese, 2009). It is essential to assess and evaluate reagent interactions holistically, both in the pulp phase and froth phase, as in addition to their primary functions, reagents may interact with one another (Bradshaw et al., 2005a).

Collectors impart hydrophobicity on valuable minerals, depressants suppress the floatability of naturally floatable hydrophobic gangue minerals, such as talc, while frothers aid with bubble formation and froth stabilisation. Activators are only added sometimes, and their role is to enhance the action of collectors. Reagents are broadly classified into three types: collectors, frothers and depressants.

2.2.1 Collectors

Collectors are hetero-polar species added to impart hydrophobicity to the mineral surface and create a link between air bubbles and mineral surfaces. These species consist of a polar reactive functional group, and a non-polar hydrocarbon radical, through which bubble-particle attachment occurs, and thus the mineral is rendered hydrophobic. The polar end of the collector is hydrophilic and is the portion through which mineral attachment to the collector occurs. The key role of collectors in froth flotation is to render the mineral hydrophobic. The mechanism of attachment for mineral-collector adsorption may result in the collector being either chemisorbed or physisorbed, depending on the collector type and mineral surface (Bradshaw, 1997). Physisorption is the adsorption through which electrostatic forces and hydrophobic bonding are involved when collectors adsorb onto the surface minerals. Chemisorption involves valence forces and is the adsorption through which the collector forms covalent bonds with the metal ions on mineral surfaces.

Collectors may be classified into different sub-groups based on their functional groups and the mineral to be collected. Thiols are the most commonly used group of collectors in the flotation of Platinum Group Minerals (PGMs) and Base Metal Sulphides (BMSs) (Wang and Forssberg, 1991, Janetski et al., 1977). Typical classes of thiol collectors include xanthates, dithiocarbonates (DTC) and

dithiophosphates (DTP). These collectors adsorb onto sulphide mineral surfaces through chemical adsorption (chemisorption), whereby there is substantial electron sharing between the adsorbent (mineral's surface) and the adsorbate (collector), resulting in the formation of an ionic or covalent bond, and thus permanently changing the mineral's surface chemistry. Fuerstenau (1982a) studied the adsorption of collectors at mineral-water interfaces and showed that at low collector concentrations, collector ions adsorb as individual ions on to the mineral's surface, while at high collector concentrations, collector ions associate into aggregates at the mineral-liquid interface.

2.2.1.1 Xanthates

Xanthates are oxidation products of sodium or potassium hydroxide, alcohol, and carbon disulphide. They are classified as anionic sulfhydryl collectors (King, 1982, Wills and Napier-Munn, 2005). Xanthate collectors are commonly utilised in the flotation of sulphide minerals because they are inexpensive, very soluble and efficient in their mineral collection role (Wiese et al., 2005, Lovell, 1982). Xanthates are non-frothing products, therefore they can be used in excess dosages without the danger of excess frothing (Dhliwayo, 2005). They decompose in alkaline conditions and have a pH stability range of 8 – 13 (Fuerstenau, 1982b). In acidic conditions, xanthate collectors tend to hydrolyse to form a weak acid (Manono, 2012, Poling, 1976).

The adsorption mechanism of xanthate on sulphide mineral surface is considered to be an electrochemical process involving the transfer of charge in chemisorption of xanthate, and oxidation of xanthate to dixanthogen, coupled with oxidation reduction (Guo et al., 2014, Miller et al., 2002, Ralston, 1991, Haung and Miller, 1978). Figure 2- 3 shows structures of some of the most widely used xanthate collectors in the flotation of sulphide minerals (Fuerstenau, 1982b). Xanthate collectors are known to generally not adsorb onto surfaces of non-sulphide minerals. Sulphide minerals can display various behaviours during flotation; the minerals can be oxidised to form hydrophilic sulfoxy species or hydrophobic sulphur rich species on the mineral's surface. The adsorption of xanthates on the surface of minerals is rapid and can occur in a few minutes (Kuopanportti et al., 2000). Studies have shown that collectors with longer alkyl-chain length have stronger induced hydrophobicity (Rao, 2013, Taguta et al., 2017). However, as the alkyl-chain length of xanthates is increased, selectivity is reduced.

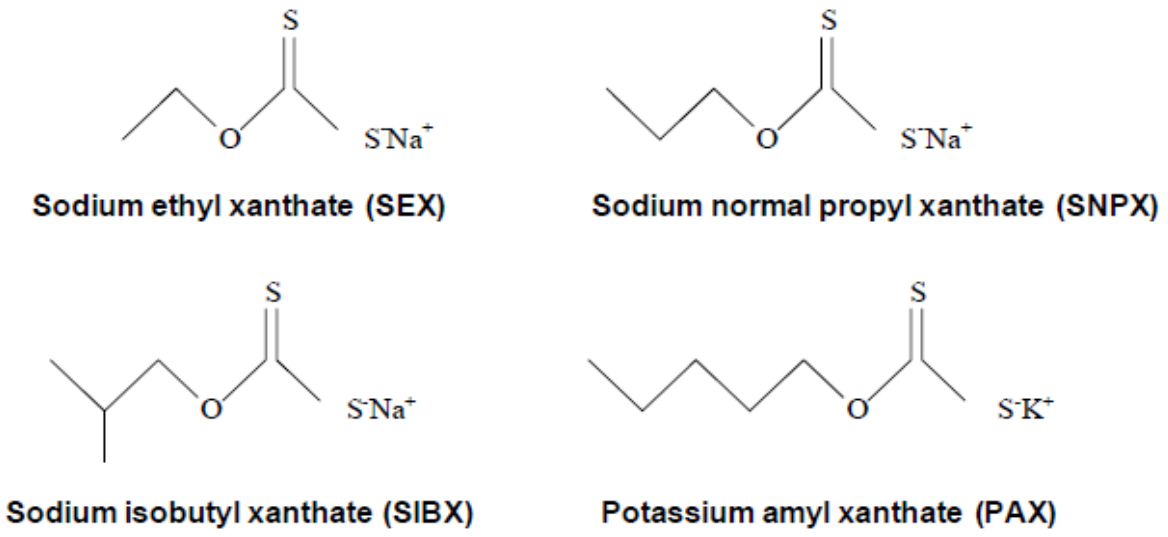

Figure 2- 3: Four common xanthate collectors (Fuerstenau, 1982b).

2.2.3 Frothers

Frothers are surface active reagents added to enhance the stability of the froth. Frothers encourage the generation of small bubbles and prevent bubble coalescence such that a stable froth is formed and selective drainage of unwanted gangue mineral particles from the froth phase occurs (Wills and Finch, 2015). Frothers decrease surface tension by preferentially adsorbing at the water-gas (air) interface (Drzymała, 2007). The surface tension of water is 72 mN/m at room temperature. The main role of a frother in froth flotation is to provide a large air-water interface and ensure that air bubbles remain intact for long enough, such that valuable mineral particles are collected as concentrate and do not fall back into the flotation pulp (Lovell, 1982). Frothers are said to have a kinetic influence on the flotation system (Klimpel and Isherwood, 1991, Klimpel, 1984); they enhance the flotation process by reducing the time required for valuable minerals to attach to the air bubbles.

A frother molecule consists of hydrophilic (polar) and hydrophobic (non-polar) components Figure 2-4 illustrates the general structure of a frother as well as two common frothers used in mineral processing operations (Finch et al., 2008).

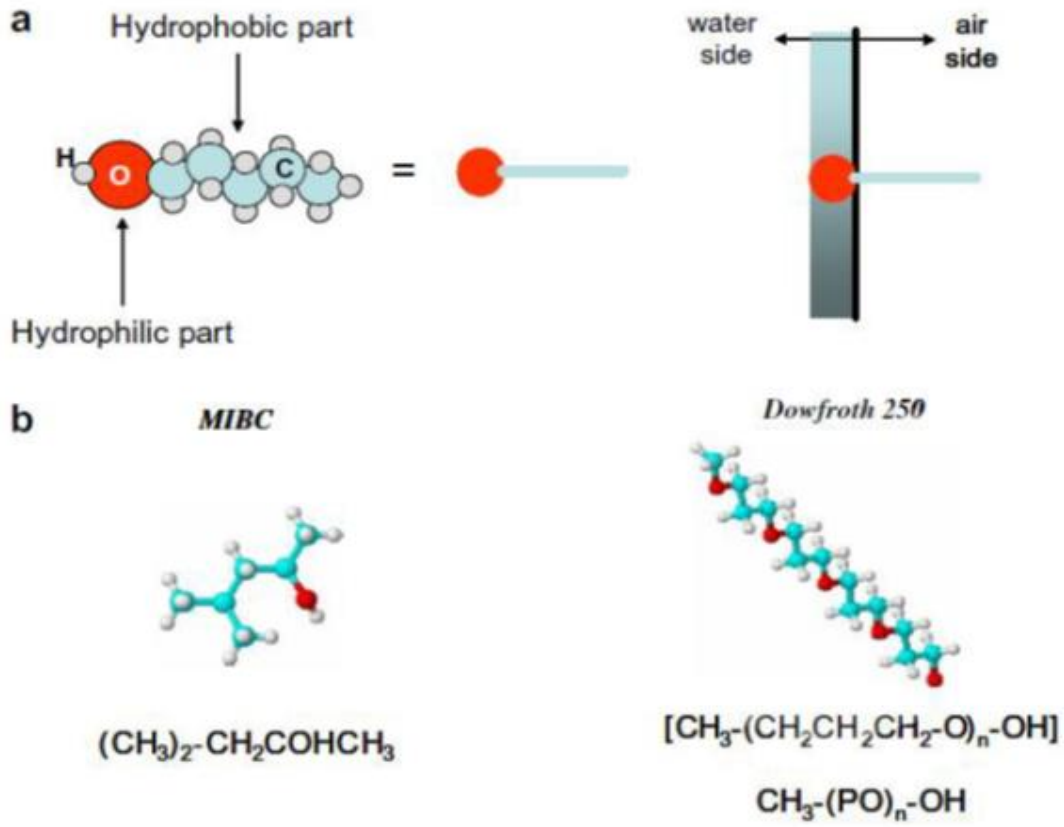

Figure 2- 4: (a) The general structure of a frother (based on alcohol) exhibiting mixed polarity and orientation at the air-water interface. (b) Two common examples of frothers, a polyglycol and an alcohol (Finch et al., 2008).

King (1982) noted that it is necessary for the flotation of sulphide ores to use reagents designed to specifically produce froth. Polyglycol ethers are efficient frothers widely used in the flotation of sulphide ores because of their strong froth stabilising effect, which aids with enhancing bubble-particle attachment in the flotation process (Sweet et al., 1997). Finch et al. (2006) proposed that surfactants control the air stream breakup at the point of injection; when frother molecules at the air-water interface

are closer together, they form a 'bulge', forcing a break away of a bubble which is smaller. Laskowski et al. (2003) proposed that frothers act to reduce the tendency of bubble coalescence, and this tendency of frothers to stabilise the froth by reducing bubble coalescence and size has been broadly studied (Corin and Wiese, 2014, Castro et al., 2013, Kowalczuk, 2013, Laskowski et al., 2003).

2.2.4 Depressants

Depressants are added to the flotation system to prevent the flotation of NFG by adsorbing onto the mineral surface and rendering the mineral hydrophilic (Steenberg and Harris, 1984, Shortridge et al., 1999, Bradshaw et al., 2005a). Bradshaw et al. (2005a) suggested that depressants reduce the flotability of naturally floatable gangue minerals such as talc. Depressants thus increase the selectivity of the flotation system by preventing the flotation of unwanted gangue minerals.

Depressants can be classified into two groups, organic and inorganic. Organic depressants such as polysaccharides, diethylenetriamine, polyacrylamides, modified lignosulfonate, etc, are natural, cheap, biodegradable, environmentally friendly and more resistant to oxidation compared to inorganic depressants (King, 1982). Inorganic depressants such as sodium dichromate, sodium cyanide and sulphur dioxide, are not routinely used and less preferred over organic depressants, and this is mostly due to their environmental intolerance.

Organic depressants can further be classified into three sub-groups, namely, polysaccharides, polyglycol ethers, and polyphenols. Polysaccharides depressants such as carboxymethyl cellulose (CMC) and guar gum (guar), are the most used industrial depressants in South Africa for the recovery of PGMs (Wills and Finch, 2015). CMCs are anionic polymer molecules which have a linear structure and high molecular weight, as shown in Figure 2- 5 (Burdukova, 2007). CMC is produced from the etherification of cellulose; cellulose is a polysaccharide with a linear structure having basic unit β and D-glucose monomers joined by C-1, 4 connections (Laskowski and Liu, 1999). CMC has a highly negative charge density which under high ionic strength conditions can lead to adsorption and create strongly dispersed pulps (Wiese et al., 2007). The molecular weight of CMC is typically in the ranges of 10^5 – 10^6 g/mol (Shortridge et al., 1999).

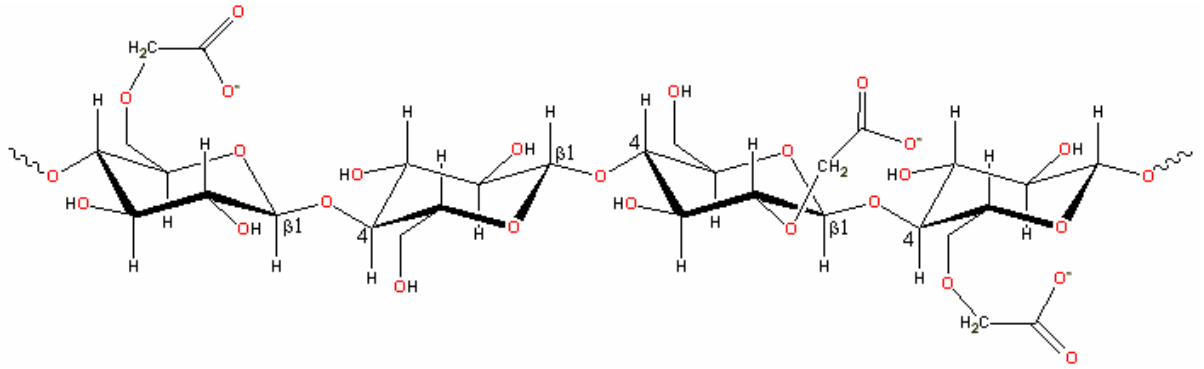

Figure 2- 5: Structure of CMC molecule (http://www.isbu.ac.uk/water/hycmc).

Generally, CMCs are classified based of three properties, namely, the active content, degree of polymerisation (Molecular weight), and degree of substitution (DS). The DS refers to the extent to which carboxyl groups replace hydroxyl groups. This substitution renders the CMC molecule negatively charged in solution. CMCs can have a degree of substitution of up to 3, but the typical range for commercial CMCs is around 0.5 – 1.5 (Laskowski et al., 2007). The DS for CMCs needs to be at least 0.5 for sufficient solubility, or for it to be soluble in polar solvents, such as water (Wiese, 2009,

Khraisheh et al., 2005). The active content indicates CMC percentage by weight in a product. The active content of CMC used in the flotation processes is approximately 70% and typically non-purified (Wiese, 2009). The negatively charged carboxyl groups in the structure of CMC are the key or main difference between CMC and natural polysaccharides, and this negative charge may increase the selectivity of the CMC toward mineral surfaces. Laskowski and Liu (1999) reported that the carboxyl groups of the CMC can interact with different forms of metallic species on minerals surfaces while the hydroxyl groups interact only with metal hydroxyl species (Bicak et al., 2007, Laskowski and Liu, 1999). Bicak et al. (2007) showed that CMC's adsorption on pyrite can be influenced by solution pH; when the pH is higher than 9, the adsorption density of CMC slightly decreases owing to the increased electrostatic repulsion between negatively charged pyrite surfaces and CMC molecules. Furthermore, Bicak et al. (2007) showed that the electrostatic forces between the pyrite surfaces and the negative CMC molecules can be diminished by the addition of Ca^{2+} cations, which in turn enhances CMC's adsorption on the mineral surfaces. High ionic strength solutions are said to cause coiling of the CMC polymer chains and increase the amount of CMC adsorbed on the mineral surface (Bicak et al., 2007, Laskowski et al., 2007).

Viscosity is defined as the resistance of a liquid to flow and is proportional to molecular weight. CMCs have high molecular weight and therefore a high viscosity.

2.3 Key Determinants of Flotation Performance

2.3.1 Froth Stability

Froth stability, among other factors, plays a key role in determining the flotation performance of a flotation system. The role of the froth phase in flotation systems is to provide an environment for valuable mineral particles to be separated from unwanted gangue and allow for the drainage of entrained material back into the flotation pulp (Harris, 1982). To attain an optimum flotation performance, it is critical for flotation systems to exhibit an optimum froth stability (Wiese et al., 2011). The froth is said to be stable when the rate of the smaller bubbles entering the froth phase from the pulp is in equilibrium with the rate of bubbles busting in the froth. Froth stability can thus be defined as the ability of air bubbles to resist bursting or coalescence. Harris (1982) defined two types of froths, namely, unstable and metastable or persistent froths. When the froth is unstable, bubbles continuously breakdown before collection, owing to coalescence and liquid drainage from entrained material back into the flotation pulp (Harris, 1982), and when the froth is metastable or persistent, not enough liquid drainage occurs and this results in high water and gangue recoveries. There are several factors which affect the stability of the froth, and the key factors include, operational effects such as particle size, shape and hydrophobicity, and chemistry effects such as collectors, frothers and depressant addition (Subrahmanyam and Forssberg, 1988, Klimpel, 1984).

During the flotation process, generated air bubbles pass through the pulp phase and emerge into the froth phase with a thin liquid film surrounding them. When at least three bubbles cluster, a plateau border containing a liquid film is formed, and when bubbles continuously cluster, polyhedral bubbles are typically formed (Ventura-Medina and Cilliers, 2002). When a bubble comes into contact with the surface of a mineral's particle, there is minimization of the total surface in pursuit of a stable configuration (Hunter et al., 2008, Binks, 2002). Horozov (2008) noted that the liquid film within plateau borders can be stabilised either by: the formation of a bilayer of hexagonally packed particles, a bridging monolayer of particles, or by a network of particle aggregates in the film. Aveyard et al. (1994) noted the key role that the contact angle plays in film rapture and froth stability; the film is stable when the contact angle is less than the critical degree of wetting, however, when the contact angle is

greater than the critical degree of wetting, particles can easily rupture the film by bridging through it as illustrated in Figure 2- 6 (Aveyard et al., 1994). These findings showed that the bridging-dewetting mechanisms of foam film rupture by solid particles can be used to explain the effects of particle hydrophobicity on froth stability (Aveyard et al., 1994, Denkov and Marinova, 2006, Frye and Berg, 1989, Garrett, 1980).

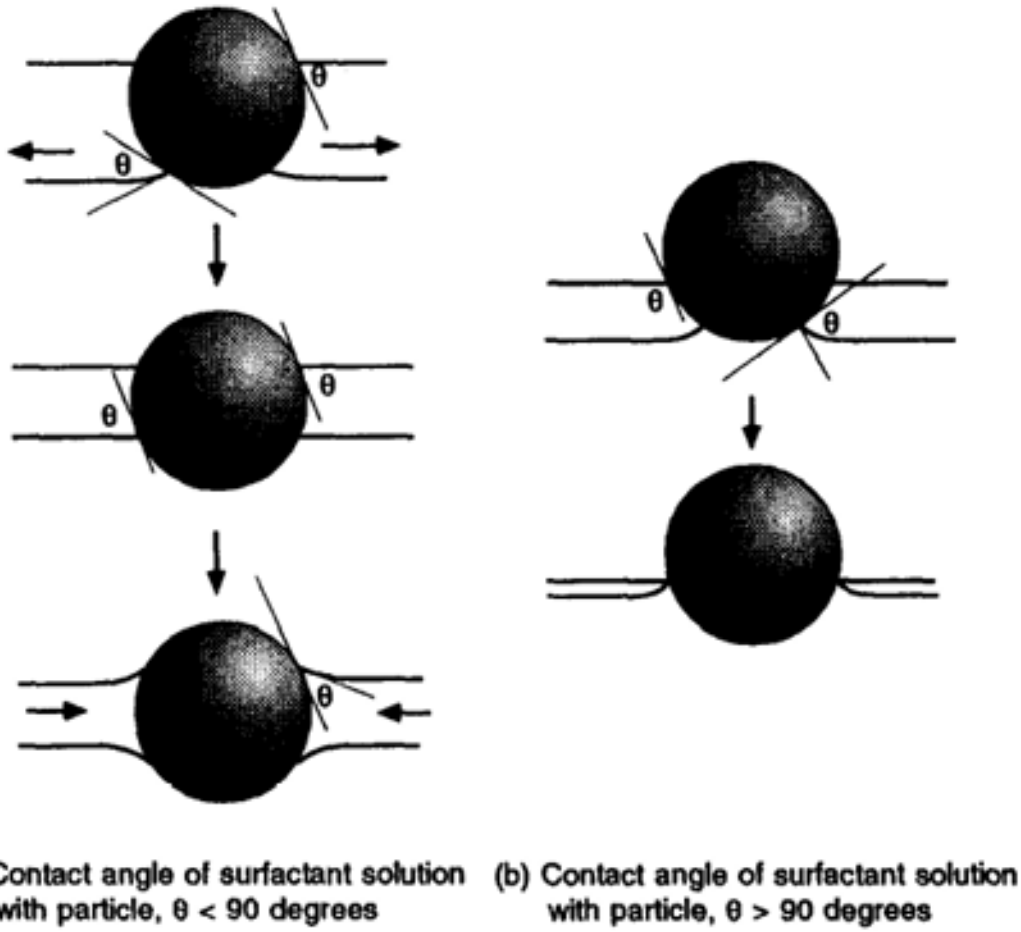

Figure 2- 6: Particles bridging through an aqueous film (a) particles of intermediate hydrophobicity (b) highly hydrophobic particles (Aveyard et al., 1994).

Particle properties such as particle hydrophobicity, shape and size are of great importance for bubble particle attachment and significantly affect froth stability. These particle properties have substantial effects on the overall flotation performance, which can be greater than the beneficial effects obtained from the pulp phase (Aktas et al., 2008). Aktas et al. (2008) reported that particle property effects on froth stability become more significant with increasing distance from the pulp-froth interface, whereby the bubble films are thinner to allow for bridging to occur (Ata et al., 2003). Furthermore, particle properties have more influence on froth stability than operational conditions (froth height, aeration rate and gas dispersion) and chemistry effects. Achaye et al. (2021) investigated the effect of mineral particle size of a synthetic pyrite-quartz ore on froth stability by making use of a bench-scale continuous column cell; their findings showed that froth stability decreased with an increase in feed particle size.

Furthermore, when transforming mineral particle size into surface area, their findings yielded a linear relationship between froth stability and particle specific surface area (Achaye et al., 2021).

2.3.2 Particle Hydrophobicity

The hydrophobicity of mineral particles is one of the key particle parameters which affect flotation performance (Prestidge and Ralston, 1996, Johansson and Pugh, 1992) and contact angle can be used to estimate hydrophobicity. Illustrated in Figure 2- 7 is an idealised particle to air bubble attachment in an aqueous solution. Contact angle is denoted by Θ and is tangential to the wetting boundary and the surface of the solid particle. The wetting boundary is the zone of contact where the three phases (solid, liquid and air) meet. Contact angle is based on surface tension and can be evaluated using Young's equation (Chau, 2009, Celik and Somasundaran, 1980), given by Equation 3.

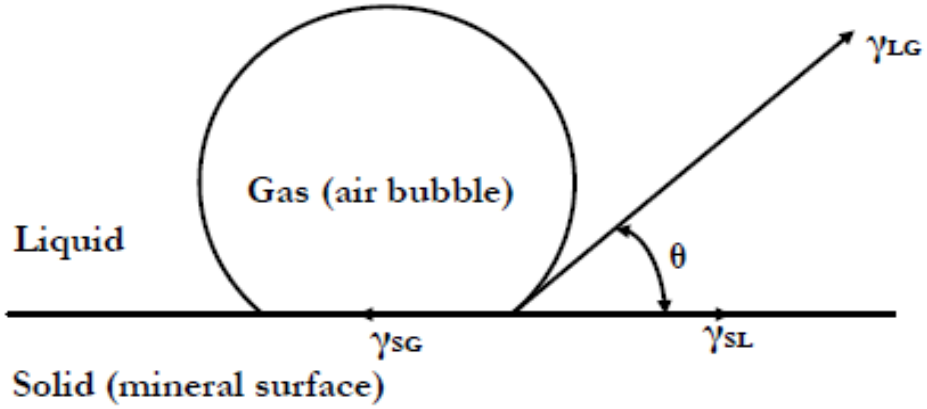

Figure 2- 7: The equilibrium contact between a solid particle and a bubble in an aqueous solution (Fuerstenau, 1982b).

$$\gamma_{SG} = \gamma_{LG}(\cos\theta) + \gamma_{SL} \qquad \text{Equation 3}$$

Where γ_{SG} is the solid-gas(air) interfacial tension, γ_{LA} is the liquid-air interfacial tension, γ_{SL} is the solid-liquid interfacial tension and Θ is the contact angel.

Young's equation is used to thermodynamically express the three phase (solid, liquid and air) contact in terms of interfacial tensions. When the diameters of the particle and the bubble are comparable, an optimal contact between the bubbles and the particles is achieved (Whelan and Brown, 1956). The change in free surface energy can be defined by Duprè's equation (Equation 4) for the work of adhesion, where ΔG is change in Gibbs free energy. Combing Duprè and Young's equation yields Equation 5 (Fuerstenau, 1982b). A chemical reaction is said to be spontaneous if the change in free energy is less than zero; therefore, it is necessary that $\Delta G_S < 0$ for bubble adhesion to occur (Fuerstenau, 1982b).

$$\Delta G = \gamma_{SG} - (\gamma_{LG} + \gamma_{SL}) \qquad \text{Equation 4}$$

$$\Delta G_S = \gamma_{LG}(\cos\theta - 1) \qquad \text{Equation 5}$$

Morris et al. (2008) proposed that the contact angles of particles in flotation froths lie between 0° to 90°, and can be divided into three separate ranges of particle hydrophobicity: 0° – 30° for low, 30° – 70° for intermediate and > 70° for highly hydrophobic particles, respectively. Schwarz and Grano (2005) studied particle hydrophobicity effects on particle and water transport across a flotation froth and concluded that increasing the contact angle to a maximum of about 63°, increased froth recovery. Beyond this maximum contact angle ($\Theta > 63°$), froth recovery started decreasing and this was attributed to increased bubble burst rate in the froth phase, which in turn increased bubble size, thereby destabilising the froth. Ata et al. (2003) carried out a study on bubble coalescence in flotation froths and showed that highly hydrophobic particles ($\Theta = 82°$) had the highest flotation recovery and were more capable of destabilising the froth more than moderately or intermediate hydrophobic particles ($\Theta = 66°$).

Johansson and Pugh (1992) studied the influence of quartz particles on froth stability and reported that weakly hydrophobic quartz particles had no influence on froth stability, while small quartz particles having an intermediate degree of hydrophobicity (Θ of about 50° – 65°) showed maximum froth stability and strongly hydrophobic particles destabilised the froths. It should be noted that the particles they used in their study had well defined size fractions with different degrees of hydrophobicity and one key finding was that froth stability increased with the concentration of small particles (having an intermediate hydrophobicity).

2.3.3 Measuring Froth Stability

Various techniques have been developed for measuring froth stability both in non-continuous and continuous flotation columns. Dynamic froth stability is the widely used technique for measuring froth stability in non-continuous froth columns (Achaye et al., 2021, Barbian et al., 2005, Iglesias et al., 1995, Bikerman, 1973) while continuous flotation columns usually use techniques such as air recovery, image analysis and water recovery (Morar et al., 2012, Hadler and Cilliers, 2009, Barbian et al., 2003, Ventura-Medina and Cilliers, 2002).

Aktas et al. (2008), Pugh (2005) and Barbian et al. (2003) suggested that there are generally two types of methods which can be identified to assess the stability of the froth or foams; these methods can be identified as dynamic methods and static methods. Dynamic methods can be used as a measure of foamability or frothability, and these methods involve making observations of the foam or froth until a state of dynamic equilibrium is reached between the rates of foam formation and decay. Static methods involve observations where the foam or froth forms, and once formed, it is allowed to decay or collapse without re-generation by input of gas or further agitation (Rossen et al., 1996).

Barbian et al. (2003) introduced a new measure for froth stability based on dynamic stability tests for non-overflowing froth columns; their findings showed that both the equilibrium froth height and the dynamic froth stability factor were strongly dependent on the air flow rate and frother concentration. The maximum equilibrium froth height was found to increase with frother concentration and aeration rate, however, when the aeration rates and frother concentrations were high, the maximum equilibrium froth height decreased, such that the froth was unstable. Consequently, the dynamic froth stability factor was also affected by the aeration rate and frother concentration.

Tao et al. (2000) used a series of coal flotation columns to relate froth stability to flotation performance. They quantified froth stability by water recovery in the froth product and found that increasing aeration stabilised the froth, however, a significant increase in ash recovery owing to entrainment was also shown when operating at superficial gas velocities higher than 2 cm/s.

The ratio of the foam volume to gas flowrate was proposed as a method for measuring froth stability by Bikerman (1973), and this is expressed as the dynamic froth stability factor, ∑, as illustrated by Equation 6. Barbian et al. (2003) also reported an improvement in flotation performance at higher froth stability conditions, when the air flow rates were lower.

$$\sum = \frac{Vf}{Qa} = \frac{Hmax \cdot A}{Qa} \qquad \text{Equation 6}$$

Where:

Vf = foam volume at equilibrium (L)

Qa = gas flow rate (L/s)

H_{max} = maximum froth height at equilibrium (cm)

A = cross sectional area of the column (cm^2)

∑ = dynamic froth stability (s)

This work considers Equation 6 to assess the dynamic froth stability. It is worth noting that the dynamic tests considered can be related to the dynamics of real flotation systems (Achaye et al., 2021, Iglesias et al., 1995, Bikerman, 1973).

2.4 Importance of Mineralogy in Sulphide Flotation

The mineralogy of an ore is one of the determining factors to its flotation performance. As previously mentioned, different ores bear different minerals and thus behave differently in the presence of chemical reagents. Ore feed grade is an important factor in mineral processing and mining industry. Ore feed grade can vary depending on the ore body type and the geological settings which formed the ore deposit. The Merensky ore deposits has a varying ore feed grade typically in the ranges 3 to 6 g/t PGM, Zambian copper ore's feed grade range between 0.6 – 4%, Upper Group Chromite No.2 (UG2) is typically in the range of 3 to 4 g/t and this highlights how feed grades can vary depending on the geological location and ore body type.

The depletion of high-grade feed grades to low-grade and complex ores has raised processing challenges for the mining industry, and is a rarely explored topic in literature, as such this study aims to contribute knowledge to this area of research in mineral processing by making use of synthetic ores as proxies for which their findings may be used in real situations by metallurgical operators.

This investigation considers synthetic ores consisting of fully liberated minerals of pyrite, galena, quartz, and talc using different water qualities. A synthetic ore mimics a real ore and allows for the isolation of distinct mineral behaviour; as such, for the purpose of this investigation, the synthetic ore allowed for the isolation of distinct sulphide mineral behaviour and for the impact ore sulphide feed grade has on froth stability, total gangue and flotation performance to be investigated. Synthetic ores have been successfully used by other authors (Achaye et al., 2021, Owusu et al., 2014, Shamaila and O'Connor, 2008, Shackleton et al., 2007a, Shackleton et al., 2007b, Dichmann and Finch, 2001, Zhang et al., 1997).

The floatability of sulphide minerals is influenced by the interactions occurring between the minerals, thus galvanic interactions between sulphide mineral play an important role in froth flotation. The flotation behaviour of a single sulphide mineral is different from that of mixed minerals and this difference may be attributed to galvanic interactions between the sulphide minerals. The contact or interaction between two sulphide minerals results in the formation of a galvanic cell, whereby a cathodic reaction occurs on the mineral surface with a higher rest potential; this mineral accepts electrons from the one with a lower rest potential (Subrahmanyam and Forssberg, 1993). Galvanic interactions between sulphide minerals are important in flotation systems. Galvanic reactions can occur on a homogenous surface through Wagner-Traud mechanism or on a heterogeneous surface via local cells (Allahkarami et al., 2017, Ahmed, 1978). Various kinds of galvanic interactions affecting mineral reactivity have been reported in literature (Pecina-Trevino et al., 2003, Rao and Finch, 1988, Moslemi et al., 2011). Qin et al. (2015) studied the effects of galvanic interactions between galena and pyrite in the presence of a butyl xanthate collector; their findings showed that galena is more active electrochemically than pyrite, and thus serves as the anode when coupled with pyrite. The recovery of galena decreased while that of pyrite increased when the minerals were mixed together, and this was attributed to the influence of galvanic interactions on the adsorption of the collector and dissolution of galena. The rest potential values for galena and pyrite in alkaline solutions have been reported to be 0.14 and 0.22 V, respectively (Cheng and Iwasaki, 1992, Babedi et al., 2023)

Collectorless flotation of sulphide minerals cannot be achieved under reducing conditions; it can only be achieved under moderate oxidation conditions and this can be controlled by pulp potential (Ralston, 1991). Oxidation can occur on the surface of minerals and change the characteristics, surface properties such as hydrophobicity and hydrophilicity of the minerals (Hampton et al., 2011). Sulphide minerals show natural flotability characteristics and can float without the addition of a collector into the flotation system when their surfaces are less oxidised and fresh; this is owing to the weak polar covalent bonds at the mineral surfaces, which makes the surfaces hydrophobic when freshly crushed or ground (Ozun et al., 2019, Ralston, 1994). Under appropriate conditions, the natural hydrophobicity of sulphide minerals can be arranged in descending order as: chalcopyrite > galena > pyrrhotite > sphalerite > pyrite > arsenopyrite (Guy and Trahar, 1984, Trahar, 1984a).

2.4.1 Pyrite

Pyrite is an iron sulphide mineral with chemical formula FeS_2. It is the most abundant sulphide mineral in the earth's crust and is sometimes referred to as 'fool's gold'. It is brass-yellow in colour and contains Fe^{2+} and S^- ions in a stochiometric ratio of 1:2. Pyrite has a Mohs scale hardness of 6 – 5 and tarnishes into dull gray-green colour post milling. It is used as a feed stock in the production of one of the most globally consumed industrial chemicals, sulphuric acid, and in the production of elemental sulphur (Ekmekçi and Demirel, 1997). In most base metal operations, pyrite is considered a non-valuable or an impurity mineral and is thus removed to minimise its contamination to the valuable minerals in the concentrate (Bulut et al., 2014, Chandra and Gerson, 2009, Wang and Forssberg, 1991). Pyrite is problematic and its presence can impact the utilisation and handling of the valuable minerals it is commonly associated with, such as gold, chalcopyrite, sphalerite and coal (Moslemi and Gharabaghi, 2017, Tu et al., 2017, Jiang et al., 1998, Dimitrijevic et al., 1996, Wang, 1995, Wang and Forssberg, 1991). Pyrite can easily report to the concentrate and dilute the grades, thus reducing the economic value of the valuable mineral component (Huang et al., 2013).

Trahar et al. (1994) reported that the reactivity and liberated surface area of pyrite in a complex ore governs the behaviour of pyrite in flotation. Pyrite may float owing to collector induced hydrophobicity, self-induced or natural hydrophobicity. The separation of pyrite in alkaline solutions from other base mineral sulphides such as galena, chalcopyrite or sphalerite can be difficult to achieve due to the

inadvertent activation of pyrite by metallic species such as Pb^{2+} and Cu^{2+}, present in solution as either contaminants from process water or dissolved from complex sulphide minerals resulting from galvanic interactions (Owusu et al., 2014, Barker et al., 2014, Pecina et al., 2006, He et al., 2005, Boulton et al., 2001, Dichmann and Finch, 2001, Ekmekçi and Demirel, 1997, Zhang et al., 1997).

Pyrite is reactive and can easily be oxidised. Raichur et al. (2000) showed that pyrite's oxidation is the fastest at pH 9. The mineral has been reported to have collector-less floatability in mildly acidic conditions. Xanthate collectors in the flotation of pyrite have been greatly studied (Wang and Forssberg, 1991, Fuerstenau et al., 1990, Fuerstenau and Mishra, 1980), including in coal-pyrite flotation, whereby pyrite is rejected by reverse flotation. A number of studies have reported that different ferric species can be formed during pyrite flotation and these ferric species are said to play a crucial role in the flotation of pyrite (Yang et al., 2018, Bulut and Atak, 2002, Jiang et al., 1998, Wang and Forssberg, 1991). Xanthate adsorption on pyrite surfaces is strongly related to the oxidation occurring on the pyrite's surface, and this is largely dependent on the conditions of the solution. Studies on the xanthate adsorption on pyrite surfaces have shown that the adsorption of xanthate in alkaline pH regions is due to physisorption of xanthate and dixanthogen ions, while in acidic pH conditions, chemisorption is more likely (Yang et al., 2018, Bulut and Atak, 2002, Jiang et al., 1998, Wang and Forssberg, 1991).

2.4.2 Galena

Galena is the most abundant lead-containing mineral and commonly found in association with other sulphide minerals such as pyrite, chalcopyrite and sphalerite (Zárate-Gutiérrez et al., 2012). Galena is metallic lead-grey in colour and contains lead cations (Pb^{+}) and sulphur anions (S^{-}) in a stochiometric ratio of 1:1. Galena belongs to the octahedral sulphide mineral group and has a cubic crystal structure (Noda et al., 1987). Furthermore, galena has a high specific gravity that makes galena mineral samples feel much 'heavier' than similar sized samples of other metallic and non-metallic minerals. Wills and Napier-Munn (2006) reported that galena feed grades range between 1 – 5% lead. As a major source of commercial lead, it is primarily used to produce lead metal for, ammunition, batteries, pipes, weights, and radiation shielding. Galena has a low electrode rest potential and this can be attributed to the fact that galena crystals possess reductive properties i.e. they are formed under a reductive atmosphere (Chen et al., 2014). The mineral has semiconductor properties, and this causes the occurrence of electrochemical reactions during galena flotation (Oertel et al., 1999).

The flotation of galena is well established in industry and in ore deposits where the mineral is associated with sphalerite, galena is usually floated first owing to it being more naturally hydrophobic. The reason for galena's natural hydrophobicity has been attributed to the formation of Pb deficient sulphur rich surface species (Rao and Leja, 2004); generally, the oxidation of galena results in the production of sulphate and the release of lead ions and oxides, elemental sulphur, intermediates and lead hydroxy-carbonate precipitate into the aqueous solution (Chernyshova, 2003, Nowak and Laajalehto, 2000, Nowak et al., 2000, Kartio et al., 1997, Manocha and Park, 1977, Kartio et al., 1996, Fornasiero et al., 1994, Hsieh and Huang, 1989). Li et al. (2019) reported that CMC has no significant effect on depressing galena, however, the depression of galena with CMC can be enhanced by the addition of $KMnO_4$ to the flotation system. To improve the flotation of strongly oxidised galena mineral surface, moderate concentrations of ethylene diamine tetraacetic acid (EDTA) and pH conditions are typically used (Wang and Forssberg, 1990); the EDTA aids with the removal of hydrophilic metal hydroxide products on the surface of galena, which in turn exposes the sulphur-rich surface to water molecules (Wang and Forssberg, 1990).

Hayes and Ralston (1988) reported that the collectorless flotation of galena occurs under moderate oxidation conditions and is inhibited under strong oxidation conditions, owing to the formation of

hydrophilic oxidation products on the mineral surface. Gu et al. (2002) reported collectorless flotation of galena at a pulp potential of less than 0.17 V and a pH greater than 12.5. Under these conditions, the elemental sulphur exceeded the oxidised lead species on the surface of galena and this in turn made the mineral hydrophobic.

Aktas et al. (2008) reported that the adsorption capabilities of xanthate on the surfaces of galena increased with condition time, with approximately 10 to 15% increase in flotation recoveries after 5 minutes of conditioning. Xanthates with straight chain lengths enhanced flotation recovery of galena when the conditioning time was shorter (up to 5 minutes), however when the conditioning time increased to 10 min, the flotation recoveries were negatively affected by the hydrophobic aggregation of the mineral particles, which led to detachment from air bubbles (Aktas et al., 2008, Kuopanportti et al., 2000). The opposite is true in the case of xanthates with branched chain lengths, i.e. lower galena recoveries were reported at shorter conditioning time (up to 5 min) owing to steric hindrance from the branched structure, however, longer conditioning time (10 min) enhanced the adsorption capabilities of the branched xanthate molecules on the surface of galena, and thus increased flotation recoveries (Aktas et al., 2008). October et al. (2021) reported a decrease in xanthate adsorption on the surfaces of galena when the ionic strength of plant water was increased. This decrease in xanthate adsorption was however overridden by zeta potential effects; zeta potential of the mineral particles increased with the ionic strength of plant water.

A study by Fuerstenau (1982b) showed that galena can be fully recovered between pH 2 and 11, while the inhibition of galena's flotation occurs at pH's less than 2 and greater than 11 (Fuerstenau and Han, 2003, Fuerstenau, 1982b).

2.4.3 Talc

Talc is an NFG mineral commonly associated with base metal sulphide ores and acts as a froth stabilising mineral in flotation systems (Parolis et al., 2008). It is a magnesium rich phyllosilicate mineral which forms through the alteration of magnesium silicates. Its structure is layered and comprises of two different surfaces; namely, a hydrophobic basal cleavage face, and hydrophilic edges (Farrokhpay et al., 2018). The cleavage face surface area is proportionally larger and is what gives talc its natural hydrophobic character. It is the only naturally floatable silicate mineral in the Merensky ore and present in other base metal ores.

Owing to its natural floatability, talc may report to the concentrate and thus lower the concentrate grade. Talc is known to have a disproportionate effect on flotation performance; it enhances froth stability and increases the entrainment of other unwanted gangue mineral particles reporting to the concentrate (Martinovic, 2005). The froth stabilising effect of talc is negated by the addition of depressants. CMC and modified guar gums have been widely used to depress the flotation of talc and thus improve the concentrate grade of ores containing talc as a gangue component (Wiese et al., 2011, Manono et al., 2018, Witney and Yan, 1997, Gong, 1999, Jenkins and Ralston, 1998). These long-chain polysaccharide depressants adsorb on to the surface of the talc and render the mineral hydrophilic.

In this study, a minor portion of talc is used within the synthetic ore to aid with the stabilisation of the froth phase.

2.4.4 Quartz

Quartz is one of the most common non-floatable gangue mineral in the earth's crust and has the chemical formula SiO_2. This mineral can undergo various modifications or transformations under different conditions of pressure, temperature, and chemical environment. In nature it exists as alpha and beta quartz, which have trigonal and hexagonal crystal structures, respectively. Although a gangue

mineral, it has various economic uses; owing to its Moh hardness scale of 7; it can be used as abrasives, filter media, and in construction materials, as well as electronics.

Quartz is commonly associated with ores which contain valuable minerals such as lead, copper, zinc, gold and iron. Hence, for the purpose of this investigation, it is used as the major hydrophilic component.

2.5 Water Quality Effect on Flotation

Environmental degradation is mainly caused by waste disposal processes, such as; process water seepage into the water table, and tailings disposals (Haggard et al., 2015). The mining industry is water-intensive with mineral processing and dust suspension accounting for most of the water used. Global restrictions and regulations on water have become more stringent, making it a necessity for mines to find alternative sources of water that meet the water demands required for operation; hence, many operations are recycling and reusing onsite process water (Mhlongo et al., 2018, Bester and Vermeulen, 2010, Naicker et al., 2003). This way of using water in a closed circuit, is key for green mining, whose focus is on recycling and reuse, minimising discharge and maintaining production targets while simultaneously addressing process water issues (Dzingai et al., 2020, Muzinda and Schreithofer, 2018). Recycling reduces the need to depend on water suppliers and thus the need for continuous access to large amounts of fresh/potable water. Furthermore, recycling reduces water discharge from flotation plants and lowers reagent consumption through the retention of some reagents as the water is recycled (Slatter et al., 2009).

Ionic strength of a solution is calculated using Equation 7 and is defined as a measure of the concentration of ions or inorganic electrolytes dissolved in that solution. It has been shown that the floatability of sulphide minerals may increase or decrease in the presence of ions, depending on the water chemistry and mineral type (Slatter et al., 2009). Recycling and reusing onsite process water increases the dissolved ions present in the water, this is ore dependent. This recycled water is usually obtained from tailings disposals after the flotation process, and thus may contain various contaminating species from the accumulation of base metals, flotation reagents, organic material and ions such as SO_4^{2-}, Mg^{2+}, Ca^{2+}, K^{+}, Na^{+}, Cl^{-} etc.

$$I = \frac{1}{2} \sum_i^n (Z_i^2 C_i) \qquad \text{Equation 7}$$

Where:

I = ionic strength

Z = charge of ion *i*

i = the ion for which the ionic strength is evaluated

C = molarity of ion *i*

n = number of ions present in solution/system

The more these ions accumulate, the more the ionic strength (IS) of the water increases, and this may in turn lead to an abnormal concentration of inorganic electrolytes in solution (Slatter et al., 2009). Water in the flotation process represents 80 – 85% of the mineral pulp and facilitates the sub-processes within froth flotation (Muzenda, 2010). Mineral beneficiation has a high dependency on the chemistry of process water, and this dependency on flotation performance is rarely known beforehand. A change

in the amount of ions present in the water may compromise the flotation process by affecting froth stability, rate of recovery, mineral pulp chemistry and flotation performance. Deleterious inorganic ions and contaminants may be introduced by recycled water and accumulate in the flotation system; and this may affect the pulp chemistry, reagent-mineral interactions, mineral surfaces, grade and recoveries, and possibly compromise the flotation process. This adds complexity to the flotation process and its chemical reagents. The complexity added to "its chemical reagents" can be better understood from the perspective of a pure vs contaminated system; in a pure system chemical reagents may perform their function better than in a contaminated one, sorely due to the fact that in a contaminated system, in this case recycled system, there are other factors at play which are directly or indirectly contributing toward performance in the flotation system. Barker (1983) showed that increasing the concentration of divalent cations, such as calcium and magnesium led to an increase in froth stability and the recovery of pyrite, while gangue recovery greatly decreased. Similarly, the author showed that pyrite recovery and froth stability increased when the concentration of sodium (monovalent cation) was increased, and gangue recovery decreased slightly. High ionic strength concentrations have been shown to have a stabilising effect on froth stability (Dzingai et al., 2020, Corin and Wiese, 2014, Manono et al., 2012, Corin et al., 2011) and this has been attributed to a decrease in bubble size and bubble coalescence in solution (Manono et al., 2012). Klassen and Mokrousov (1963) attributed this to the fact that inorganic electrolytes reduce the surface hydration of naturally hydrophobic minerals and provide attractive forces between the mineral particles and air bubbles.

A closed water circuit may be key to green mining, and a good alternative source of water for the mining industry, however, this recycling changes the water chemistry and may have a compromising effect on the flotation process as highlighted above, and this may further compromise the efficiency of the reagents involved (Slatter et al., 2009). Hence, a fundamental understanding of how these changes in water chemistry may impact the flotation system is paramount for mineral processing (Corin et al., 2011, Mooruth and Booley, 2009, Slatter et al., 2009).

2.6. Gaps in Knowledge

The depletion of high-feed grade ore deposits to low-grade and more complex ore deposits has posed the mining industry with a processing challenge owing to the growing demand to increase metal production for our technologically driven future. Although evidently critical, ore feed grade is in most cases not controlled and hence rarely explored in literature. An understanding of the impact of depleting ore feed grades is vital not only meeting metal production demands, but also for exploring alternative processing methods and mitigating environmental degradation issues as mines dig deeper. Stringent water restrictions and regulations have forced mining operations to recycle onsite process water. This recycling changes the water quality overtime and may compromise the flotation process. Previous studies have considered the effects that operational properties (such as particle hydrophobicity, shape, and size) and chemistry properties (such as collectors, frothers and pH) have on froth flotation, but not much has been reported on the effects of depleting ore feed grades under degrading water quality. This study considers synthetic sulphide ores to investigate the impact of varying ore feed grade on froth stability, total gangue recovery and flotation performance under varying water qualities.

Chapter 3. Hypotheses, Key Questions and Objectives

3.1 Hypotheses

(i) Froth stability is determined by the hydrophobic components within an ore. A higher feed grade yields a more stable froth when the feed grade is higher owing to a higher proportion of hydrophobic minerals.

(ii) The Ionic Strength of plant water is a strong determinant of froth stability due to its effects on the behaviour of hydrophobic and hydrophilic components. A low feed grade at a high ionic strength water causes an increase in water and gangue minerals recovery, which in turn yields a more stable froth.

3.2 Key Questions

(i) What effect does varying the ore feed grade have on froth stability and flotation performance?

(ii) How does a simultaneous change in ore feed grade and ionic strength of plant water affect froth stability and flotation performance?

(iii) How does a combination of varying ore feed grade and ionic strength of plant water affect gangue recovery?

(iv) What effect does varying the ore feed grade have on pulp chemistry as measured by Eh, pH, DO, EC and TDS?

3.3 Objectives

Considering the previous work conducted within the CMR on water quality in flotation, the objectives of this investigation read as follows;

(i) Develop a better understanding into the impact of ore feed grade on flotation performance, froth stability and entrainment under changing water quality.

(ii) Monitor changes in pulp chemistry; Eh, pH, DO, EC, TDS, with changes in ore feed grade and water quality.

(iii) Determine whether a froth column can be used as a simple technique for indicating the potential flotation performance of an ore, for known feed grade and process water quality.

3.4 Research Approach

To investigate process variables, a standard experimental approach commonly used is one variable at a time. However, this method of investigation does not consider other variable(s) responses which may be contributing to the overall response (Nanthakumar and Kelebek, 2007, Dean et al., 2015). A factorial experimental design was consisted for this investigation for determining the possible number of experiments required to address the study's objectives. Factorial experimental designs are used to investigate experimental designs consisting of more than one independent variables; each having discrete levels and whose experimental units take on all possible combinations across all factors or variables. A three level, three factor factorial design, denoted 3^3, was considered for this investigation. The three factors varied in this investigation were ore feed grade, ionic strength and depressant dosage for three levels; Low (L), intermediate(M) and High(H). This equates to 27 experiments; however, for this investigation, one level, M, for one factor, ionic strength, was dropped, thus 9 experiments had to be removed, which equated to a total of 18 single run experiments, as outlined in Table 1.

The full factorial design for the batch flotation experiments in this project consisted of a total of seventy-two experimental runs (inclusive of repeats); 36 batch flotation tests for the pyrite and galena-based synthetic ore, respectively. Design Expert software gave a confidence level of 95% for this factorial design. Furthermore, a total of 12 column runs were conducted for the pyrite and galena-based synthetic ore, respectively. This study thus consisted of a total of ninety-six experiments.

Table 3.1: Batch flotation factorial experimental design for pyrite and galena-based ore(s), respectively.

Factor	Low Level	Intermediate Level	High Level
Ore Feed Grade (%)	3	6	12
Ionic Strength (SPW)	3	-	10
Depressant Dosage (g/t)	0	100	500

3.5 Sustainable Development Goals

Figure 3- 1 shows the 17 global Sustainable Development Goals (SDGs) developed by the United Nations as a blueprint to aid the world in achieving a better and more sustainable future for all. SDGs 6 and 12 are addressed in this study. Goal 6 is addressed through the use of recycled water in the flotation circuit; this reduces the amount of contaminated water discharged to the environment, thereby reducing effluents from the processing circuits that may harm or pollute freshwater resources. Furthermore, the amount of freshwater used for processing is reduced. Responsible consumption and production are achieved in this way, thus also addressing sustainability goal 12. Goals 13, 14 and 15 are indirectly addressed; life is preserved for the living species on the land and below water, and climate change effects are also lowered by reducing the use of fresh water for processing and effluents discharged to the environment.

Figure 3- 1: United Nations Sustainable Development Goals ("Communications materials - United Nations Sustainable Development," n.d.).

Chapter 4. Experimental Materials and Methods

This chapter details the materials, equipment and methods used to meet the objectives of this research. All experiments were conducted using predefined synthetic ore types and water qualities. This study consisted of two main experimental tests; batch flotation and froth stability column tests.

4.1 Ore

Two synthetic ore types were considered in this investigation;

- Pyrite-based where pyrite was considered as the valuable mineral.
- Galena-based where galena was considered as the valuable mineral.

Each synthetic ore was investigated in isolation using the same experimental approach to better understand the behaviour(s) of pyrite and galena-based ores with varying feed grades and in varying ionic strengths of process water.

Table 4- 1 show the pure mineral samples which were used in this study. Included in the table are their respective purity and the suppliers they were obtained from. To determine each minerals purity and confirm the absence of other sulfide minerals, Powder X-ray diffraction (XRD) spectra analysis was carried using a Bruker D8 Advance powder diffractometer with LynxEye detector and fixed divergence, receiving slits with Co-kα radiation. Table 4- 2 shows the mineral samples and their respective purity.

Table 4- 1: Mineral samples and their respective purity.

Mineral	Chemical formula	Supplier	Purity (%)
Pyrite	FeS_2	Minerals World, Cape Town, South Africa	95,1
Galena	PbS	Minerals World, Cape Town, South Africa	78,0
Talc	$Mg_3Si_4O_{10}(OH)_2$	Central South University, China	88,03
Quartz	SiO_2	Cape Silica Suppliers, Cape Town, South Africa.	95,89

Table 4- 2: XRD analysis for the pure minerals used.

	Proportion of crystalline phases (mass %)			
Mineral phase	**Pyrite**	**Galena**	**Talc**	**Quartz**
Pyrite	95,1	-	-	-
Galena	-	78,0	-	-
Talc	0,7	-	88,0	-
Quartz	0,4	-	-	95,9
Anglesite	-	11,8	-	-
Cerrusite	-	10,2	-	-
Sulphur	1,0	-	-	-
Jarosite	0,8	-	-	-
Gypsum	0,6	-	-	-
Calcite*	0,2	-	-	-

Dolomite	-	-	9,7	-
Mica	0,8	-	2,3	1,8
Chlorite	0,4	-	-	-
Corundum	-	-	-	2,3
Total	**100,0**	**100,0**	**100,0**	**100,0**

Note: Anglesite and Cerussite had no major effect on the flotation of galena (Rashchi et al., 2005, Herrera-Urbina et al., 1999, Fuerstenau et al., 1987).

The pure mineral samples were hammered into chunks, if needed. The talc was placed into a pulverising ring mil bowl and pulverised for 30 s, using a pulveriser supplied by The Ferguson Industrial Equipment Group, Johannesburg, South Africa. The pulverised talc samples were then dry screened using a 2.36 mm screen. The size fractions above 2.36 mm were pulverised for a further 5 s and dry screened similarly using the 2.36 mm screen. Pure mineral samples of pyrite and galena were crushed separately, using Terminator Joial Jaw crusher, supplied by Mineral Innovative Technologies. The mineral samples were separately dry screened using the 2.36 mm screen, riffled and split using a rotary splitter and placed into two airtight plastic bags. The riffler and rotary splitter were supplied by Dickie & Stockler, Johannesburg, South Africa. The quartz was supplied as size fractions 2 – 4 mm; this was considered suitable for feed to mill samples and thus the quartz sample was only riffled and split using a rotary splitter and placed into airtight plastic bags.

Three different ore feed sulfide grades were considered, namely, 3, 6 and 12% sulfide. To generate the synthetic ore, a total mass of 1 kg was considered. A constant 2% concentration of talc was maintained in all ore samples, while the quartz mass balanced the synthetic ore composition(s).

4.2 Water

All batch flotation and column tests were conducted using UCT synthetic plant water (SPW); a water recipe whereby distilled water is modified using inorganic salts of analytical grade to ensure that the water contains similar amounts of ions typically found in plant water (Wiese et al., 2005). The synthetic plant water was prepared in bulk fresh every second day after running out, or when there was too little SPW remaining to conduct a float. The water was stored in a 40 L container. To simulate water recirculation and thereby allow for the effects of ionic strength to be investigated, baseline plant water (1 SPW) was increased by 3 and 10 times respectively (Manono et al., 2018), as shown in Table 4- 3.

Table 4- 3: ion concentrations of synthetic plant water.(Manono et al., 2018, Wiese et al., 2005)

Water Type	Ca^{+} (mg/L)	Mg^{2+} (mg/L)	Na^{+} (mg/L)	Cl^{-} (mg/L)	SO_4^{2-} (mg/L)	NO_3^{-} (mg/L)	NO_2^{-} (mg/L)	CO_3^{2-} (mg/L)	TDS (mg/L)	Ionic Strength [M]
1 SPW	80	70	153	287	240	176	-	17	1023	0.0242
3 SPW	240	210	459	861	720	528	-	51	3069	0.0727
10 SPW	800	700	1530	2870	2400	1760	-	850	10230	0.2426

4.3 Flotation Reagents

4.3.1 Collector

Sodium Isobutyl Xanthate (SIBX) collector, supplied by AECI Mining Chemicals, was used in this investigation and its properties are shown in Table 4- 4. A 1% (w/v) solution of SIBX was prepared

fresh each day by hydration in distilled water. The collector dosage was kept constant at 150 g/t for all batch flotation and 3-phase column tests. The dosage was not corrected for active content (i.e calculated on an 'as is' basis). The remaining collector solution was discarded as per the requirements of the Material Safety Data Sheet (MSDS).

Table 4- 4: SIBX properties.

Collector	M_r, g/mol	Density, g/mL	% Purity	Dosage, g/t
SIBX	200	1	90	150

4.3.2 Depressant

Sodium carboxymethyl cellulose (Na-CMC), supplied by Merck, South Africa, was used as the gangue depressant. A 1% (w/v) solution of the Na-CMC depressant was prepared fresh every 2nd day for all batch flotation tests; by hydration in distilled water for two hours using a magnetic stirrer to ensure complete dissolution. In an attempt to differentiate the entrained from floating gangue, this investigation considered the UCT high depressant method. The method assumes that at a high depressant dosage (>300 g/t), all floatable gangue is depressed and any gangue reporting to the concentrate is owing to entrainment (Corin et al., 2011, Wiese and Harris, 2012, Wiese, 2009). This therefore allows for the amount of NFG reporting to the concentrate to be determined at lower depressant dosages. Table 4- 5 shows the properties of the Na-CMC depressant.

Table 4- 5: CMC properties.

Depressant	M_r, g/mol	Relative Density, g/mL	% Purity	Degree of Substitution	Dosage, g/t
Na-CMC	250 000	1.59	98.7	0.7	0, 100 and 500

4.3.3 Frother

A polyglycol ether, Dowfroth 200 (Dow 200), supplied by Betachem, was used in all the batch flotation and column tests in this investigation. The frother was used in its pure form and a frother dosage of 40 g/t was maintained in all experimental tests. Table 4- 6 shows the properties of the Dow200.

Table 4- 6: Dow200 properties.

Depressant	M_r, g/mol	Density, g/mL	% Purity	Dosage, g/t
Dow200	200	0.965	100	40

4.4 Calibration Probe

A multiparameter meter (multiprobe) supplied by HANNA instruments, South Africa, shown in Figure 4- 1 was used to monitor the pulp chemistry, namely, redox potential (Eh), pH, dissolved oxygen (DO), electrical conductivity (EC) and total dissolved solids (TDS) (calculated from EC). The multiprobe was inserted into the batch flotation cell during the collection of concentrate one (C1) and at the end of each flotation test (Tails). C1 measurements were taken once the pulp was conditioned and the aeration maintained at a constant flow rate of 7 L/min, and once the C4 collection was complete and aeration

turned off, the multiprobe was re-inserted into the flotation cell and tails measurements were recorded. The impeller was turned on throughout all the pulp chemistry measurements. The oxidation of the mineral surfaces within the pulp phase is due to DO and affects the rate of adsorption of the xanthate, due to oxygen being a necessity for the electrochemical reactions on the mineral surface of sulfide minerals (Corin et al., 2013, Wills and Finch, 2015). Sulphide mineral hydrophobicity can be reduced by oxidation on the surface of the minerals which can inhibit the separation the sulfide mineral from unwanted gangue in during flotation (Hayes and Ralston, 1988). Electrical conductivity in aqueous solutions measures the ability of the solution to conduct current. Inorganic electrolytes can carry current, and thus the higher the amount of inorganic electrolytes in solution, the higher the EC. The measured EC in this study was used as a proxy for ionic strength.

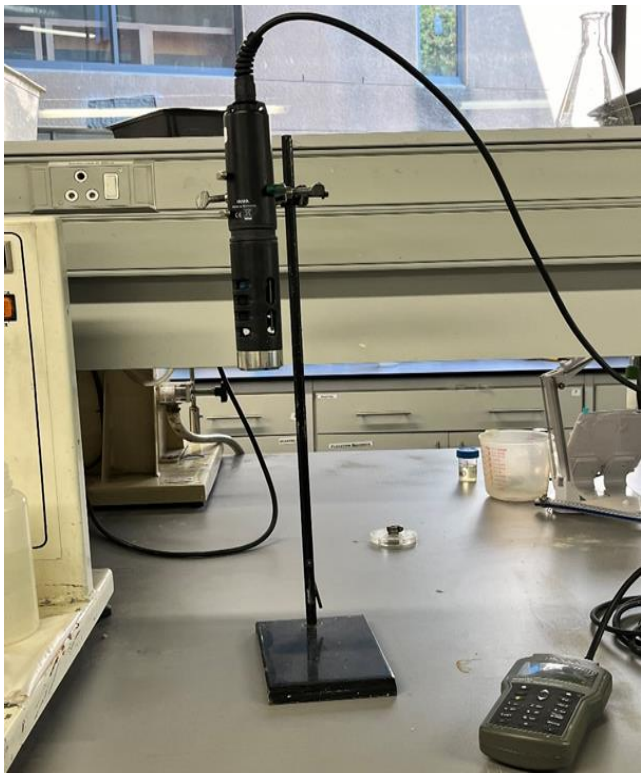

Figure 4- 1 Multiparameter meter instrument.

4.5 Milling

A 200 mm diameter Eriez stainless steel rod mill, charged with 20 stainless steel rods of varying diameter ratios, 8 x 20 mm, 6 x 25 mm and 6 x 16 mm, was used to mill the ore in this investigation. 1 kg synthetic ore sample was milled at 66% solids in synthetic plant water of known ionic strength to achieve a grind of 60% passing 75 µm. This grind size represents the primary rougher grind that is used by industrial mining operations processing Merensky ore. Figure 4- 2 shows the milling curve generated for this study; the milling time for the target grind was determined by interpolation to be 25 min and 48 s. Collector was added during the milling process.

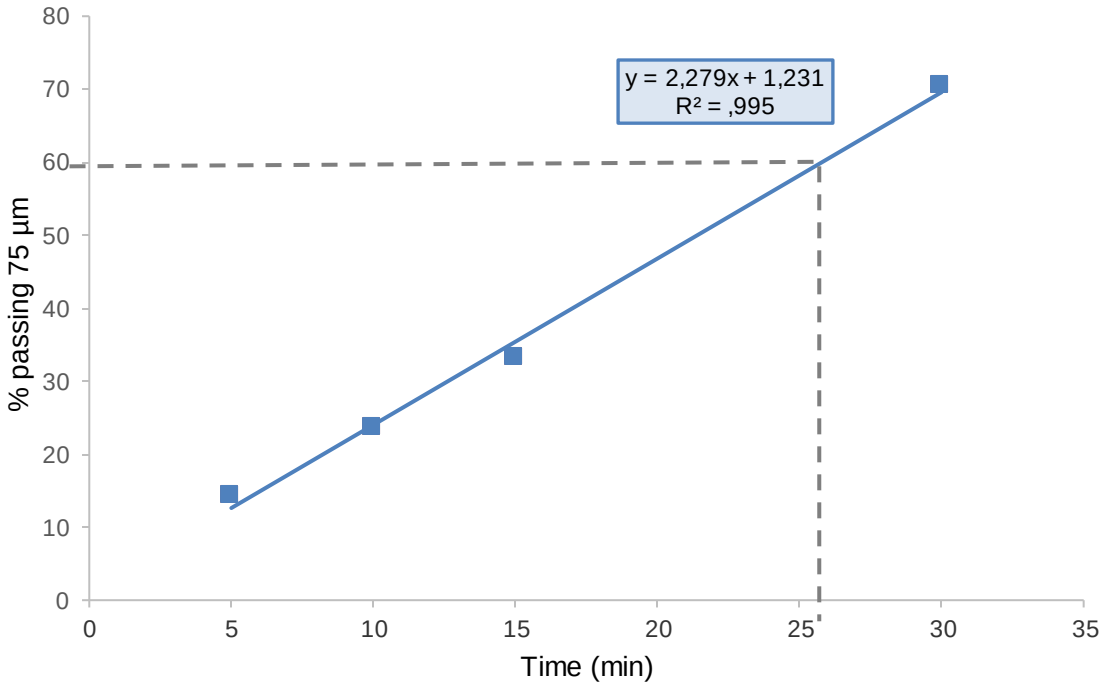

Figure 4- 2: Milling curve for 1 kg batch float.

4.6 Batch Flotation Equipment

Batch flotation tests were conducted to evaluate water and solid recoveries, valuable mineral recoveries and grades as well as those of gangue minerals. This was done by making use of the UCT 3 L Barker laboratory flotation cell shown in Figure 4- 3. Table 4- 7 shows the standard conditions, reagent types and dosages, including the variables considered when operating the flotation cell in this study. The flotation pulp level was controlled manually, and three variables were varied, namely, ore feed grade, water quality and depressant dosage, respectively. Aeration rate, impeller speed, collector type and dosage as well as frother type and dosage remained constant throughout all tests.

Table 4- 7: Standard and variable flotation cell conditions.

Constants	**Variables**
Cell conditions	
Aeration rate: 7 L/min Impeller speed: 1200 rpm	Ore feed sulphide grade: 3%, 6% and 12% Synthetic Plant water type: 3 and 10SPW
Reagent type and dosage	
Collector: 150 g/t of SIBX Frother: 40 g/t of Dow200	Depressant: 0, 100 and 500 g/t of Na-CMC

Figure 4- 3: The UCT 3L Barker laboratory flotation cell.

4.6.1 Batch Flotation Procedure

A representative 1 kg ore sample, milled in the presence of the SIBX collector, was used. The milled ore slurry was transferred to the flotation cell and the required synthetic plant water was added to make up a volume of 3 L to achieve a solids percentage of 35%. An impeller speed of 1200 rpm was used. A feed sample was taken before each flotation test. CMC depressant was dosed into the slurry and allowed to condition for two minutes. The multiparameter meter (multiprobe) was inserted into the flotation cell to monitor pulp chemistry. Dow200 frother was added and allowed to condition for 1 minute. The aeration was turned on and kept at a constant flow rate of 7 L/min. A froth height of 2 cm was kept constant throughout the flotation experiments by manually adding top-up water at regular intervals. Four concentrates were collected as follows; C1 for 2, C2 for 4, C3 for 6, and C4 for 8 minutes, respectively, allowing a total of 20 minutes for flotation. The froth was manually collected by scraping the froth from the top of the flotation cell at a fixed depth every 15 seconds. The multiprobe was removed from the flotation cell after the collection of C1 and reinserted into the flotation cell after the collection of C4 when the air was turned off. The samples were filtered, dried, and weighed before X-ray fluorescence (XRF) analysis was carried out for elemental analysis. A Olympus Vanta™ C Series handheld XRF analyzer was used for all Iron (Fe) and Lead (Pb) analysis. Water recovery was monitored and measured throughout. Table 4- 8 shows a summary of the batch flotation procedure followed in this study. All batch flotation tests were performed in duplicates to minimise uncertainty, standard error between duplicate tests was found to be within 5 and 10% for solids and water recoveries, respectively. The standard error is represented by error bars on the graphs in Chapter 5, the Results Chapter.

Furthermore, the study intents to show entrainment, a non-selective process responsible for the recovery of both valuable and unwanted gangue mineral particles reporting to the concentrate. The method used to determine an entrainment factor was the UCT high depressant method; the method assumes that all

floatable gangue has been depressed at high depressant dosages (>300 g/t), and any gangue reporting to the concentrate is owing to entrainment (Corin et al., 2011, Wiese and Harris, 2012, Wiese, 2009). An entrainment factor or degree of entrainment refers to the proportionality between the total gangue and water recovered, i.e the gradient line, and is used for calculating the floating gangue.

Table 4- 8: Summary of the batch flotation procedure followed in this investigation.

Action	Conditioning Time (minutes)
Milling	25.80
Collector dosed to the mill	Added to the mill before grinding
Feed sample drawn	Post slurry transfer to cell
Depressant dosed to the flotation cell	0
Frother dosed to the flotation cell	2
Multiprobe inserted into the flotation cell	2.5
Air turned on and froth allowed to develop	3
C1	5
Multiprobe removed from the flotation cell	5.5
C2	9
C3	15
C4	23
Air turned off and Multiprobe reinserted into the flotation cell	23
2 Tails samples drawn	23

4.7 Froth Stability Column

Figure 4- 4 shows a laboratory scale froth stability column set up. The column is a non-overflowing stability column which is constructed from Perspex. It has a height of 1 m and an internal diameter of 9.4 cm. A pore-4 sintered glass frit with a 60 mm disc diameter and height of 4.2 mm, was placed at the bottom of the column. The same frit was used for conducting all column test work. Furthermore, all the 3-phase column test work made use of a stainless-steel impeller which was inserted inside the column to keep the solids in suspension and aid with bubble-particle collision and attachment.

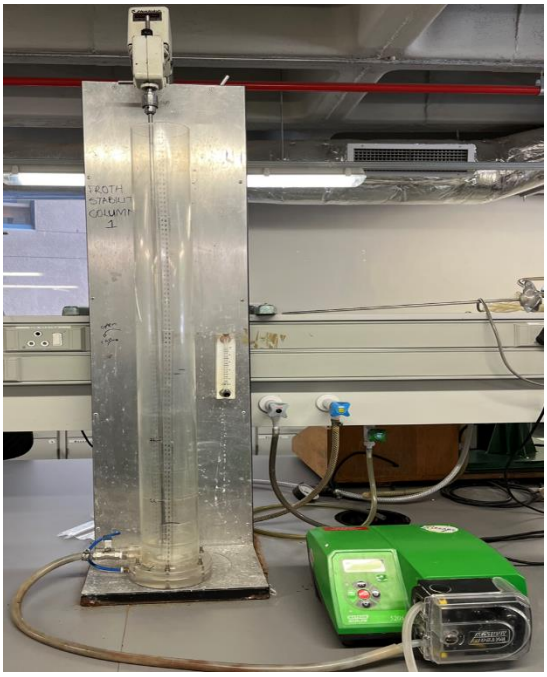

Figure 4- 4: Froth stability column set up.

4.7.1 Froth Column Procedure

To conduct the 2-phase column tests; a 3 L feed bucket was used to condition the SPW containing the required reagent before running each column test. A frother dosage of 40 g/t was added to each plant water type and once conditioned, the solution was pumped through an inlet near the bottom of the column. The level attained by the solution was noted as the initial height. Air was introduced into the column and maintained at a flow rate of 7 L/min. The height attained by the foam was tracked as a function of time and once equilibrium foam height (H_{max}) was achieved, the air was turned off. The solution was then pumped out of the column and discarded.

Similarly, for conducting all the 3-phase column tests, a feed bucket was used to condition the slurry post milling, before running each column test. Milling was conducted in the same manner as that given for flotation test work in Section 4.5. The feed bucket was topped up to the 3 L mark using the required SPW type. Furthermore, 40 g/t of Dow200 frother was added and once well-mixed, the slurry was pumped into the column through an inlet near the bottom of the column with the impeller turned on to keep the solid particles in suspension. The initial height attained by the slurry was noted and air was introduced into the column, maintained at a flow rate of 7 L/min for all runs. The froth height attained was tracked as a function of time until an equilibrium froth height (H_{max}) was achieved. Once the H_{max} was achieved, the air was turned off and the slurry was pumped out of the column for no further analysis. Dynamic froth stability was calculated using Equation 6 as discussed in Section 2.3.2.

4.8 Reproducibility

To minimise and determine the standard error associated with the experimental results, each batch flotation test was carried out in duplicate for each of the conditions tested. The variables used to determine the reproducibility of the tests are solids and water recoveries, concentrate assays and metal recoveries. The values presented in this thesis are therefore calculated averages and thus the error bars represent the standard error between the duplicate tests. To calculate the sample standard error, the sample standard deviation was divided by the square root of the sample size. The standard error required

by the UCT standard batch flotation procedure for solids and water recovered is 5 and 10%, respectively. The standard error calculated for all the batch flotation tests presented in this thesis was found to be within acceptable limits.

Chapter 5. Results

The result section in this thesis is sub-divided into 3;

- pyrite-based synthetic ore results.
- galena-based synthetic ore results.
- and batch flotation kinetics results for both synthetic ores considered, obtained by making use of the classical first order kinetics model.

5.1 Pyrite

This section evaluates the effects of varying pyrite feed grade, ionic strength of plant water and depressant dosage on the flotation performance of the pyrite-based synthetic ore, by comparison of; solids and water recovered, iron (Fe) grades and recoveries, foam and froth stability, and total gangue recovered. The colours blue, orange and grey represent the three pyrite feed grades, 3, 6 and 12%, respectively. 3 and 10 Synthetic Plant Water types (SPW) are represented by solid and dashed coloured lines, respectively, while the markers represent the three CMC depressant dosages; 0, 100 and 500 g/t, represented by the triangle, diamond, and square-shaped markers, respectively.

5.1.1 Cumulative Solids vs. Time

Figure 5- 1 illustrates cumulative solids vs. time for 3, 6 and 12% pyrite feed, under 3 and 10SPW, for the three CMC depressant dosages, 0, 100 and 500 g/t. Solids recovered per unit time increased with pyrite feed grade, as illustrated predominantly by the grey curves at the top of the graph, with the solids increasing in the order 3% (blue) < 6% (orange) < 12% (grey), with most solids generally being recovered within the first 2 minutes. Solids recovered per unit time decreased with an increase in depressant dosage for all pyrite feed grades. This effect is more clearly illustrated by the 12% pyrite feed grade (grey), whereby an increase in depressant dosage from 0, 100 to 500 g/t is illustrated by the triangle (0 g/t) > diamond (100 g/t) > square (500 g/t). As the ionic strength of plant water was increased, from 3SPW (solid curves) to 10SPW (dashed curves), solids recovered per unit time increased for all pyrite feed grades. This is clearly illustrated by the dashed lines falling above their solid counterparts in most cases. The highest solids recovered by the 12% was ~162 g, 6% was ~100 g and 3% was ~75 g.

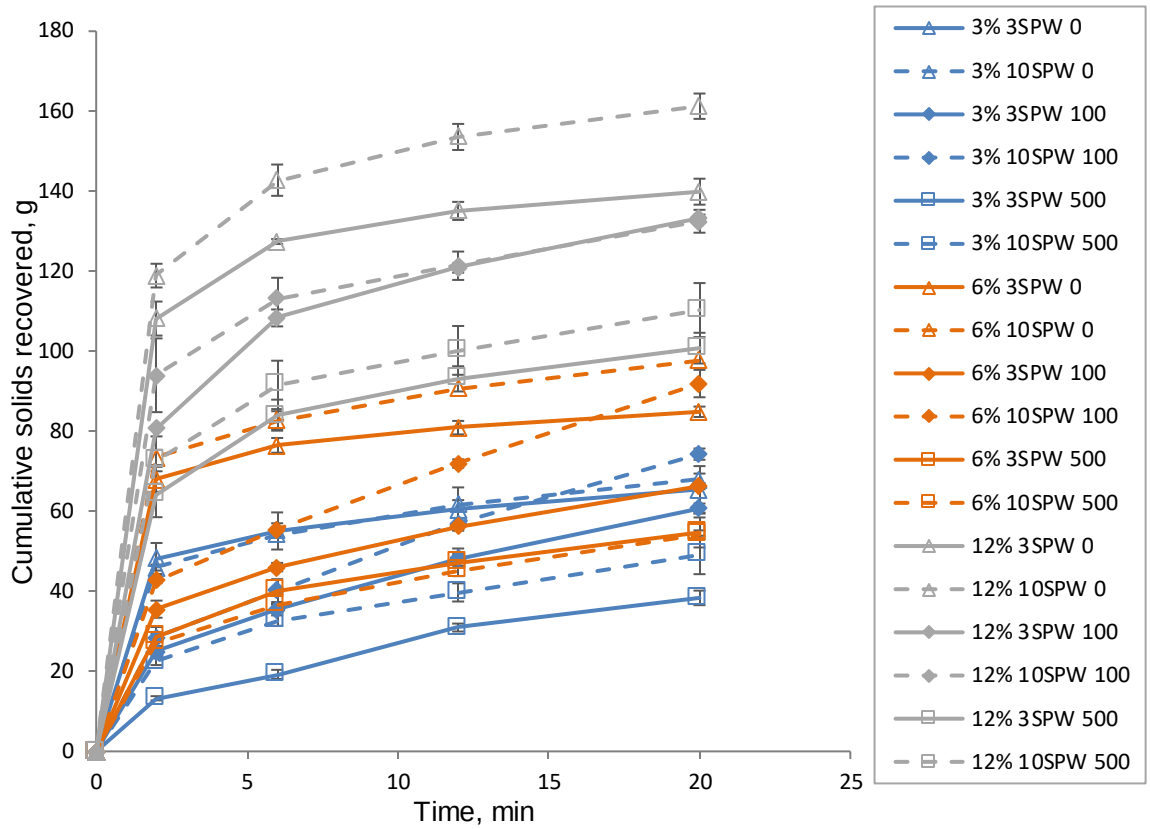

Figure 5- 1: Cumulative solids recovered Vs. Time for 3(blue), 6(orange) and 12% (grey)) pyrite feed, under 3(solid) and 10 (dashed) Synthetic Plant Water type(s), for 0(triangle), 100(diamond) and 500 (square) g/t CMC depressant dosage(s), respectively. The error bars included in the figure represent the standard error between duplicate tests.

5.1.2 Cumulative Water vs. Time

Figure 5- 2 illustrates cumulative water vs. time for 3, 6 and 12% pyrite feed grade, under 3 and 10SPW, for the three CMC depressant dosages, 0, 100 and 500 g/t. Water recovered per unit time increased with pyrite feed grade, as illustrated predominantly by the grey curves at the top of the graph, with water recoveries increasing in the order 3% (blue) < 6% (orange) < 12% (grey). To clarify the overlaps in Figure 5- 2 and thereby allow for a better illustration of this observation, the feed grades are separated into individual cumulative water recovery vs time, as shown in Appendix A1. As the ionic strength of plant water increased from 3 (solid curves) to 10SPW (dashed curves), water recovered per unit time increased for all pyrite feed grades; this is clearly depicted by the dashed lines falling above their solid counter parts in all cases. The highest water recovered by the 12% was ~ 1400 g, 6% was ~ 1200 g and 3% was ~ 1100 g. Generally, water recovered per unit time decreased with increasing depressant dosage for all pyrite feed grades as illustrated predominantly by the triangle markers (0 g/t) at the top of the graph, with water recoveries decreasing in the order square (500 g/t) < diamond (100 g/t) < triangle (0 g/t).

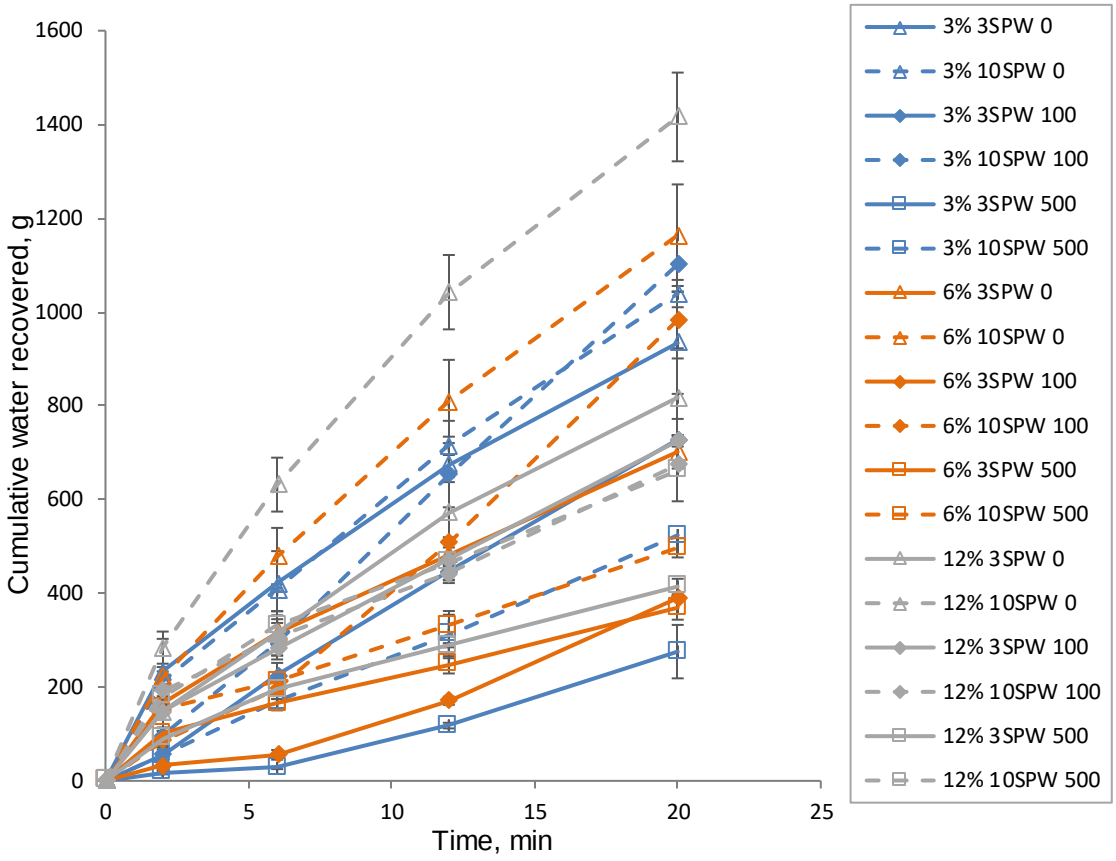

Figure 5- 2: Cumulative water recovered vs. Time for 3(blue), 6(orange) and 12%(grey) pyrite feed, under 3(solid) and 10(dashed) Synthetic Plant Water type(s), for 0(triangle), 100(diamond) and 500(square) g/t CMC depressant dosage(s), respectively. The error bars included in the figure represent the standard error between duplicate tests.

5.1.3 Solids and Water Recoveries

Figure 5- 3 illustrates the cumulative solids and water recoveries for 3, 6 and 12% pyrite feed grade, under the two SPW conditions considered, 3 and 10SPW, for three CMC depressant dosages, 0, 100 and 500 g/t. Solids and water recovered increased with increasing pyrite feed grade, as illustrated predominantly by the grey curves at the top of the graph, with solids and water recovery increasing in the order 3% (blue) < 6% (orange) < 12% (grey). As the ionic strength of plant water was increased from 3 (solid curves) to 10SPW (dashed curves), solids and water recovery increased for all pyrite feed grades; this is clearly illustrated by the dashed lines falling above their solid counter parts in most cases. The highest solids recovered in order of increasing pyrite feed grade was ~75 g for 3% (blue) < 100 g for 6% (orange) < 162 g for 12% (grey). The highest water recovered by the 3% (blue) was ~1100 g < 6% (orange) ~1180 g < 3% (grey) ~1400 g. Water and solids recovered decreased with increasing depressant dosage for all the investigated pyrite feed grades. This is clearly illustrated by the 12% pyrite feed grade (grey), whereby an increase in depressant dosage from 0, 100 to 500 g/t is shown by the triangle (0 g/t) > diamond (100 g/t) > square (500 g/t).

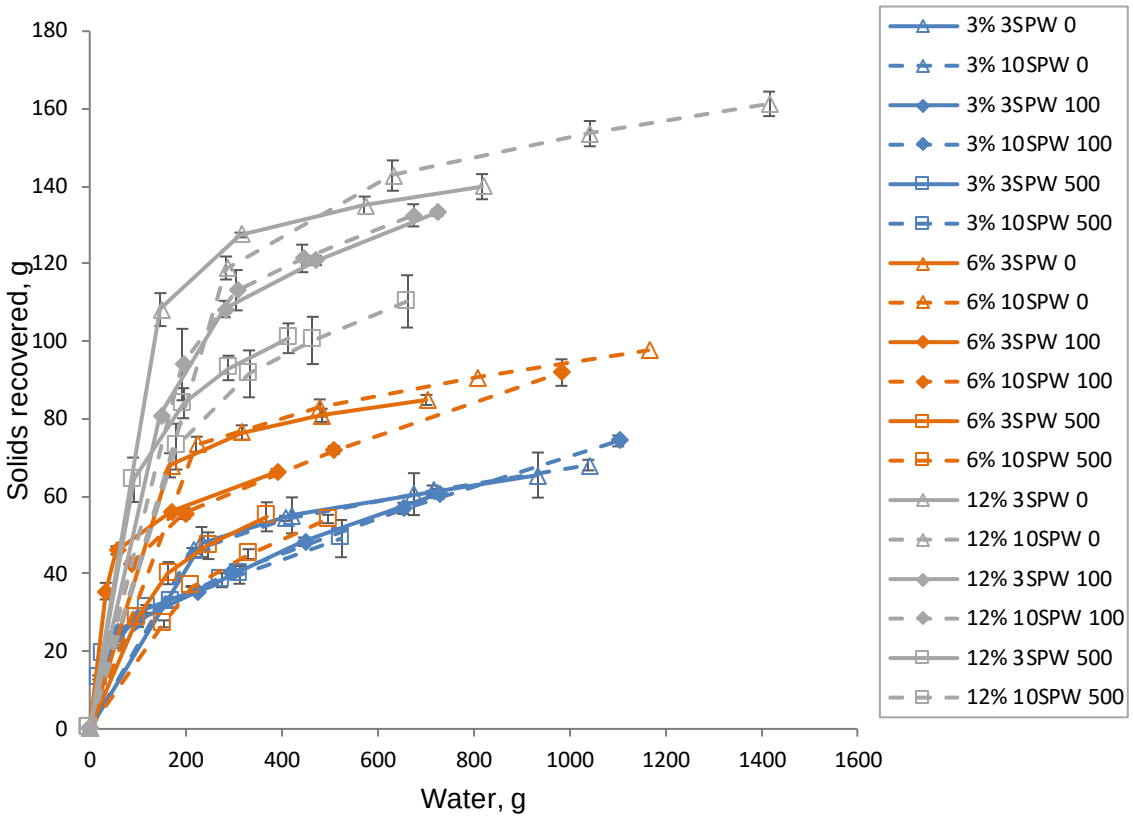

Figure 5- 3: Cumulative solids and water recoveries for 3 (blue), 6 (orange) and 12% (grey) pyrite feed, under 3 (solid) and 10 (dashed) Synthetic Plant Water type(s), for 0 (triangle), 100 (diamond) and 500 (square) g/t CMC depressant dosage(s), respectively. The error bars included in the figure represent the standard error between duplicate tests.

5.1.4 Final Solids and Water Recoveries

Figure 5- 4 illustrates final total solids and water recovered for the conditions tested. As the pyrite feed grade was increased for each ionic strength, solids (brown bars) recovered increased, while water (light blue bars) recovered generally decreased for the 3SPW, and increased for the 10SPW. At each depressant dosage, solids (brown bars) and water (light blue bars) recovered increased with increasing ionic strength of plant water for the 3, 6 and 12% pyrite feed grade. At each pyrite feed grade and synthetic plant water type, solids (brown bars) and water (light blue bars) recovered decreased with increasing CMC depressant dosage (with the exception of 3% pyrite feed, 10SPW). Furthermore, as the pyrite feed grade and ionic strength were simultaneously increased, solids (brown bars) and water (light blue bars) recovered increased for each depressant dosage. The highest solid (brown bars) recovered for each feed grade was ~ 75 g for the 3% pyrite feed grade < ~ 100 g for 6% pyrite feed grade < ~ 162 g for the 12% pyrite feed grade. These highest solids recovered were generally obtained at high ionic strength, 10SPW under 0 g/t CMC depressant dosage for all the pyrite feed grades.

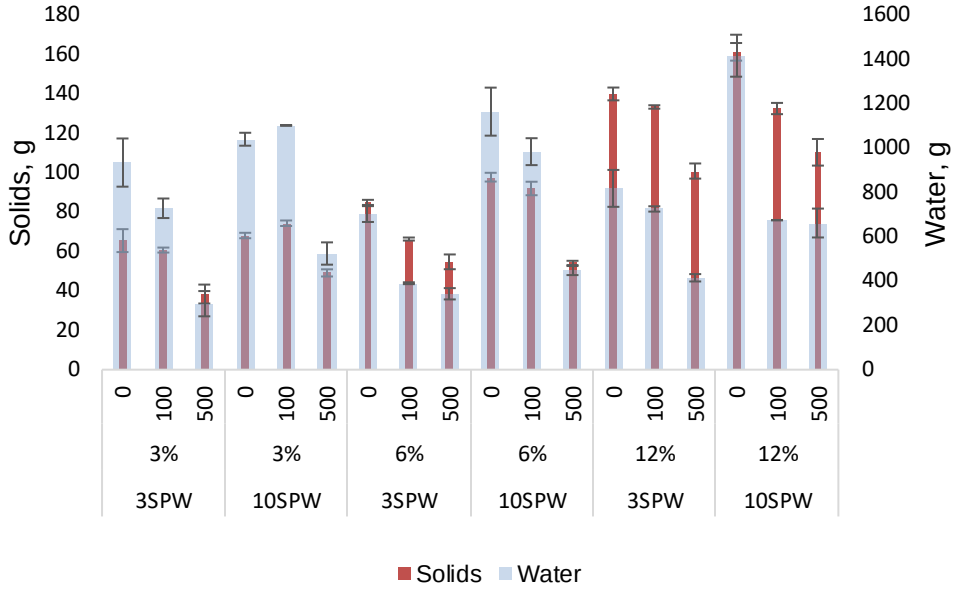

Figure 5- 4: Final solids and water recoveries for 3, 6 and 12% pyrite feed, under 3 and 10 Synthetic Plant Water type(s), for 0, 100 and 500 g/t CMC depressant dosage(s), respectively. The error bars included in the figure represent the standard error between duplicate tests.

5.1.5 Concentrate Grade and Recoveries

This section evaluates the effects of varying pyrite feed grade, ionic strength of plant water and depressant dosage on the flotation performance of the pyrite-based synthetic ore, through comparison of iron (Fe) grades and recoveries.

5.1.5.1 Cumulative Fe Recovery vs. Time

Figure 5- 5 illustrates cumulative Fe recovery vs. time for 3, 6 and 12% pyrite feed, under 3SPW and 10SPW conditions, for the three CMC depressant dosages; 0, 100 and 500 g/t. The majority of the Fe was recovered within the first 2 minutes for each pyrite feed grade. Generally, Fe recovery increased with increasing pyrite feed grade as illustrated by the cumulative Fe recovery curves in the order blue (3%) < orange (6%) < grey (12%). Increasing the depressant dosage, generally decreased the Fe recovery per unit time for all pyrite feed grades. This effect is more clearly illustrated by the 6% pyrite feed grade (orange), whereby Fe recovery per unit time decreased with an increase in depressant dosage as illustrated by the triangle (0 g/t) > diamond (100 g/t) > square (500 g/t). To clarify the overlaps in Figure 5- 5 and thereby allow for a better illustration of these observations, the feed grades are separated into individual cumulative Fe recovery vs. time, as shown in Appendix B1. The greatest CMC depression was observed at 500 g/t under the 6% (orange) pyrite feed grade, for both 3 and 10SPW, respectively. The effect of ionic strength is not clearly illustrated in this figure.

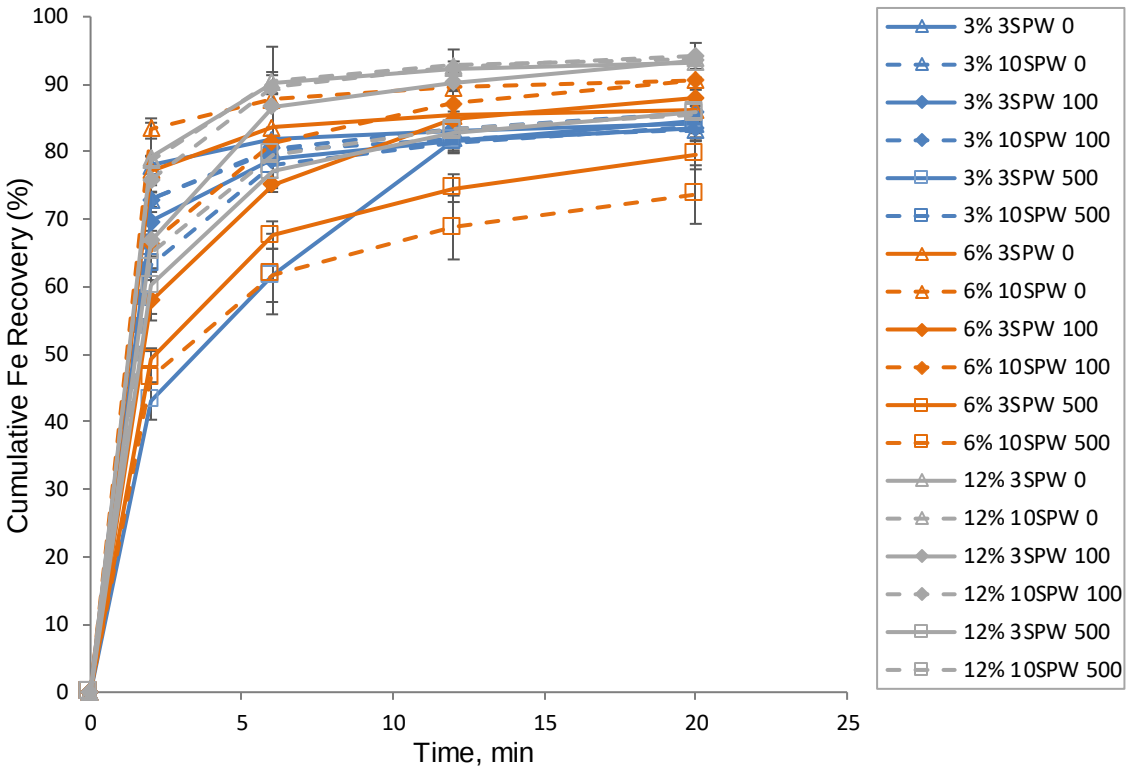

Figure 5- 5: Cumulative Fe recovery vs. Time for 3, 6 and 12% pyrite feed under 3 and 10 Synthetic Plant Water type(s), for 0, 100 and 500 g/t CMC depressant dosage(s), respectively. The error bars included in the figure represent the standard error between duplicate tests.

5.1.5.2 Cumulative Fe Recovery vs. Water Recoveries

Figure 5- 6 illustrates the cumulative Fe recoveries as a function of cumulative water recovered for 3, 6 and 12% pyrite feed grade, under 3SPW and 10SPW conditions, for the three CMC depressant dosages, 0, 100 and 500 g/t. Generally, as the pyrite feed grade was increased, cumulative Fe and water recovery increased, as illustrated by the grey curves at the top of the graph, with the Fe recovery increasing in the order 3% (blue) < 6% (orange) < 12% (grey). To clarify the overlaps in Figure 5- 6 and thereby allow for a better illustration of these observations, the feed grades are separated into individual cumulative Fe recovery vs. cumulative water recovered, as shown in Appendix B1. The effects of ionic strength of plant water type are not clearly illustrated in this figure. Similarly, the same can be said for the depressant effects. Similar amounts of final Fe were recovered for the 3% (blue) pyrite feed grade for the tested conditions, with the majority of the Fe recovery collected within 200 g of synthetic plant water utilised for the flotation process. The 6% (orange) pyrite feed grade, under 10SPW, at 500 g/t CMC depressant dosage, recorded the lowest amount of Fe recovery compared to the 3% (blue) and 12% (grey) for the same depressant dosage condition under both 3 and 10SPW, respectively.

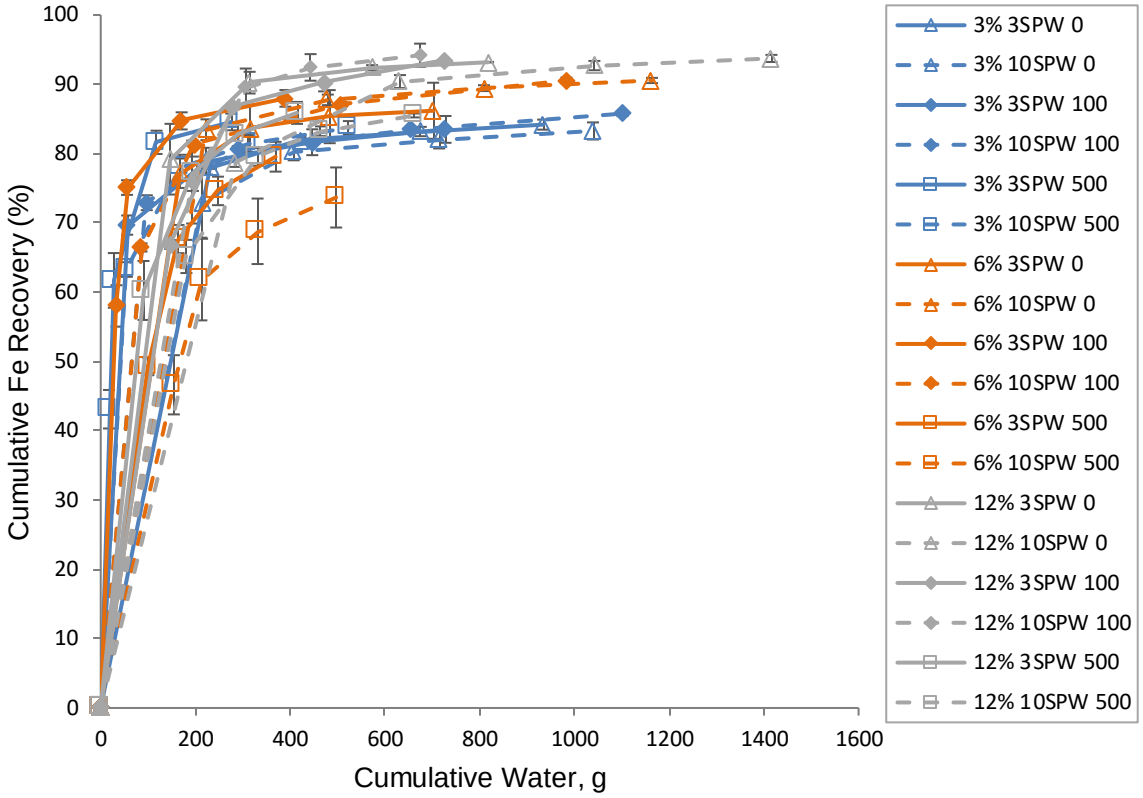

Figure 5- 6: Cumulative Fe recovery Vs. cumulative water recovered for 3, 6 and 12% pyrite feed, under 3 and 10 Synthetic Plant Water type(s), for 0, 100 and 500 g/t CMC depressant dosage(s), respectively. The error bars included in the figure represent the standard error between duplicate tests.

5.1.5.3 Final Fe Grade and Recovery

Figure 5- 7 illustrates the final Fe grade and recovery for 3, 6 and 12% pyrite feed, under 3 and 10SPW, for 0, 100 and 500 g/t CMC depressant dosages. Generally, the final Fe recoveries as illustrated by the grey bars, fall within similar ranges for each feed grade; ~ 80 to 85% for the 3% pyrite feed grade < ~ 86 to 90% for the 6% pyrite feed grade < ~ 84 to 94% for the 12% pyrite feed grade. These minimal changes in cumulative final Fe recoveries suggest that neither varying pyrite feed grade nor ionic strength nor depressant dosage affected the Fe recoveries. As the pyrite feed grade was increased for each ionic strength of plant water type and depressant dosage condition, final Fe grade (brown bars) recovered increased. At each pyrite feed grade and ionic strength of plant water type condition, final Fe grade (brown bars) recovered increased with increasing depressant dosage. At each feed grade, Fe grade (brown bars) recovered decreased with an increase in ionic strength of plant water type, for each depressant dosage. Final Fe grade (brown bars) recovered increased with a simultaneous increase in pyrite feed grade and ionic strength, for each depressant dosage. The highest final Fe grade (brown bars) recovered was ~ 27% for 3% pyrite feed grade < ~34% for 6% pyrite feed grade < ~ 35% for 12% pyrite. These highest Fe grade recoveries were obtained under 3SPW, 500 g/t CMC depressant dosage for the 3 and 6% pyrite feed grade, and under 3SPW 100 g/t for the 12% pyrite feed grade.

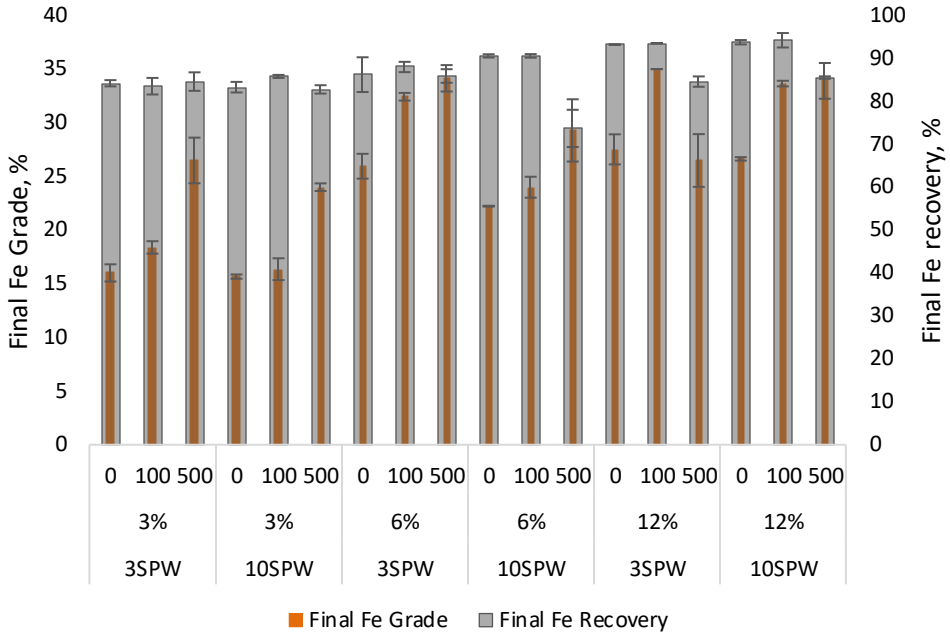

Figure 5- 7: Final Fe grade and recovery for 3, 6 and 12% pyrite feed, under 3 and 10 Synthetic Plant Water type(s), for 0, 100 and 500 g/t CMC depressant dosage(s), respectively. The error bars included in the figure represent the standard error between duplicate tests.

5.1.5.4 Fe Grade and Recoveries for 3 SPW

Figure 5- 8 illustrates Fe grade vs. Fe recovery for 3, 6 and 12% pyrite feed under 3SPW, for 0, 100 and 500 g/t CMC depressant dosages. It is clear from the figure that for this ionic strength, 3SPW, most of the Fe recoveries fall between 80 to 90% for all the tested conditions. The Fe grade recoveries fall between 15 to 42% across the three pyrite feed grades. As the pyrite feed grade was increased for this SPW, Fe grades and recoveries increased as illustrated by the 12% (grey) curves falling predominantly on top of the graph, with Fe grades and recoveries in the order 3% (blue) < 6% (orange) < 12% (grey). The figure clearly illustrates that Fe grade recoveries increased with depressant dosage from 0 to 100 g/t for all pyrite feed grades. The 500 g/t depressant dosage for 6 (orange) and 12% (grey) pyrite feed grade are seen to decrease recovery for almost the same grade as 100 g/t (diamond) CMC depressant dosage, while for the 3% (blue) pyrite feed grade, the Fe grade increased for almost the same recovery as the 100 g/t depressant dosage. Furthermore, highest grade recoveries for the 6 (orange) and 12% (grey) pyrite feed grade are seen at 100 g/t (diamond) depressant dosage, while for the 3% (blue) pyrite feed grade, the highest grade are seen at 500 g/t. This illustrates that Fe grades were maximized at higher depressant dosages.

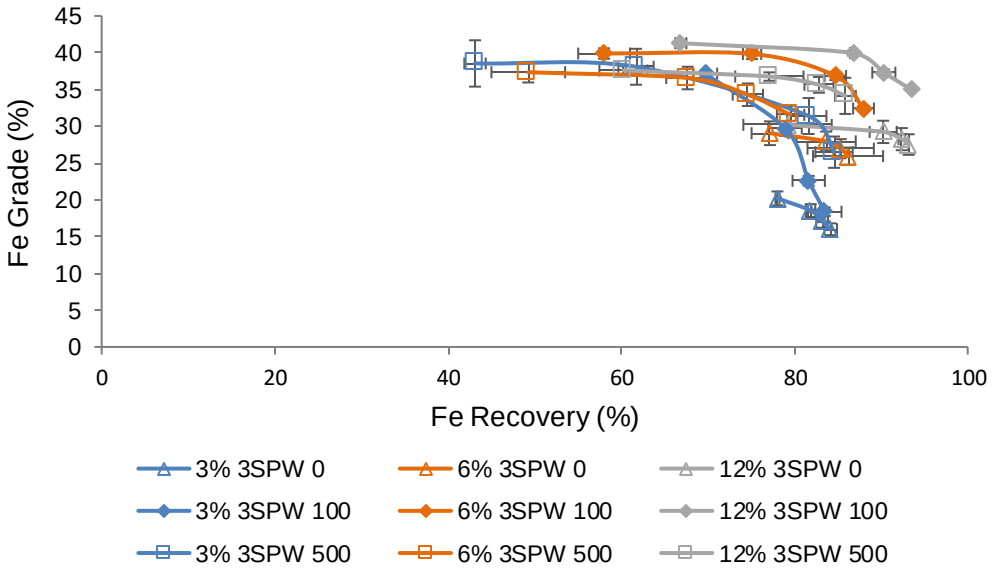

Figure 5- 8: Fe grade Vs. Fe recovery for 3, 6 and 12% pyrite feed under 3SPW, for 0, 100 and 500 g/t CMC depressant dosage(s), respectively. The error bars included in the figure represent the standard error between duplicate tests.

5.1.5.5 Fe Grade and Recoveries for 10 SPW

Figure 5- 9 illustrates the Fe grade vs. Fe recovery for 3, 6 and 12% pyrite feed under 10 SPW, for 0, 100 and 500 g/t CMC depressant dosages, respectively. The Fe recoveries for this synthetic plant water type, 10SPW, generally fall between 75 – 90% for the tested conditions, with the exception of the 6% (orange) pyrite feed grade, under 500 g/t (square) CMC depressant dosage. The Fe grade recoveries fall between 15 – 38% across all the three pyrite feed grades. As the pyrite feed grade was increased for this SPW, Fe grades and recoveries increased as illustrated by the 12% (grey) curves falling predominantly on top of the graph, with Fe grades and recoveries in the order 3% (blue) < 6% (orange) < 12% (grey). The figure clearly illustrates that Fe grade recoveries increased with depressant dosage from 0 to 100 g/t for all pyrite feed grades. The 500 g/t (square) depressant dosage for the 3 (blue) and 12% (grey) pyrite feed grade are seen to decrease recovery for almost the same grade as 100 g/t (diamond) CMC depressant dosage, while for the 6% (orange) pyrite feed grade, the Fe grade recoveries are seen to decrease to below the 3% (blue) pyrite feed grade, 100 g/t (diamond) CMC depressant dosage. The figure clearly illustrates that Fe grade recoveries were maximized at higher depressant dosages.

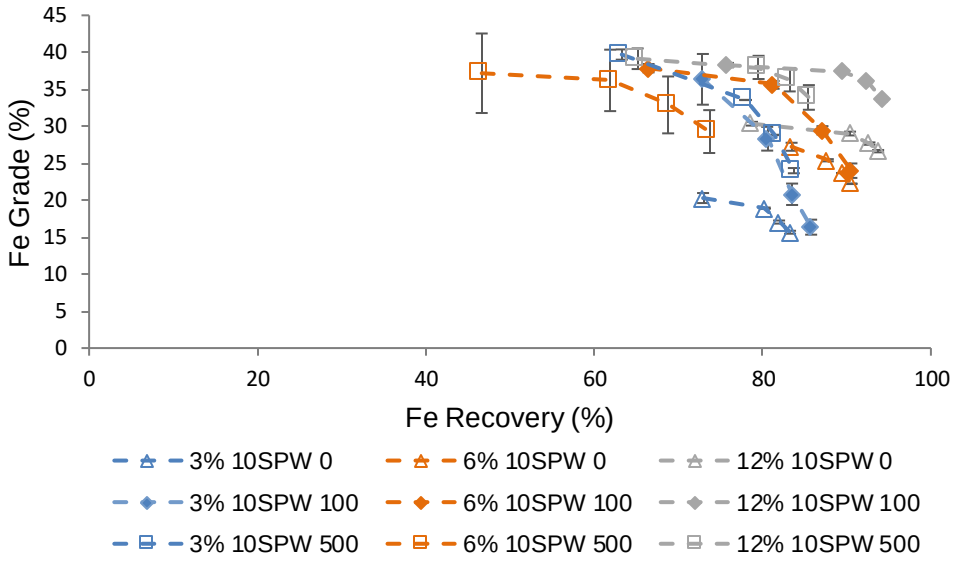

Figure 5- 9: Fe grade Vs. Fe recovery for 3, 6 and 12% pyrite feed under 10 SPW, for 0, 100 and 500 g/t CMC depressant dosage(s), respectively. The error bars included in the figure represent the standard error between duplicate tests.

5.1.6 Foam Column

Foam can be defined as a two-phase structure consisting of liquid and air. Pure liquids are incapable of foaming without the aid of surfactant. The addition of a surfactant to pure liquids allows for a stronger air-liquid interface, thereby foaming. Figure 5- 10 illustrates the maximum foam height and foam stability for the 3SPW and 10SPW. The surfactant used for carrying out these tests was Dow200 frother. Maximum foam height is represented by the light blue bars, while the dark blue represents the foam stability. The foam stability and foam height of 3SPW and 10SPW were about 1 s and 1.8 cm, and 3 s and 5 cm, respectively. Thus, as the ionic strength of plant water was increased from 3SPW to 10SPW, foam height and foam stability also increased. Knowledge of two-phase foams can be used to describe three phase systems (solid, liquid and air bubbles).

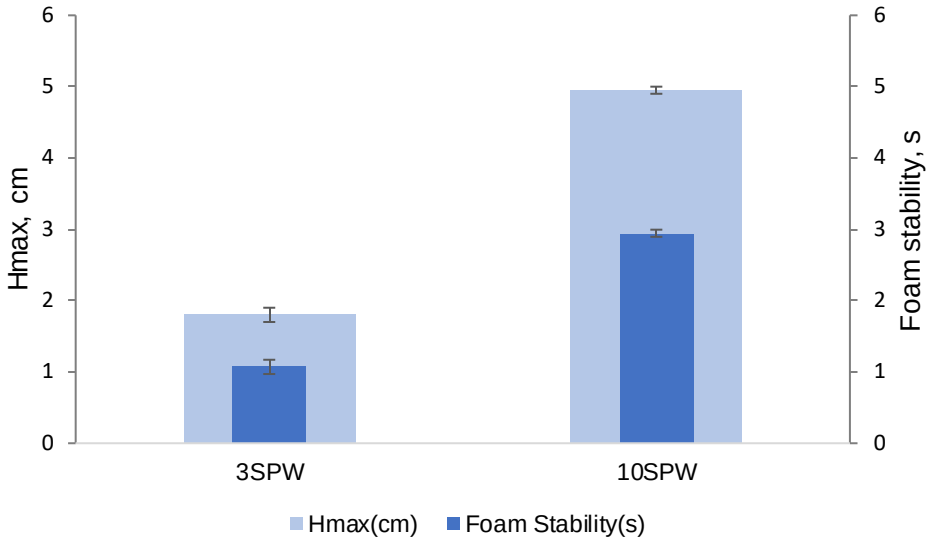

Figure 5- 10: Maximum foam height and foam stability for 3SPW and 10SPW, respectively. A frother dosage of 40g/t Dow200 was used. The error bars included in the figure represent the standard error between duplicate tests.

5.1.7 Froth Column

Froth can be defined as a three-phase structure consisting of solid, liquid and air. Figure 5- 11 illustrates the maximum froth height and froth stability for 3, 6 and 12% pyrite feed grade, under the 3SPW and 10SPW. Maximum froth height and froth stability are represented by the light blue and dark blue bars for all the pyrite feed grades investigated. Generally, for each pyrite feed grade, froth height (light blue bars) and froth stability (dark blue bars) increased with increasing ionic strength of plant water from 3SPW to 10SPW. The froth stability and froth height for the 3, 6 and 12% pyrite feed grade, under 3SPW, were 11.5 s and 19.3 cm, 8.4 s and 14.1 cm, and 12.2 s and 20.5 cm, respectively. This illustrated that froth stability and froth height did not linearly increase as pyrite feed grade was increased from 3, 6 to 12% pyrite feed grade. A positive parabolic relationship between froth stability and pyrite feed grade is depicted, whereby froth stability goes through a minimum at the 6% pyrite feed grade, after which it reaches a maximum froth stability at 12%. There was not much variation observed at higher ionic strength, 10SPW, as the pyrite feed grade was varied from 3, 6 to 12%. These small differences in froth stability between the 3, 6 and 12% pyrite feed grade under 10 SPW suggest that froth stability was the same as the pyrite feed grade was increased.

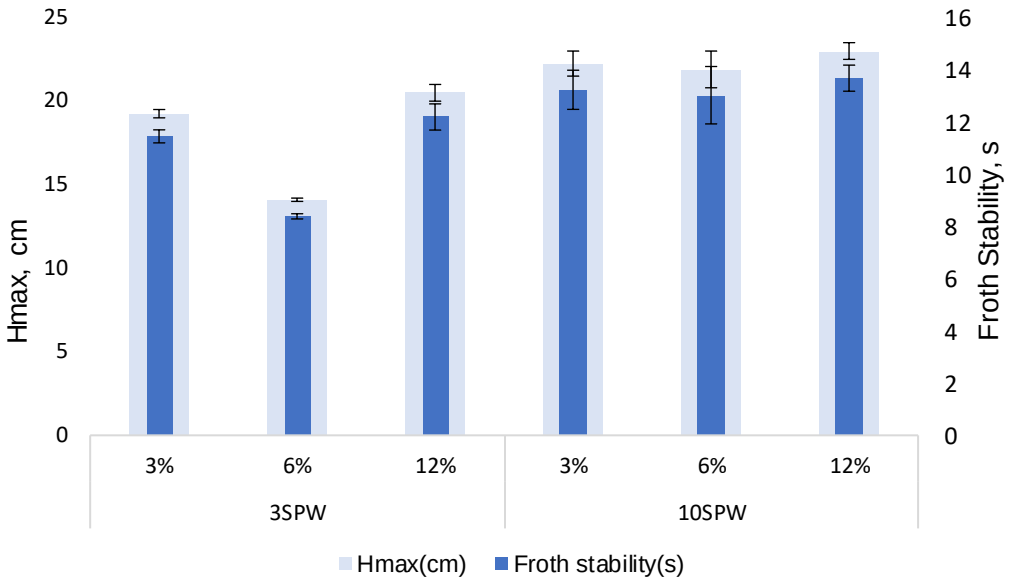

Figure 5- 11: Maximum froth height and froth stability for 3, 6 and 12% pyrite feed, under 3 and 10SPW, respectively. Reagents used include 150 g/t SIBX collector and 40 g/t Dow200 frother. The error bars included in the figure represent the standard error between duplicate tests.

5.1.8 Total Gangue Recoveries

Figure 5- 12 illustrates the total gangue vs. water recovered for 3, 6 and 12% pyrite feed under 3SPW and 10SPW, for 500 g/t CMC depressant dosages. The intention of the results presented in this section was to show entrainment; a non-selective process responsible for the recovery of both valuable and unwanted gangue mineral particles reporting to the concentrate. Generally, the rate of recovery of the total gangue recovered (per unit water) increased with increasing pyrite feed grade. Total gangue and water recoveries increased with increasing pyrite feed grade, as illustrated predominantly by the grey curves at the top of the graph, with total gangue recovery increasing in the order 3% (blue) < 6% (orange) < 12% (grey). The total gangue increased with increasing ionic strength from 3 SPW to 10 SPW as illustrated by the dashed lines falling above their solid counterparts in most cases. Furthermore, the results illustrated suggest that not all the Naturally Floating Gangue (NFG) was completely depressed at depressant dosages greater than 500 g/t. The galena-based synthetic ore proved this observation to be true; the depressant dosage was increased to 700 and 800 g/t and an entrainment factor was still not attained as described in Section 5.2.7.

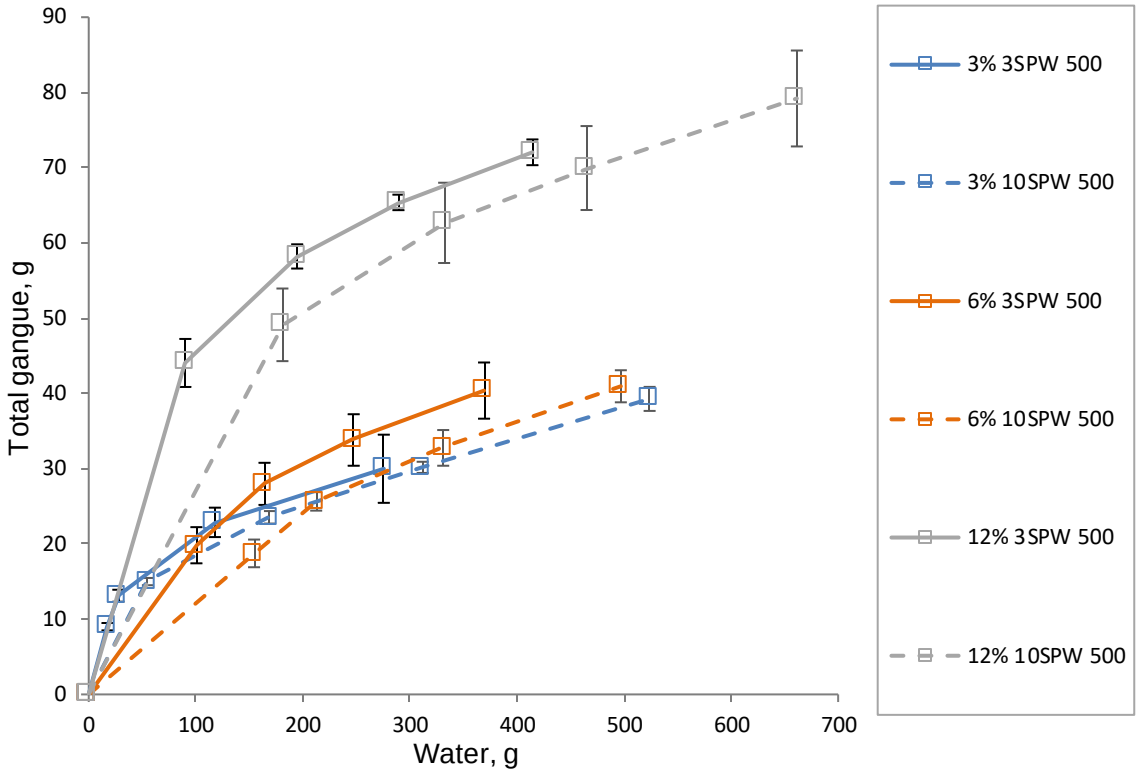

Figure 5- 12: Total gangue Vs. water recovered for 3, 6 and 12% pyrite feed under 3 and 10 Synthetic Plant Water type(s), for 500 g/t CMC depressant dosages. The error bars included in the figure represent the standard error between duplicate tests.

5.2 Galena

This section evaluates the effects of varying galena feed grade, ionic strength of plant water and depressant dosage on the flotation performance of the galena-based synthetic ore, by comparison of; solids and water recovered, lead (Pb) grades and recoveries, froth stability, and total gangue recovered.

5.2.1 Cumulative Solids vs. Time

Figure 5- 13 illustrates cumulative solids vs. time for 3, 6 and 12% galena feed, under 3 and 10SPW, for 0, 100 and 500 g/t CMC depressant dosages. Solids recovered per unit time increased with galena feed grade, as illustrated predominantly by the grey curves at the top of the graph, with the solids increasing in the order 3% (blue) < 6% (orange) < 12% (grey), with most solids generally being recovered within the first 2 minutes. Solids recovered per unit time decreased with an increase in depressant dosage for all the galena feed grades. This effect is illustrated by each galena feed grade, whereby an increase in depressant dosage from 0, 100 to 500 g/t is illustrated by the triangle (0 g/t) > diamond (100 g/t) > square (500 g/t). As the ionic strength of plant water was increased, from 3 (solid curves) to 10SPW (dashed curves), solids recovered per unit time increased for all galena feed grades. This is clearly shown by the dashed lines falling above their solid counterparts in most cases (with the exception of 12% galena feed grade, 10SPW for 0 g/t CMC depressant dosage). The highest solids recovered by the 12% was ~160 g, 6% was ~100 g and 3% was ~85 g.

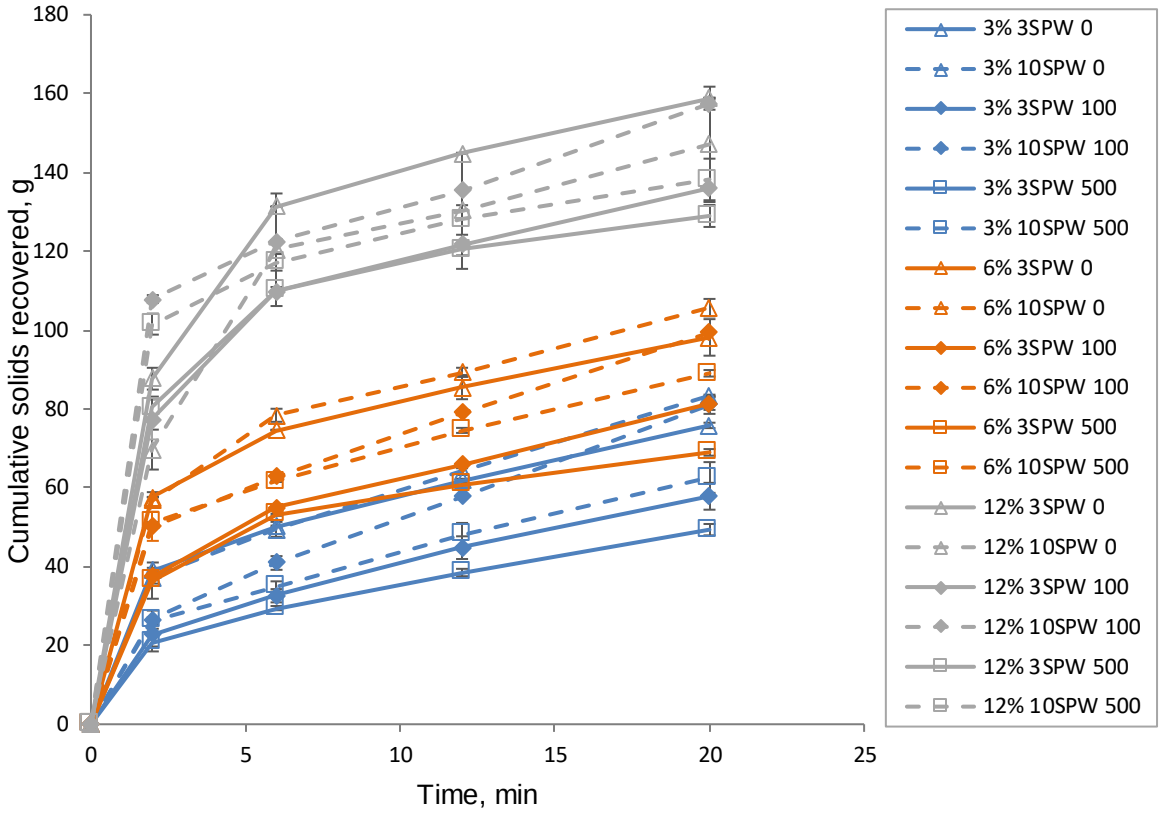

Figure 5- 13: Cumulative solids recovered Vs Time for 3(blue), 6(orange) and 12%(grey) galena feed, under 3(solid) and 10(dashed) Synthetic Plant Water type(s), for 0, 100 and 500 g/t CMC depressant dosage(s), respectively. The error bars included in the figure represent the standard error between duplicate tests.

5.2.2 Cumulative Water vs. Time

Figure 5- 14 illustrates cumulative water vs. time for 3, 6 and 12% galena feed grade, under 3 and 10SPW, for the three CMC depressant dosages, 0, 100 and 500 g/t. Generally, water recovered per unit time decreased with increasing galena feed grade, as illustrated predominantly by the blue curves at the top of the graph, with water recoveries decreasing in the order 3% (blue) > 6% (orange) > 12% (grey). To clarify the overlaps in Figure 5- 14 and thereby allow for a better illustration of this observation, the feed grades are separated into individual cumulative water recovery vs time, as shown in Appendix A2. As the ionic strength of plant water increased from 3 (solid curves) to 10SPW (dashed curves), water recovered per unit time increased for all galena feed grades; this is clearly illustrated by the dashed lines falling above their solid counterparts in all cases. The highest water recovered by the 3% was ~ 1600 g, 6% was ~ 1400 g and 12% was ~ 1200 g. Furthermore, the figure clearly illustrates that more water was recovered under 10SPW (dashed), 100 g/t (diamond) CMC depressant dosage, for all galena feed grades, with water recovered per unit time decreasing in the order 3% (blue) > 6% (orange) > 12% (grey).

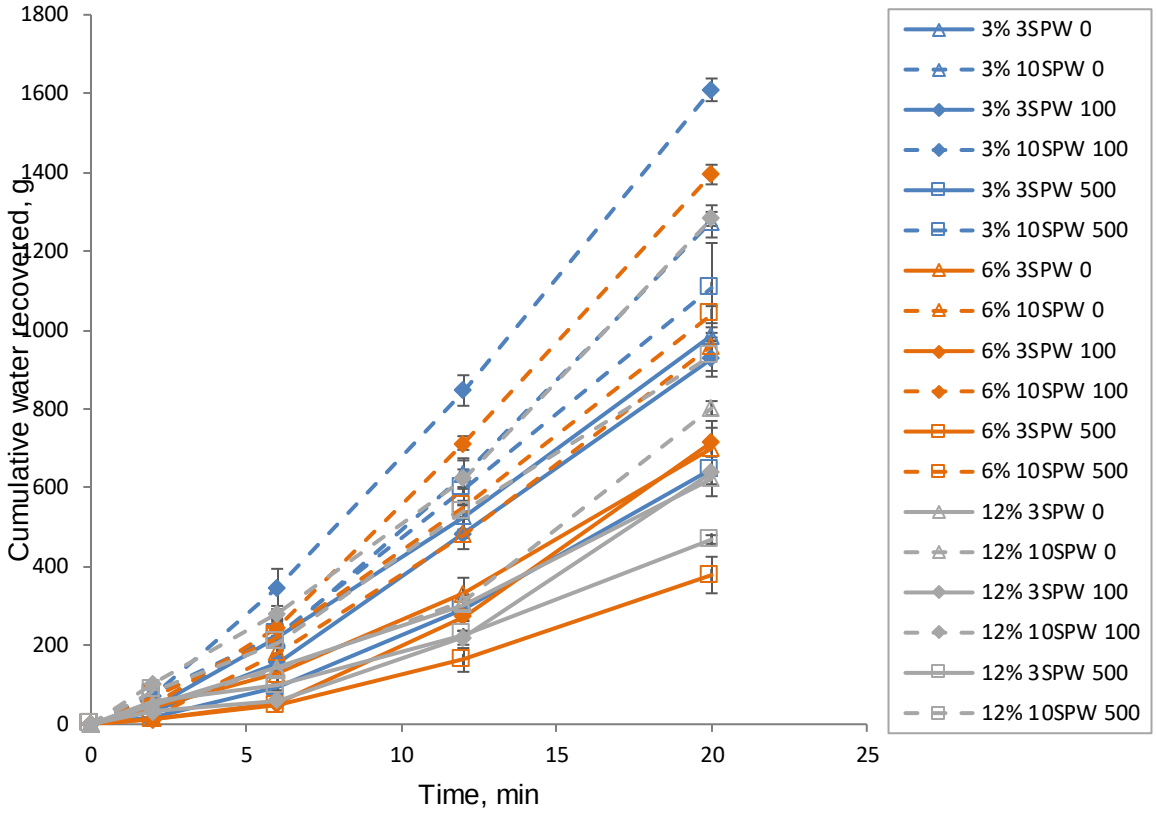

Figure 5- 14: Cumulative water recovered Vs. Time for 3(blue), 6(orange) and 12%(grey) galena feed, under 3(solid) and 10(dashed) Synthetic Plant Water type(s), for 0(triangle), 100(diamond) and 500(square) g/t CMC depressant dosage(s), respectively. The error bars included in the figure represent the standard error between duplicate tests.

5.2.3 Solids and Water Recoveries

Figure 5- 15 illustrates the cumulative solids and water recoveries for 3, 6 and 12% galena feed grade, under 3 and 10SPW, for three CMC depressant dosages, 0, 100 and 500 g/t. Solids recovered increased with increasing galena feed grade, as illustrated predominantly by the grey curves at the top of the graph, with solids recovery increasing in the order 3% (blue) < 6% (orange) < 12% (grey). Water recovered decreased with increasing galena feed grade as illustrated by the cumulative water recovery (x-axis) decreasing in the order 3% (blue) > 6% (orange) > 12% (grey). As the ionic strength of plant water was increased from 3SPW (solid curves) to 10SPW (dashed curves), solids and water recovery increased for all galena feed grades (with the exception of 12% galena feed grade, 10SPW, 0g/t), this is clearly shown by the dashed lines falling above their solid counterparts in most cases. The highest solids recovered by the 12% (grey) was ~160 g > 6% (orange) ~105 g > 3% (blue) ~85 g. The highest water recovered by (12%) was ~1300 g < orange (6%) ~1400 g < blue (3%) ~1600 g. Solids recovered decreased with increasing depressant dosage for all the investigated galena feed grades. This effect is illustrated by all the galena feed grades, whereby an increase in depressant dosage from 0, 100 to 500 g/t is shown by the triangle (0 g/t) > diamond (100 g/t) > square (500 g/t).

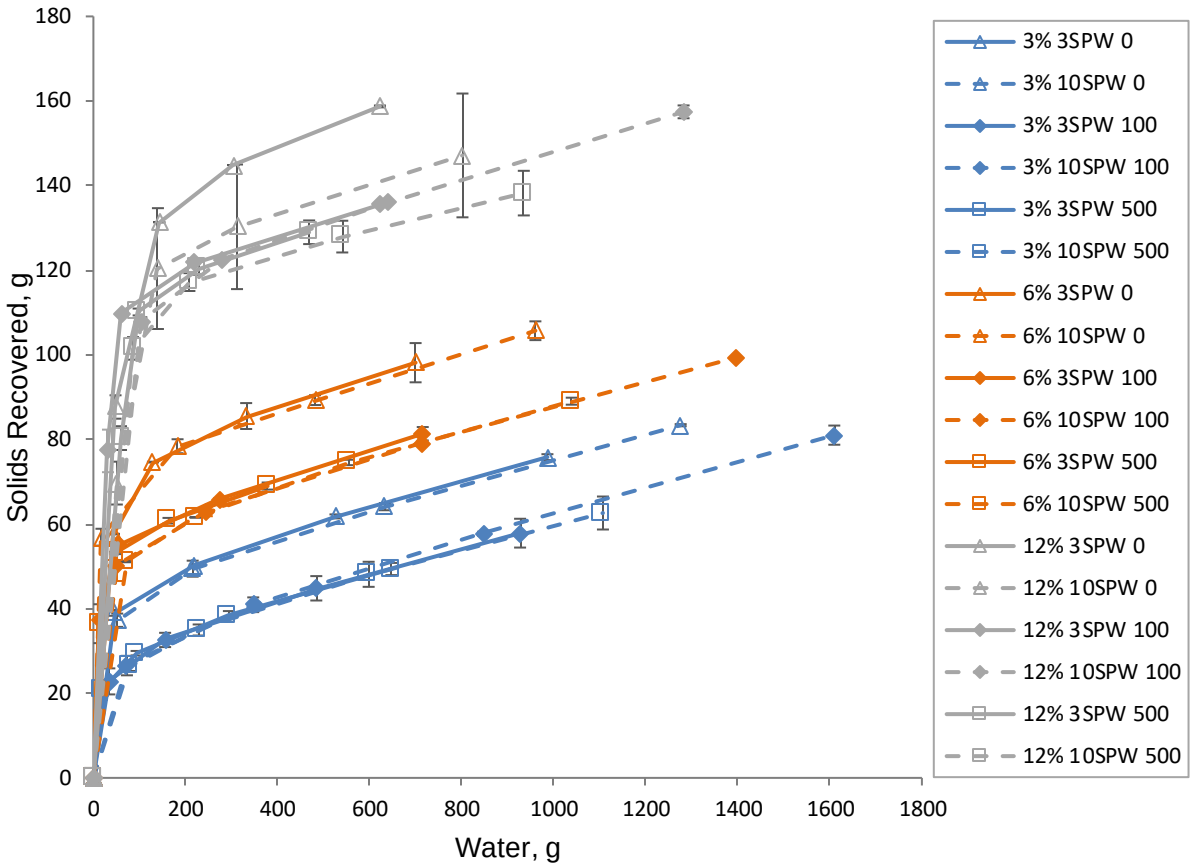

Figure 5- 15: Cumulative solids and water recoveries for 3(blue), 6(orange) and 12%(grey) galena feed, under 3(solid) and 10(dashed) Synthetic Plant Water type(s), for 0, 100 and 500 g/t CMC depressant dosage(s), respectively. The error bars included in the figure represent the standard error between duplicate tests.

5.2.4 Final Solids and Water Recoveries

Figure 5- 16 illustrates the final total solids and water recovered for the conditions tested. As the galena feed grade was increased for each ionic strength and depressant condition, solids (black bars) recovered increased while water (light blue bars) decreased. At each depressant dosage, solids (black bars) recovered increased with increasing ionic strength of plant water, while water recovered (light blue bars) decreased with increasing ionic strength for the 3, 6 and 12% galena feed grades. At each galena feed grade and synthetic plant water type, solids (black bars) and water (light blue bars) recovered decreased with increasing CMC depressant dosage (with exceptions of 10SPW for 3, 6 and 12% galena feed grade). Furthermore, as the galena feed grade and ionic strength were simultaneously increased, solids (black bars) and water (light blue bars) recovered increased for each depressant dosage. The highest final solids (black bars) recovered was ~ 84 g for 3% galena feed grade < ~ 106 g for 6% galena feed grade < ~ 158 g for 12% galena feed grade. These highest final solid recoveries were obtained under 10SPW, 0 g/t for the 3 and 6% galena feed grade, and under 3SPW, 0 g/t for the 12% galena feed grade.

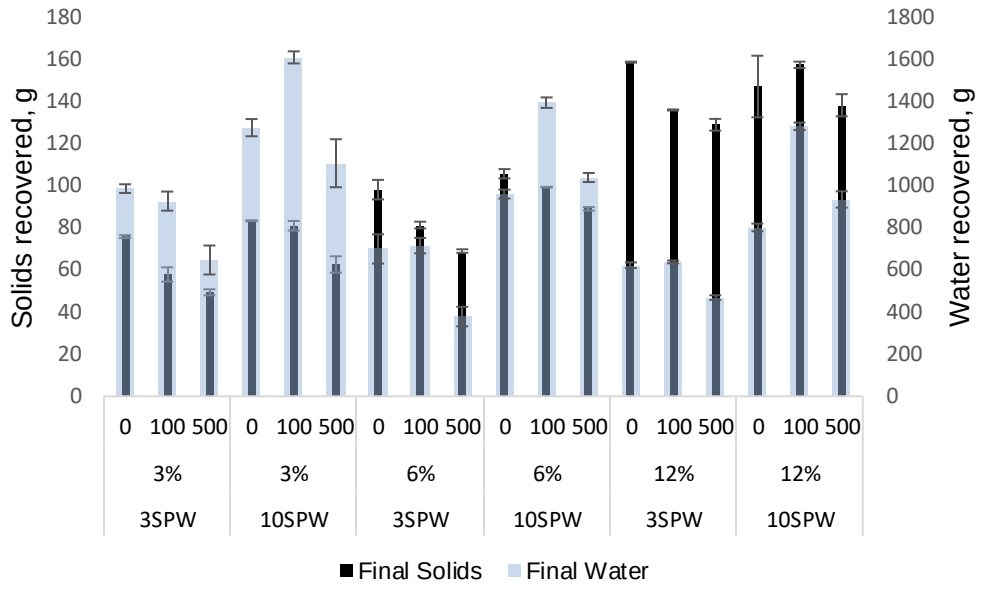

Figure 5- 16: Final solids and water recovered for 3, 6 and 12% galena feed, under 3 and 10 Synthetic Plant Water type(s), for 0, 100 and 500 g/t CMC depressant dosage(s), respectively. The error bars included in the figure represent the standard error between duplicate tests.

5.2.5 Concentrate Grade and Recoveries

This section evaluates the effects of varying galena feed grade, ionic strength of plant water and depressant dosage on the flotation performance of the galena-based synthetic ore, through comparison of Lead (Pb) grades and recoveries.

5.2.5.1 Cumulative Pb Recovery vs. Time

Figure 5- 17 illustrates cumulative Pb recovery vs. time for 3, 6 and 12% galena feed grade, under 3SPW and 10SPW conditions, for the three CMC depressant dosages 0, 100 and 500 g/t. The majority of the Pb was recovered within the first 2 minutes for each galena feed grade. Generally, Pb recovery increased with increasing galena feed grade as illustrated by the cumulative Fe recovery curves in the order 3% (blue) < 6% (orange) < 12% (grey). Increasing the depressant dosage, generally decreased the Pb recovery per unit time for all galena feed grades. This effect is illustrated by the markers arranged in the order triangle (0 g/t) > diamond (100 g/t) > square (500 g/t). To clarify the overlaps in Figure 5-17 and thereby allow for a better illustration of these observations, the feed grades are separated into individual cumulative Pb recovery vs. time, as shown in Appendix B2. The greatest CMC depression was observed at 500 g/t under the 3% (blue) galena feed grade, for 3SPW type. The effect of ionic strength is not clearly illustrated in this figure.

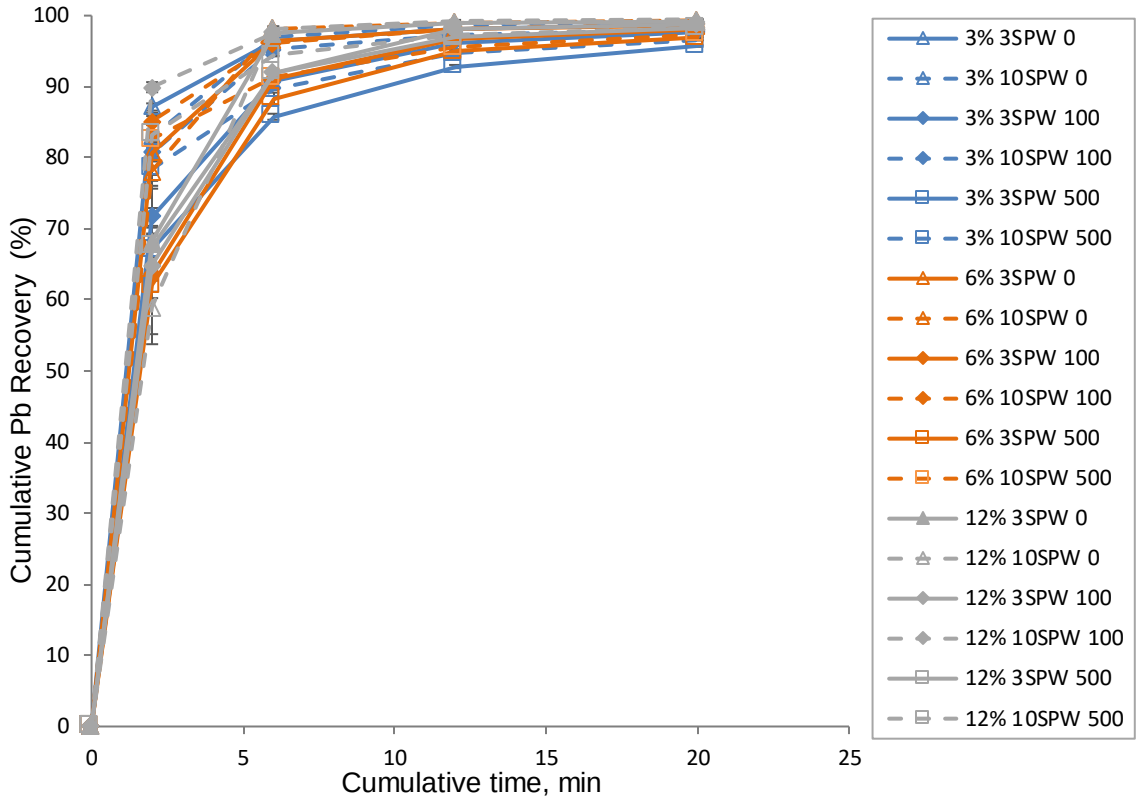

Figure 5- 17: Cumulative Pb recovery vs. Time for 3, 6 and 12% galena feed, under 3 and 10 Synthetic Plant Water type(s), for 0, 100 and 500 g/t CMC depressant dosage(s), respectively. The error bars included in the figure represent the standard error between duplicate tests.

5.2.5.2 Cumulative Pb Recovery Vs. Water Recoveries

Figure 5- 18 illustrates the cumulative Pb recoveries as a function of cumulative water recovered for 3, 6 and 12% pyrite feed grade, under 3SPW and 10SPW conditions, for the three CMC depressant dosages, 0, 100 and 500 g/t. Generally, as the galena feed grade was increased, cumulative Pb recovered increased, as illustrated by the grey curves at the top of the graph, with the Pb recovery increasing in the order 3% (blue) < 6% (orange) < 12% (grey). Cumulative water recovered decreased with increasing galena feed grade, as illustrated by cumulative water recoveries (x-axis) decreasing in the order 3% (blue) > 6% (orange) > 12% (grey). The effects of ionic strength of plant water type are not clearly illustrated in this figure. Increasing the depressant dosage, generally decreased the Pb recovery per unit water for all galena feed grades. This effect is illustrated by the markers generally arranged in the order triangle (0 g/t) > diamond (100 g/t) > square (500 g/t). To clarify the overlaps in Figure 5- 18 and thereby allow for a better illustration of this observation, the feed grades are separated into individual cumulative Pb recovery vs. Cumulative water recovery, as shown in Appendix B2. Generally, similar amounts of Pb were recovered for the 6% (orange) and 12% (grey) galena feed grade, as illustrated by the grey and orange curves falling on top of one another for the tested conditions, with the majority of the Pb recovery collected within 200 g of synthetic plant water utilised for the flotation process. The 3% (blue) galena feed grade, under 10SPW, at 500 g/t CMC depressant dosage, recorded the lowest amount of Pb recovery compared to the 6 (orange) and 12% (grey) under the same conditions.

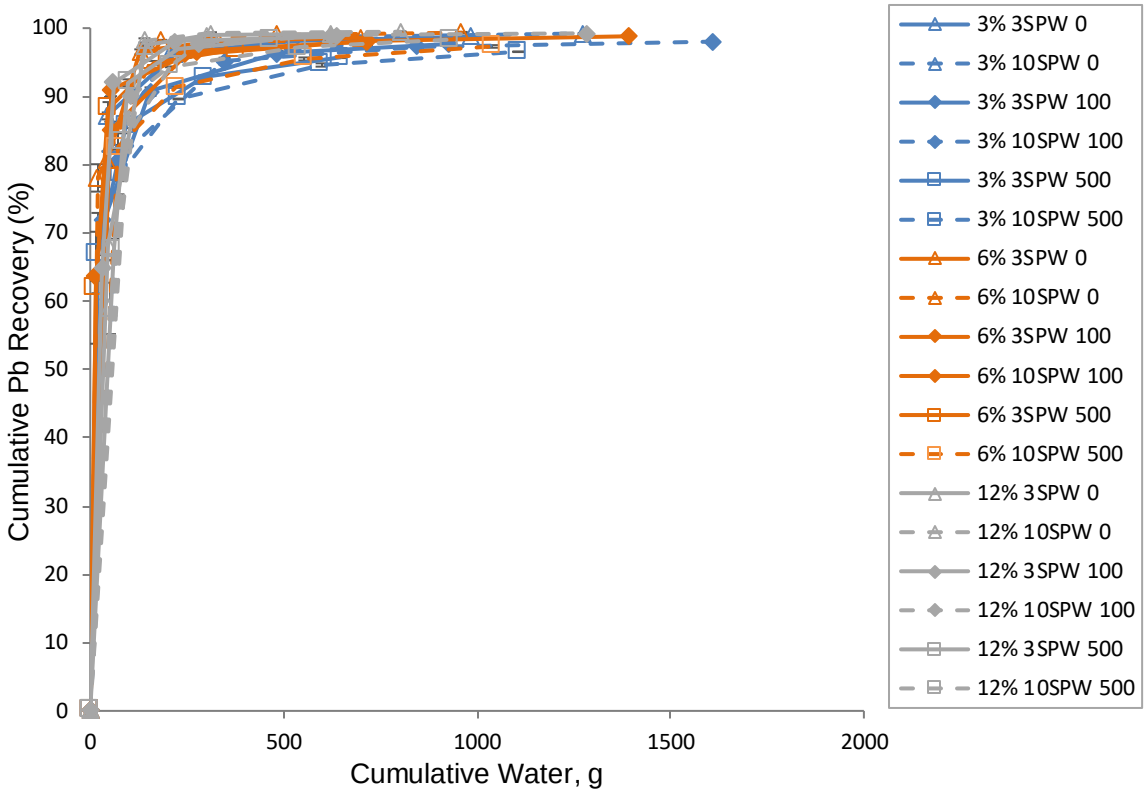

Figure 5- 18: Cumulative Pb recovery vs. cumulative water recovered for 3, 6 and 12% galena feed under 3 and 10 Synthetic Plant Water type(s), for 0, 100 and 500 g/t CMC depressant dosage(s), respectively. The error bars included in the figure represent the standard error between duplicate tests.

5.2.5.3 Final Pb Grade and Recoveries

Figure 5- 19 illustrates final cumulative lead (Pb) grades and recoveries for the conditions tested. As the galena feed grade was increased for each ionic strength and depressant condition, Pb grades (purple bars) increased. As the ionic strength was increased for each galena feed grade, the final Pb grade decreased for each depressant dosage condition. At each galena feed grade and ionic strength condition, final Pb grade (purple bars) recovered increased with increasing depressant dosage. Final Pb grade (purple bars) recovered increased with a simultaneous increase in galena feed grade and ionic strength, for each depressant dosage. The final Pb recoveries (light grey bars) fall within same range of about 97 to 98% for all the galena feed grades, suggesting that Pb recoveries were generally not affected by the variation of pyrite feed grade, ionic strength nor depressant dosage. The highest final Pb grade (purple bars) recovered was ~ 34% for 3% galena feed grade < ~ 47% for 6% galena feed grade < ~ 50% for 12% galena feed grade. These highest final Pb grade recoveries were obtained under 3SPW, 500 g/t CMC depressant dosage for all the galena feed grades.

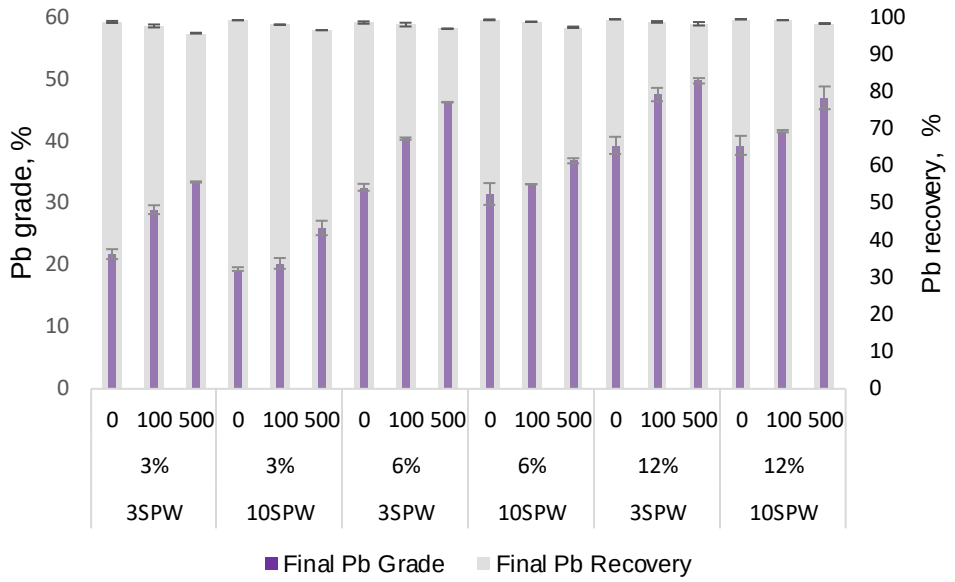

Figure 5- 19: Final Pb grade and recovery for 3, 6 and 12% galena feed under 3 and 10 Synthetic Plant Water type(s), for 0, 100 and 500 g/t CMC depressant dosage(s), respectively. The error bars included in the figure represent the standard error between duplicate tests.

5.2.5.4 Pb Grade and Recoveries for 3 SPW

Figure 5- 20 illustrates Pb grade vs. Pb recovery for 3, 6 and 12% galena feed under 3SPW, for 0, 100 and 500 g/t CMC depressant dosages. It is clear from the figure that for this ionic strength, 3SPW, most of the final Pb recoveries fall between 95.74 to 99.48% for all the tested conditions. The final Pb grade recoveries fall between 21.75 to 49.75% across the three galena feed grades. As the galena feed grade was increased for this ionic strength, Pb grades and recoveries increased as illustrated by the 12% (grey) curves falling predominantly on top of the graph, with the Pb grades and recoveries curves in the order 3% (blue) < 6% (orange) < 12% (grey). Generally, as the depressant dosage was increased, Pb grade increased for all galena feed grades. This increase was more pronounced between 0 (triangle) and 100 g/t (diamond) compared to 500 g/t (square) and 100 g/t (diamond). Furthermore, the highest Pb grades for the 3 (blue), 6 (orange) and 12% (grey) galena feed grade are seen at higher depressant dosages 100 (diamond) and 500 g/t (square).

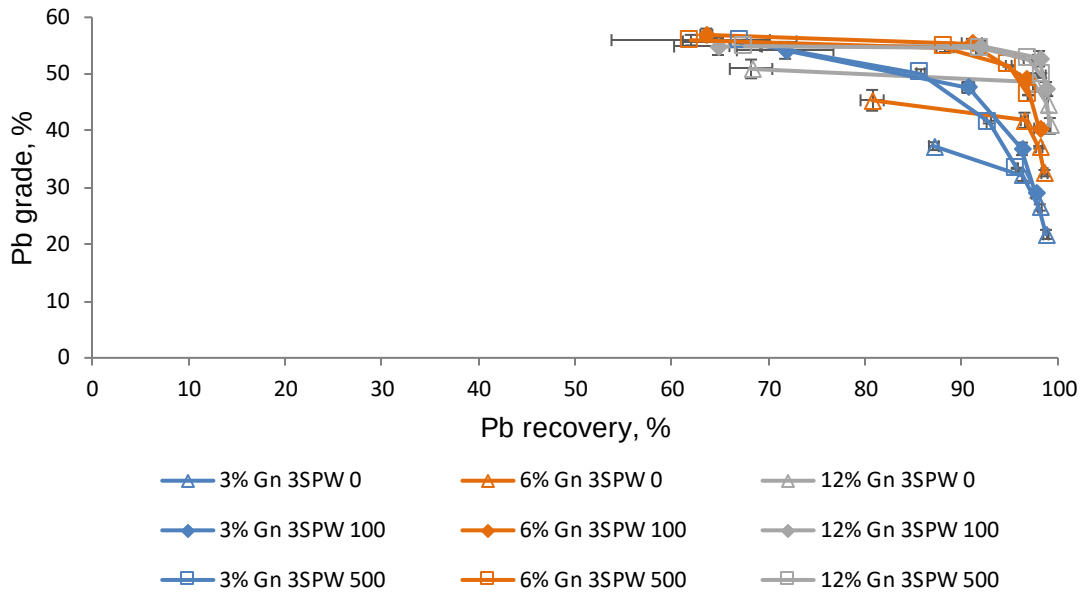

Figure 5- 20: Pb grade vs. Pb recovery for 3, 6 and 12% galena feed under 3 SPW, for 0, 100 and 500 g/t CMC depressant dosage(s), respectively. The error bars included in the figure represent the standard error between duplicate tests.

5.2.5.5 Pb Grade and Recoveries for 10 SPW

Figure 5- 21 illustrates the Pb grade vs. Pb recovery for 3, 6 and 12% pyrite feed under 10 SPW, for 0, 100 and 500 g/t CMC depressant dosages, respectively. The final Pb recoveries for this synthetic plant water type, 10SPW, generally fall between 96.54 to 99.48% for the tested conditions. The final Pb grades fall between 19.34 to 46.99% across all the three galena feed grades. As the galena feed grade was increased for this ionic strength, Pb grades and recoveries increased as illustrated by the 12% (grey) curves falling predominantly on top of the graph, with Pb grades and recoveries in the order 3% (blue) < 6% (orange) < 12% (grey). Generally, as the depressant dosage was increased, Pb grade increased for all galena feed grades, with 500 g/t (square) for the 3 (blue) and 12% (grey) galena feed grades seen to decrease recovery for almost the same amounts of Pb grade as the 100 g/t (diamond), while for the 6% (orange) galena feed grade, the Pb grade recoveries for the 500 g/t (square) are seen to decrease below the 100 g/t CMC depressant dosage. The highest Pb grade are seen at higher depressant dosages 100 (diamond) and 500 g/t (square), for the 3 (blue) and 12% (grey) galena feed grade, while for the 6% (orange), highest Pb grades are observed at 100 g/t (diamond).

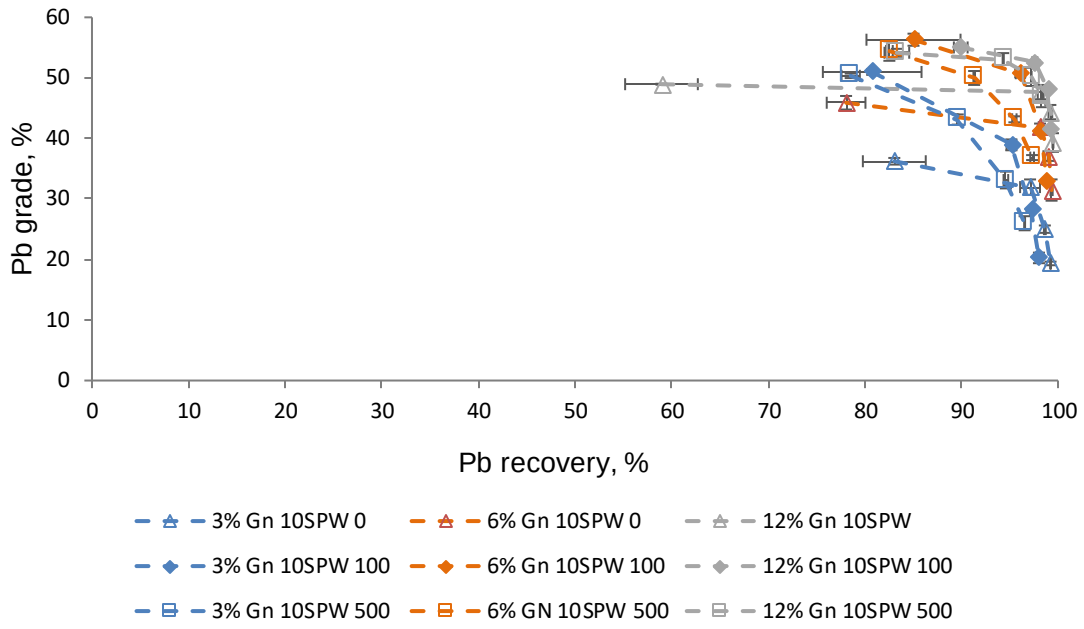

Figure 5- 21: Pb grade Vs. Pb recovery for 3, 6 and 12% galena feed under 10 SPW, for 0, 100 and 500 g/t CMC depressant dosage(s), respectively. The error bars included in the figure represent the standard error between duplicate tests.

5.2.6 Froth Column

Froth can be defined as a three-phase structure consisting of solid, liquid and air. Figure 5- 22 illustrates the maximum froth height and froth stability for 3, 6 and 12% galena feed grade, under the 3SPW and 10SPW. The foam results presented in Section 5.1.6 for the pyrite-based synthetic ore is of relevance to the galena-based synthetic ore as well, as the foam results does not contain any minerals. Maximum froth height and froth stability are represented by the light blue and dark blue bars for all the galena feed grades investigated. Generally, for each galena feed grade, froth height (light blue bars) and froth stability (dark blue bars) increased with increasing ionic strength of plant water from 3SPW to 10SPW. The highest froth stability and froth height for the 3, 6 and 12% were 5.06 s and 9 cm, 3.06 s and 5 cm, and 2.32 s and 4 cm, respectively. These values were all observed at 10SPW. Furthermore, this illustrates that for the 10SPW, there was a decrease in froth stability and froth height as the galena feed grade was increased from 3, 6 to 12%. The same trend was observed under the 3SPW, with froth stability and froth height in the order 12% < 6% < 3%.

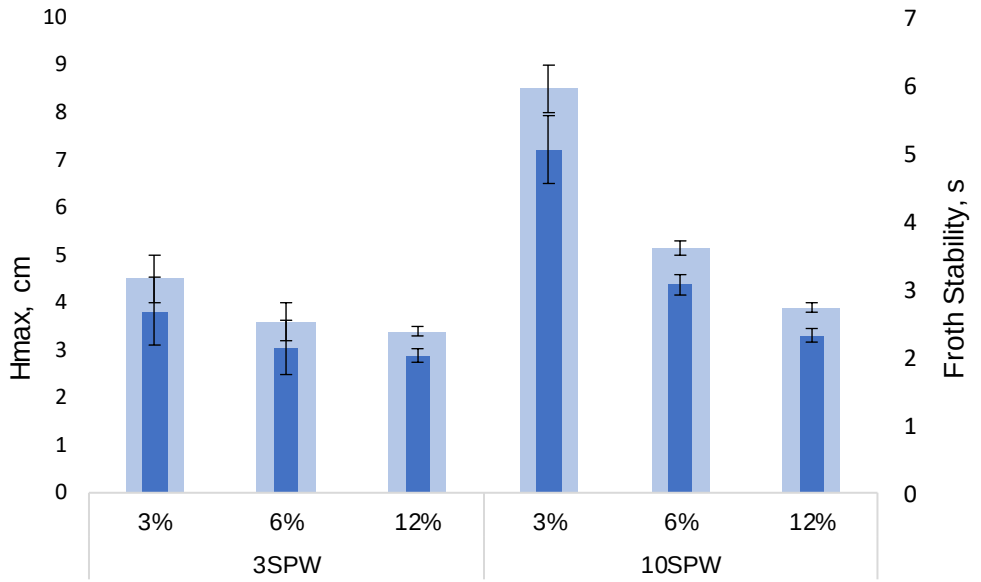

Figure 5- 22: Maximum froth height and froth stability for 3, 6 and 12% galena feed, under 3 and 10SPW, respectively. Reagents used include 150 g/t SIBX collector and 40 g/t Dow200 frother. The error bars included in the figure represent the standard error between duplicate tests.

5.2.7 Total Gangue Recoveries

Figure 5- 23 illustrates the total gangue vs. water recovered for 3, 6 and 12% galena feed under 3SPW and 10SPW, for 500 g/t CMC depressant dosages. The intention of the results presented in this section was to show entrainment; a non-selective process responsible for the recovery of both valuable and unwanted gangue mineral particles reporting to the concentrate. Generally, the rate of recovery of the total gangue recovered (per unit water) increased with increasing galena feed grade. Total gangue recovered increased with increasing galena feed grade, as illustrated predominantly by the grey curves at the top of the graph, with total gangue recovered increasing in the order 3% (blue) < 6% (orange) < 12% (grey). Cumulative water recovered decreased with increasing galena feed grade for both 3SPW (solid curves) and 10SPW (dashed curves), with water recovered decreasing in the order 3% (blue) < 6% (orange) <12% (grey). The total gangue and water recovered increased with increasing ionic strength from 3SPW to 10SPW as illustrated by the dashed lines falling above their solid counterparts in most cases. The results illustrated suggest that not all the Naturally Floating Gangue (NFG) was completely depressed at 500 g/t CMC depressant dosage. The CMC depressant dosage was increased to 700 and 800 g/t as illustrated by Figure 5- 24. The figure clearly illustrates similar trends and proves that not all the NFG was completely depressed at depressant dosages greater than 500 g/t, and thus for the synthetic ores considered in this investigation, an entrainment factor was not achieved.

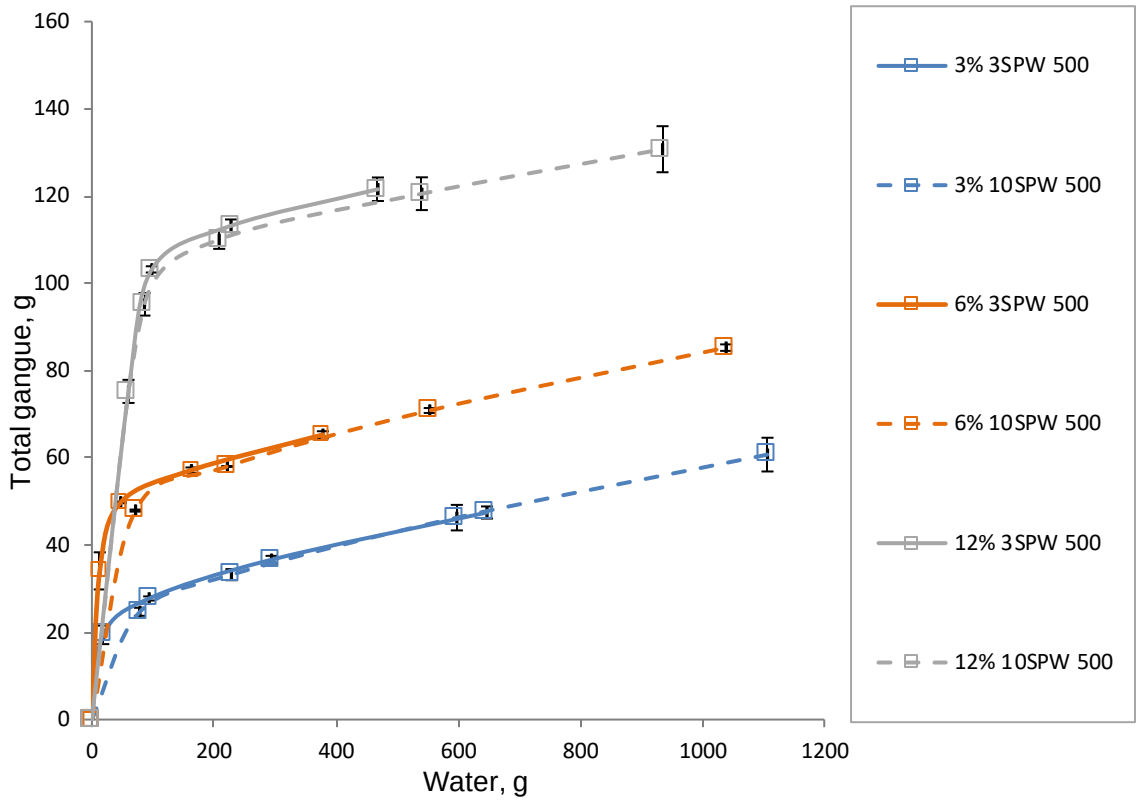

Figure 5- 23: Total gangue vs. water recovered for 3, 6 and 12% galena feed, under 3 and 10SPW, for 500 g/t CMC depressant dosages, respectively. The error bars included in the figure represent the standard error between duplicate tests.

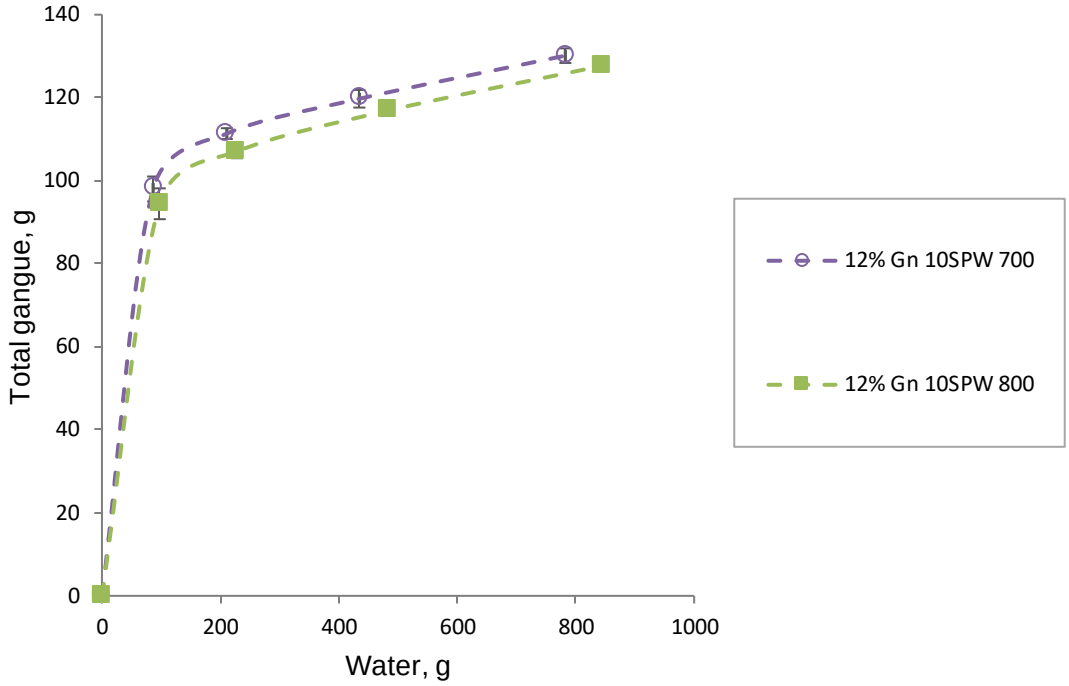

Figure 5- 24: Total gangue vs. water recovered for 12% galena feed, under 10SPW, for 700 and 800 g/t CMC depressant dosages, respectively. The error bars included in the figure represent the standard error between duplicate tests.

5.3 Determination of Batch Flotation Kinetics Using the Classical Model

Presented in this section are the flotation kinetics parameters of the batch flotation tests carried out in this investigation, subject to varying ore feed sulphide grade, ionic strength of plant water and depressant dosage. The classical first order kinetics model, as represented by Equation 2, was fitted to the experimental data to investigate the effects of varying ore feed sulphide grade, ionic strength of plant water and depressant dosage on flotation performance. The classical first order kinetics model is represented by the following equation:

$$R = R_{max}\left(1 - e^{-kt}\right) \qquad \text{Equation 2}$$

The equation allows for the possibility of isolating R_{max} and k and see how they were individually affected by changes in variables considered.

5.3.1 Classical Model for Pyrite

Presented in this section are the flotation kinetics parameters obtained from the batch flotation tests of the pyrite-based synthetic ore.

5.3.1.1 Classical First Order Model for Fe under 3, 6 and 12% Pyrite Feed Grade

Figure 5- 25 illustrates the fitted kinetic models of the cumulative Fe recovery vs time for 3, 6 and 12% pyrite feed grade, under 3 and 10SPW, for 0, 100 and 500 g/t CMC depressant dosages. A total of ten fitted kinetic models were obtained from the experimental batch flotation data of the pyrite-based synthetic ore. Figure 5- 25 does not clearly illustrate which kinetic models correspond to which pyrite

feed grade and hence for better clarity and depiction of the kinetics models to their respective pyrite feed grades, the three pyrite feed grades are illustrated on separate figures; Figure 5- 26, Figure 5- 27 and Figure 5- 28, which correspond to the fitted kinetics models for the 3, 6 and 12% pyrite feed grade, respectively.

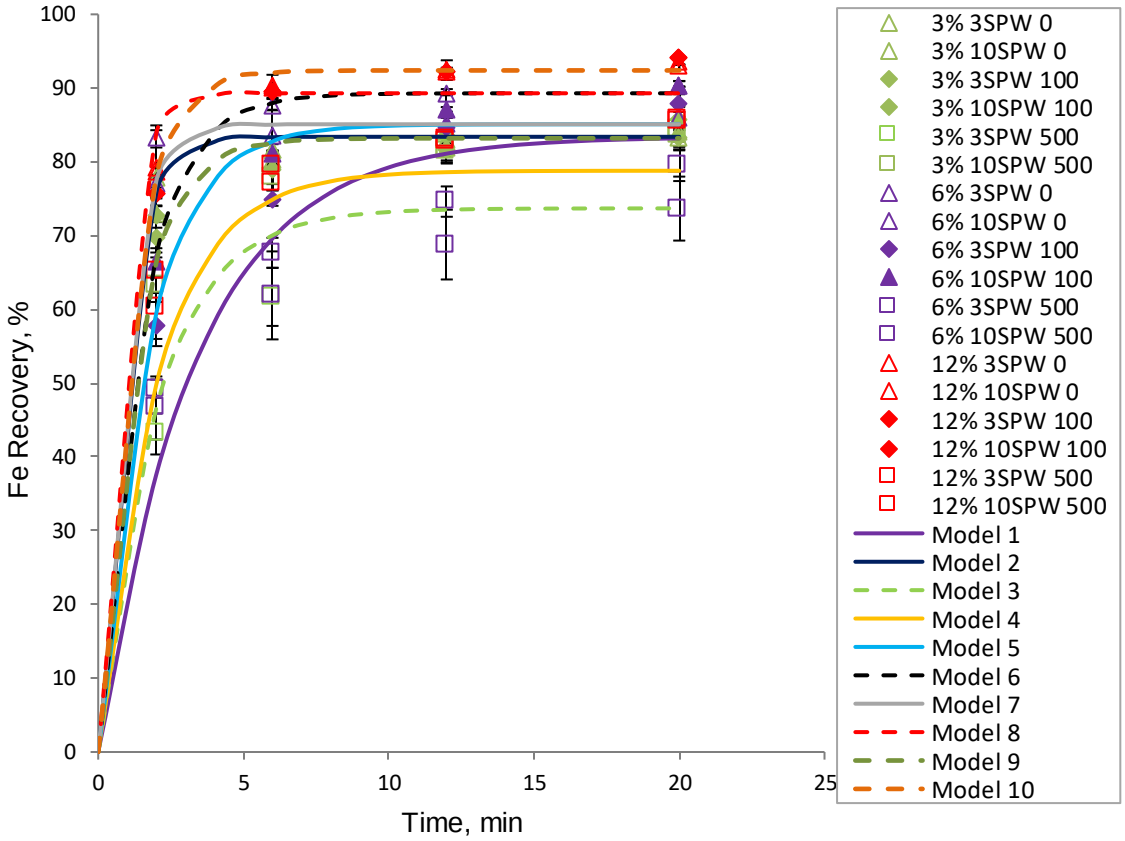

Figure 5- 25: Cumulative Fe recovery vs Time for the fitted kinetics model, for 3, 6 and 12% pyrite feed under 3 and 10SPW, for 0, 100 and 500 g/t CMC depressant dosages. The error bars included in the figure represent the standard error between duplicate tests.

5.3.1.2 Classical First Order Model for Fe under 3% Pyrite Feed Grade

Figure 5- 26 illustrates the fitted kinetic models of the cumulative Fe recovery vs time for 3% pyrite feed grade, under 3 and 10SPW, for 0, 100 and 500 g/t CMC depressant dosages. Two fitted kinetic models were obtained from the experimental batch flotation data under this pyrite feed grade. The figure illustrates that flotation rate of Fe for this pyrite feed grade increased from slowest to fastest in the order Model 1 < Model 2, and this corresponds to test runs 3% 3SPW 500 < 3% 3SPW 0 and 100 = 3% 10SPW 0,100 and 500.

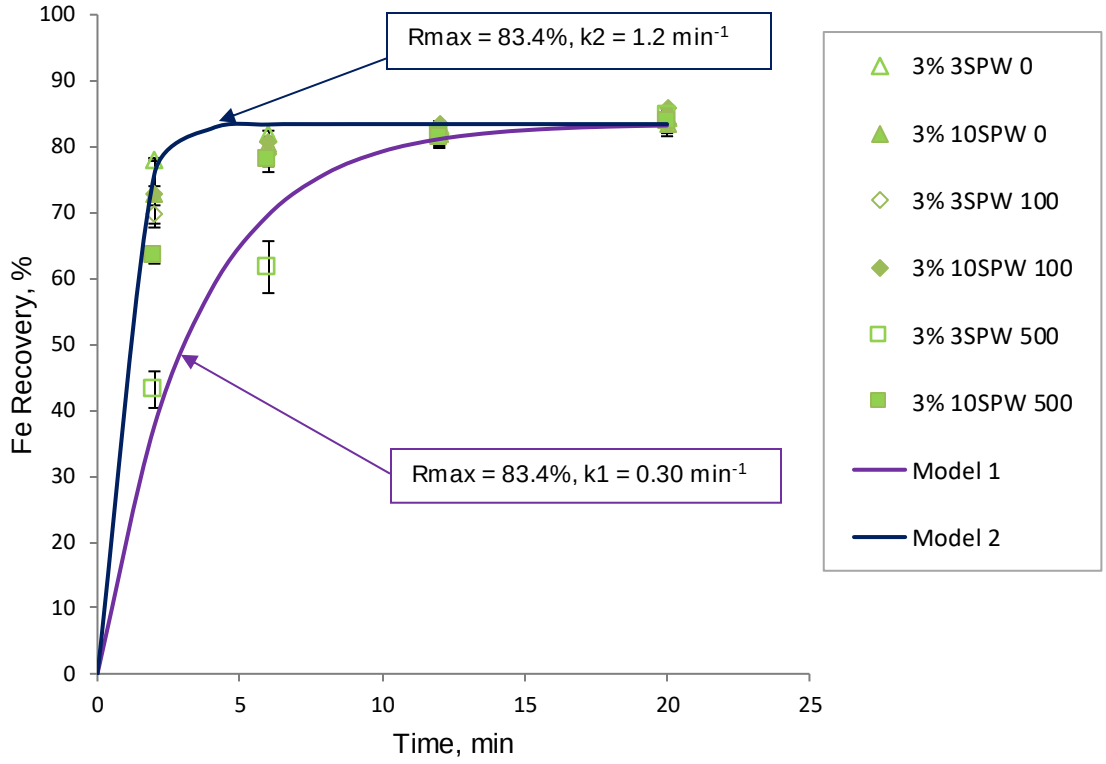

Figure 5- 26: Cumulative Fe recovery vs Time for the fitted kinetics model, for 3% pyrite feed under 3 and 10SPW, for 0, 100 and 500 g/t CMC depressant dosages. The error bars included in the figure represent the standard error between duplicate tests.

5.3.1.3 Classical First Order Model for Fe under 6% Pyrite Feed Grade

Figure 5- 27 illustrates the fitted kinetic models of the cumulative Fe recovery vs time for 6% pyrite feed grade, under 3 and 10SPW, for 0, 100 and 500 g/t CMC depressant dosages. Six fitted kinetic models were obtained from the experimental batch flotation data under this pyrite feed grade. The figure illustrates that flotation rate of Fe for this pyrite feed grade increased from slowest to fastest in the order Model 3< Model 4 < Model 5 < Model 6 < Model 7 < Model 8, and this corresponds to test runs 6% 10SPW 500 < 6% 3SPW 500 < 6% 3SPW 100 < 6% 10SPW 100 < 6% 3SPW 0 < 6% 10SPW 0.

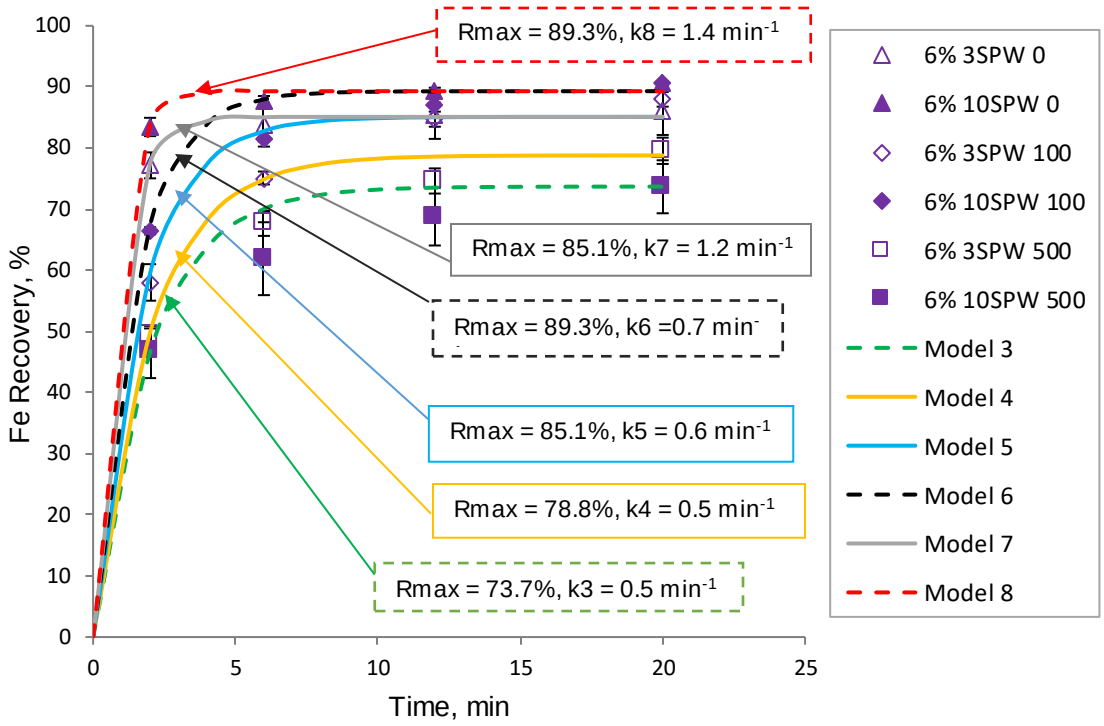

Figure 5- 27: Cumulative Fe recovery vs Time for the fitted kinetics model, for 6% pyrite feed under 3 and 10SPW, for 0, 100 and 500 g/t CMC depressant dosages. The error bars included in the figure represent the standard error between duplicate tests.

5.3.1.4 Classical First Order Model for Fe under 12% Pyrite Feed Grade

Figure 5- 28 illustrates the fitted kinetic models of the cumulative Fe recovery vs time for 12% pyrite feed grade, under 3 and 10SPW, for 0, 100 and 500 g/t CMC depressant dosages. Two fitted kinetic models were obtained from the experimental batch flotation data under this pyrite feed grade. The figure illustrates that flotation rate of Fe for this pyrite feed grade increased from slowest to fastest in the order Model 9 < Model 10, and this corresponds to test runs 12% 3SPW 500 = 12% 10SPW 500 < 12% 3SPW 0 = 12% 3SPW 100 = 12% 10SPW 0 = 12% 3SPW 100.

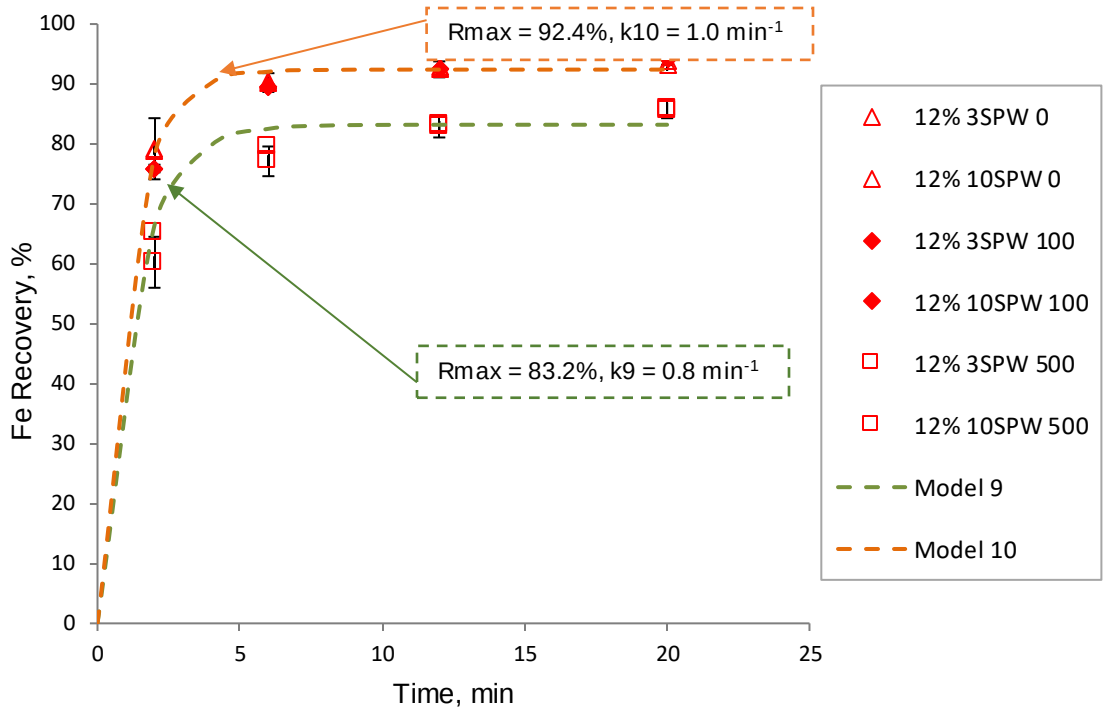

Figure 5- 28: Cumulative Fe recovery vs Time for the fitted kinetics model, for 12% pyrite feed under 3 and 10SPW, for 0, 100 and 500 g/t CMC depressant dosages. The error bars included in the figure represent the standard error between duplicate tests.

5.3.1.5 Summary of Fe Flotation Kinetics

Table 5- 1 shows the detailed R_{max} and k values obtained from the kinetics models of the pyrite-based synthetic ore's batch flotation tests. The flotation rate constants of Fe for the 3, 6 and 12% pyrite feed grade fall within the range 0.30 – 1.4 min^{-1}. The lowest (0.30 min^{-1}) flotation rate of Fe correspond to 3% pyrite feed grade, under 3SPW for 500 g/t CMC depressant dosage. The highest (1.4 min^{-1}) flotation rate of Fe correspond to 6% pyrite feed grade, under 10SPW for 0 g/t CMC depressant dosage. This is graphically illustrated in Figure 5- 25

Table 5- 1: A summary of the flotation kinetics rate constant (k) and maximum recovery (R_{max}) for Fe.

IRON (Fe)					
Ore feed sulphide grade (%)	**Plant water type (SPW)**	**Depressant (g/t)**	**R_{max} (%)**	**k (min^{-1})**	**Model number**
3	3SPW	0 100 500	83.4	1.2 1.2 0.30	2 2 1
	10SPW	0 100 500	83.4	1.2	2
6	3SPW	0 100 500	85.1 85.1 78.8	1.2 0.6 0.5	7 5 4
	10SPW	0 100 500	89.3 89.3 73.7	1.4 0.7 0.5	8 6 3
	3SPW	0	92.4	0.93	10

12		100 500	92.4 83.2	0.93 0.8	10 9
	10SPW	0 100 500	92.4 92.4 83.2	0.93 0.93 0.8	10 10 9

5.3.2 Classical Model for Galena

Presented in this section are the flotation kinetics parameters obtained from the batch flotation tests of the galena-based synthetic ore.

5.3.2.1 Classical First Order Model for Pb under 3,6 and 12% Galena Feed Grade

Figure 5- 29 illustrates the fitted kinetic models of the cumulative Pb recovery vs time for 3, 6 and 12% galena feed grade, under 3 and 10SPW, for 0, 100 and 500 g/t CMC depressant dosages. A total of six fitted kinetic models were obtained from the experimental batch flotation data of the galena-based synthetic ore. Generally, the figure does not clearly illustrate which kinetic models corresponds to which galena feed grade, and hence for better clarity and depiction of the kinetic models to their respective galena feed grades, the three galena feed grades are illustrated on separate figures; Figure 5- 30, Figure 5- 31 and Figure 5- 32, which corresponds to the fitted kinetics models for the 3, 6 and 12% galena feed grade, respectively.

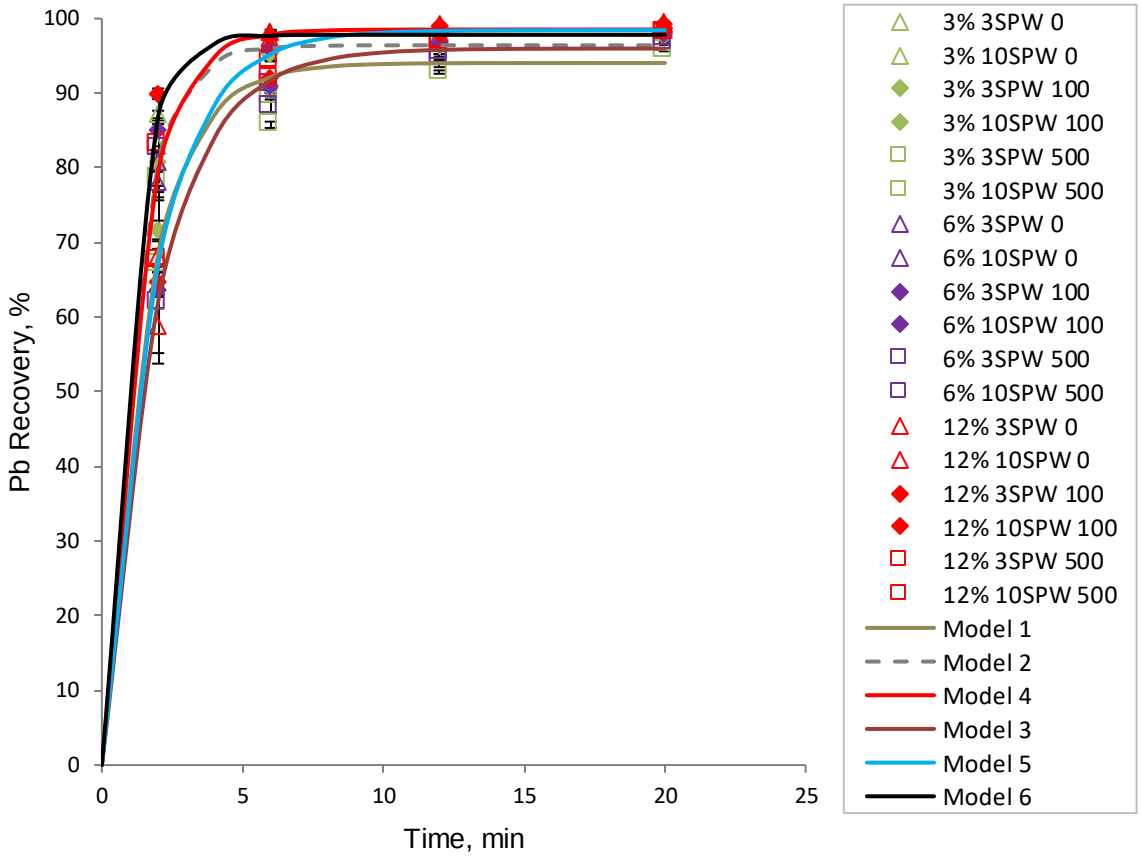

Figure 5- 29: Cumulative Fe recovery vs Time for the fitted kinetics model, for 3,6 and 12% galena feed under 3 and 10SPW, for 0, 100 and 500 g/t CMC depressant dosages. The error bars included in the figure represent the standard error between duplicate tests.

5.3.2.2 Classical First Order Model for Pb under 3% Galena Feed Grade

Figure 5- 30 illustrates the fitted kinetic models of the cumulative Pb recovery vs time for 3% galena feed grade, under 3 and 10SPW, for 0, 100 and 500 g/t CMC depressant dosages. Two fitted kinetic models were obtained from the experimental batch flotation data under this galena feed grade. The figure illustrates that the flotation rate of Pb for this galena feed grade increased from slowest to fastest in the order Model 1 < Model 2, and this corresponds to test runs 3% 3SPW 100 = 3% 3SPW 500 < 3% 3SPW 0 = 3% 10SPW 0, 100 and 500.

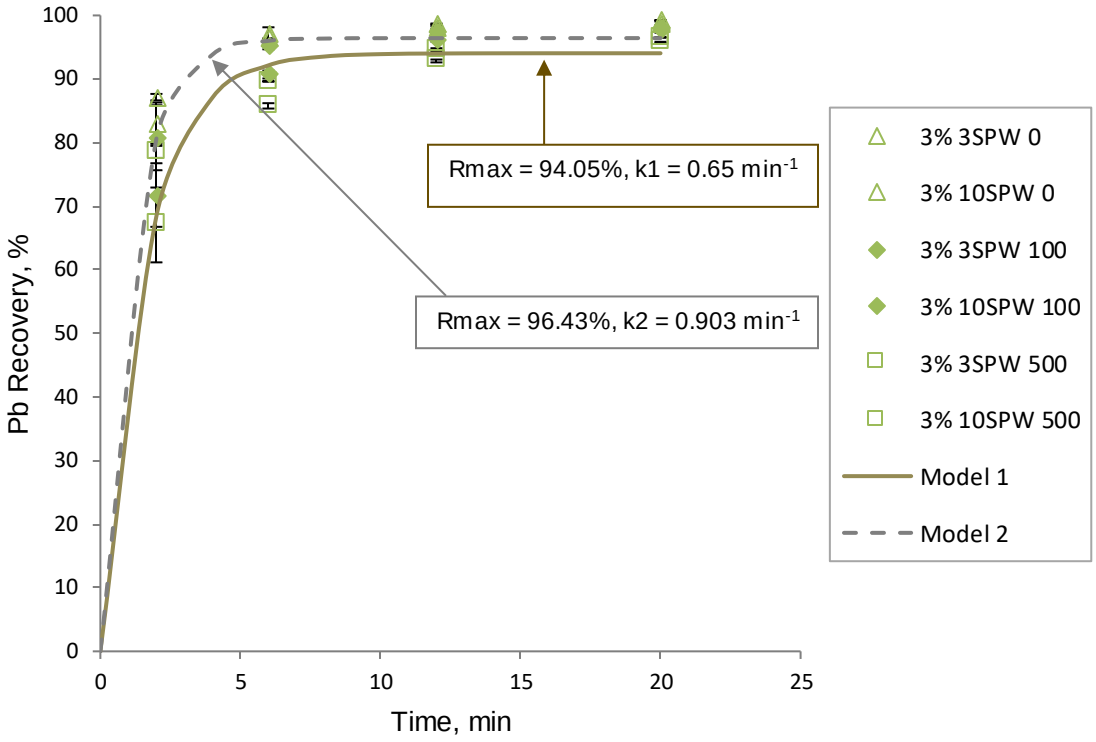

Figure 5- 30: Cumulative Fe recovery vs Time for the fitted kinetics model, for 3% galena feed under 3 and 10SPW, for 0, 100 and 500 g/t CMC depressant dosages. The error bars included in the figure represent the standard error between duplicate tests.

5.3.2.3 Classical First Order Model for Pb under 6% Galena Feed Grade

Figure 5- 31 illustrates the fitted kinetic models of the cumulative Pb recovery vs time for 6% galena feed grade, under 3 and 10SPW, for 0, 100 and 500 g/t CMC depressant dosages. Two fitted kinetic models were obtained from the experimental batch flotation data under this galena feed grade. The figure illustrates that the flotation rate of Pb for this galena feed grade increased from slowest to fastest in the order Model 3 < Model 4, and this corresponds to test runs with 6% 3SPW 100 = 6% 3SPW 500 < 6% 3SPW 0 = 6% 10SPW 0,100 and 500.

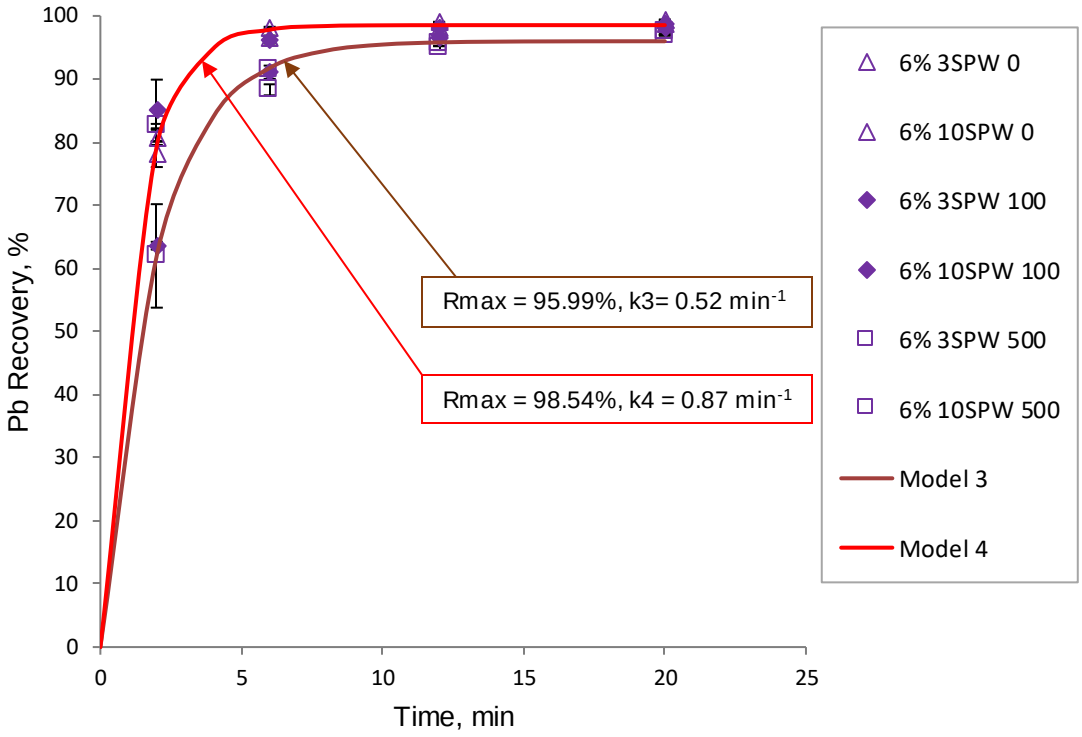

Figure 5- 31: Cumulative Fe recovery vs Time for the fitted kinetics model, for 6% galena feed under 3 and 10SPW, for 0, 100 and 500 g/t CMC depressant dosages. The error bars included in the figure represent the standard error between duplicate tests.

5.3.2.4 Classical First Order Model for Pb under 12% Galena Feed Grade

Figure 5- 32 illustrates the fitted kinetic models of the cumulative Pb recovery vs time for 12% galena feed grade, under 3 and 10SPW, for 0, 100 and 500 g/t CMC depressant dosages. Two fitted kinetic models were obtained from the experimental batch flotation data under this galena feed grade. The figure illustrates that the flotation rate of Pb for this galena feed grade increased from slowest to fastest in the order Model 5< Model 6, and this corresponds to test runs 12% galena 3SPW for 0,100 and 500 = 12% 10SPW 0 < 12% 10SPW 100 = 12% 10SPW 500.

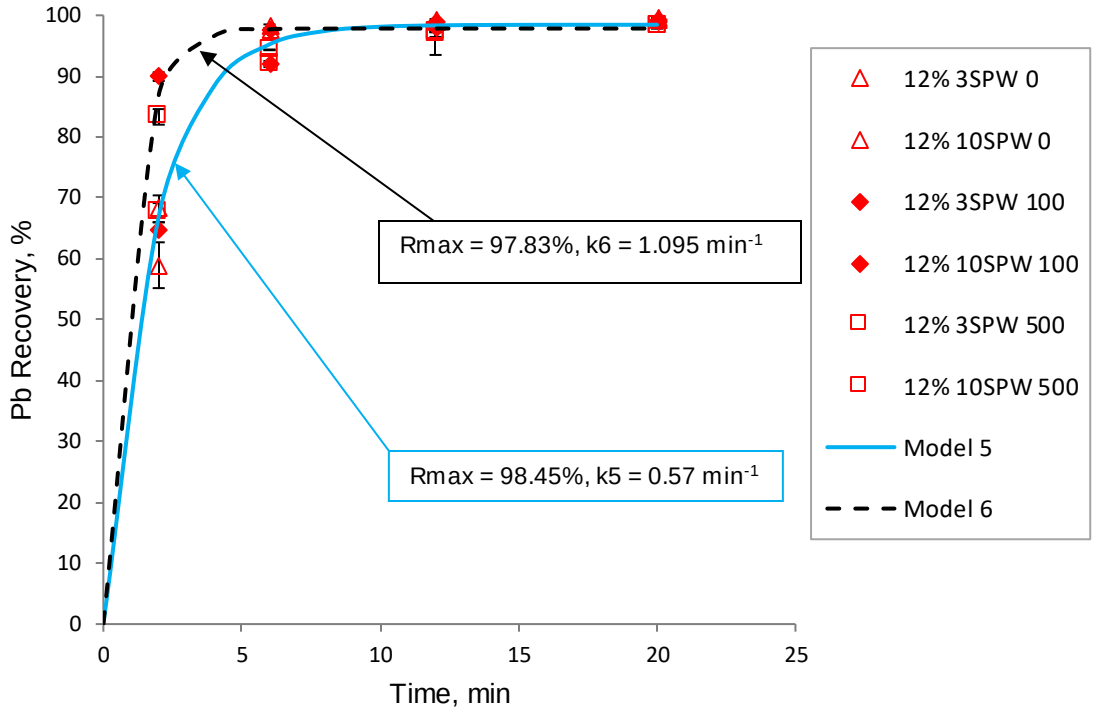

Figure 5- 32: Cumulative Fe recovery vs Time for the fitted kinetics model, for 12% galena feed under 3 and 10SPW, for 0, 100 and 500 g/t CMC depressant dosages. The error bars included in the figure represent the standard error between duplicate tests.

5.3.2.5 Summary of Pb Flotation Kinetics

Table 5- 2 shows the detailed R_{max} and k values obtained from the kinetic models of the galena-based synthetic ore's batch flotation tests. The flotation rate constants of Pb for the 3, 6 and 12% galena feed grade fall within the range 0.52 – 1.095 min^{-1}. The lowest (0.52 min^{-1}) flotation rate of Pb corresponds to 6% galena feed grade under 3SPW, for 100 and 500 g/t, while the highest (1.095 min^{-1}) flotation rate of Pb corresponds to 12% galena feed grade, under 10SPW, for 100 and 500 g/t CMC depressant dosage. This is graphically illustrated in Figure 5- 29.

Table 5- 2: A summary of the flotation kinetics rate constant (k) and maximum recovery (R_{max}) for Pb.

Lead (Pb)					
Ore feed sulphide grade (%)	**Plant water type (SPW)**	**Depressant (g/t)**	**R_{max} (%)**	**k (min^{-1})**	**Model number**
3	3SPW	0	96.43	0.903	2
		100	94.05	0.65	1
		500	94.05	0.65	1
	10SPW	0	98.47	0.903	
		100	97	0.903	2

		500	93.83	0.903	
6	3SPW	0	98.54	0.82	4
		100	95.99	0.52	3
		500	95.99	0.52	3
	10SPW	0	98.54	0.82	
		100	98.54	0.82	4
		500	98.54	0.82	
12	3SPW	0	98.45	0.57	
		100	98.45	0.57	5
		500	98.45	0.57	
	10SPW	0	98.45	0.57	5
		100	97.83	1.095	6
		500	97.83	1.095	6

Chapter 6. Discussion

The aim of this study was to investigate the impact of varying ore feed grade on froth stability, entrainment and flotation performance under varying water qualities. The key indicators evaluated for the flotation performance include; (i) solids and water recovery, (ii) foam and froth stability, (iii) valuable mineral recovery and concentrate grade. Two synthetic ore types were considered; pyrite-based synthetic ore, where pyrite was the valuable mineral, and galena-based synthetic ore, where galena was the valuable mineral. The ores were investigated in the presence of SIBX, CMC and a Dow 200 frother. Water quality was defined by varying the ionic strength of synthetic plant water (Wiese et al., 2005) over two levels, 3SPW and 10SPW. Owing to the interactive effects which may be present in the sub-processes of flotation, interpretation of the flotation response can be complex (Bradshaw et al., 2005b). To achieve the objectives of this study, various tests were conducted as outlined and evaluated in Chapter 4. Chapter 6 presents a critical discussion of the results presented in Chapter 5 in the context of available literature, and in view of the hypothesis and key questions outlined in Chapter 3. The key questions of this study were:

(i) What effect does varying the ore feed grade have on froth stability and flotation performance?
(ii) How does a simultaneous change in ore feed grade and ionic strength of plant water affect froth stability and flotation performance?
(iii) How does a combination of varying ore feed grade and ionic strength of plant water affect gangue recovery?
(iv) What effect does varying the ore feed grade have on pulp chemistry as measured by Eh, pH, DO, EC and TDS?

Considering that these key questions were put forward for both synthetic ores, Chapter 6 therefore presents the findings of this study in view of each ore, such that for each key question a critical discussion will be presented for the pyrite and galena systems.

6.1 Effect of varying ore feed grade on froth stability and flotation performance?

6.1.1 Pyrite System

The findings of this study showed that as the pyrite feed grade increased, solids and water reporting to the concentrate increased with ionic strength of plant water at all depressant dosages. This may have been primarily due to the increased hydrophobic component in the ore as the pyrite feed grade was increased. Depending on the type of mineral present and water chemistry, the floatability of sulphide minerals may decrease or increase in the presence of inorganic electrolytes (Slatter et al., 2009). Studies have shown that high concentrations of inorganic electrolytes stabilise the froth (Dzingai et al., 2020, Corin and Wiese, 2014, Manono et al., 2012, Corin et al., 2011) and attributed this to bubble size reduction and retardation of bubble coalescence when there are high amounts of dissolved inorganic electrolytes in solution (Manono et al., 2012). Klassen and Mokrousov (1963) attributed this to the fact that inorganic electrolytes reduce the surface hydration of naturally hydrophobic minerals and provide attractive forces between the mineral particles and air bubbles. Dishon et al. (2009) postulated that naturally hydrophobic minerals have specific cation adsorptions at high ionic strength of solution, which may change the surface charge of the mineral particles and yield strong attractive forces between the mineral particles. Chapter 5 (Figure 5- 3 and Figure 5- 4) illustrated that, as the ionic strength of plant water was increased, the amount of solids and water reporting to the concentrate increased with the pyrite feed grade at all depressant dosages. This could be a result of two factors; (i) increased ionic

strength of plant water increases surface tension at the air liquid interface, generating smaller and more stable bubbles with increased surface area. These bubbles carry more water and therefore more solids. (ii) the increase in the concentration of the valuable hydrophobic mineral (pyrite) reporting to the froth phase as pyrite feed grade was increased. These two factors may have had a direct effect on one another and the stability of the froth.

The primary role of a depressant is to prevent the flotation of naturally floatable gangue (NFG) by adsorbing onto the NFG surface and thus rendering the minerals hydrophilic (Bradshaw et al., 2005a, Steenberg and Harris, 1984, Shortridge et al., 1999). Changes in ionic strength of plant water and pulp pH have been shown to affect the adsorption strength of polymeric depressants such as CMC (Wang et al., 2005, Khraisheh et al., 2005, Bicak et al., 2007, Parolis et al., 2008). In this study, the amount of solids and water reporting to the concentrate decreased with increasing CMC depressant dosage at each pyrite feed grade and synthetic plant water type. This decrease varied with ionic strength of plant water at each pyrite feed grade as illustrated in Figure 5- 3 and Figure 5- 4. Furthermore, since plant water of higher ionic strength 10SPW, recovered more solids than the plant water of lower ionic strength, 3SPW, the depressant action at 10SPW was not the same as that at 3SPW when the same depressant dosage was used. Studies have shown that the amount of inorganic electrolytes in the flotation system have an effect on the degree to which CMC and guar depressed the floating gangue (Corin et al., 2011, Manono et al., 2012). The decrease in water recovery with an increase in depressant dosage at each pyrite feed grade indicates a reduction in froth stability. This is owing to the removal of the NFG froth stabilising talc (Wiese et al., 2011, Bradshaw et al., 2005b, Steenberg and Harris, 1984, Shortridge et al., 1999, Corin et al., 2011).

In this study, two-phase foam stability tests were conducted using a laboratory froth column to quantify the effect of the ionic strength of plant water on foam height and foam stability. Knowledge of two-phase (liquid and air bubbles) foams can be used to describe three phase systems (solid, liquid and air bubbles). Corin et al. (2011) showed that the increase in froth stability in the presence of solids (three-phase) can be directly related to the increase in the two-phase foam stability of the frother rather than any changes in the hydrophobicity of the solid particles entering the froth. The findings of this study showed that as the ionic strength of synthetic plant water was increased from 3SPW to 10SPW, foam height and foam stability increased as illustrated in Figure 5- 10. This indicates that the amount of inorganic electrolytes in solution enhanced the foam stability or foamability of the flotation system. It has been reported that high concentrations of inorganic electrolytes stabilise the froth (Dzingai et al., 2020, Corin and Wiese, 2014, Manono et al., 2012, Corin et al., 2011) and this is owing to bubble size reduction and retardation of bubble coalescence when there are high amounts of dissolved inorganic electrolytes in solution (Manono et al., 2012). Furthermore, the surfactant used for conducting these tests was a polyglycol ether, Dow 200, which is non-ionic, and its dosage was fixed at 40 g/t, therefore its performance could not have been significantly affected by the inorganic electrolyte changes as the ionic strength of plant water was increased. Section 5.1.7 (Chapter 5) evaluated the froth height and froth stability of the pyrite-based synthetic ore. The findings showed a concurrent increase in froth height and froth stability as the ionic strength of synthetic plant water was increased at all pyrite feed grades. This complemented the 2-phase foam stability findings evaluated in Section 5.1.6 (Chapter 5). This can be attributed to the increased amount of inorganic electrolytes in solution as the ionic strength of synthetic plant water was increased; which increased the surface tension at the air liquid interface, generating smaller and more stable bubbles with increased surface area. These bubbles carry more water and therefore more solids. These findings are in agreement with previous studies (Dzingai et al., 2020, Manono et al., 2018, Manono et al., 2012, Corin et al., 2011). It is unclear as to why the foam height and dynamic froth stability data does not correlate with the batch flotation data when varying the pyrite feed grade at each synthetic plant water type.

Figure 5- 7 in Chapter 5 evaluated the final concentrate grades and recoveries and showed that the final Fe recoveries were generally within similar ranges for each pyrite feed grade; ~ 80 to 85% for the 3%; ~ 86 to 90% for the 6%; ~ 84 to 94% for the 12%. The changes in final Fe recoveries were minimal and generally not affected by neither varying pyrite feed grade nor ionic strength of plant water nor depressant dosage. The final Fe grades increased at all depressant dosages and synthetic plant water types as the pyrite feed grade was increased. This can be attributed to the increased pyrite concentration as the pyrite feed was increased. As the ionic strength of plant water was increased, final Fe grades increased with pyrite feed grade at all depressant dosages. This increase could be owing more to the increased sulphide mineral (pyrite) concentration as the pyrite feed was increased, and less to do with increased amount of inorganic electrolytes in the system. The reason for this postulation is owing to the fact that increasing the ionic strength of plant water type at each pyrite feed grade, led to a decrease in final Fe grades at all depressant dosages as illustrated in Figure 5- 7. Thus, increasing ionic strength of plant water may have an indirect effect on the final Fe grades in the flotation system.

Final Fe grades increased in conjunction with an increase in depressant dosage at each pyrite feed grade for both synthetic plant water types. This is owing to the reduction in the amount of NFG reporting to the concentrate (Corin et al., 2011, Wiese et al., 2011, Bradshaw et al., 2005b, Steenberg and Harris, 1984) , thus less dilution of the grade. The highest final grade for each pyrite feed grade was; ~27% for 3%; ~34% for the 6%; ~ 35% for the 12%. This showed that the increase in Fe grades was not directly proportional to the pyrite feed grade. Furthermore, this showed that generally, the highest Fe grades were obtained at a CMC dosage of 500g/t, under 3SPW, and this is owing to a reduction in entrainment of the NFG reporting to the concentrate (which dilutes the grade) and thus results in a reduction in froth stability (Corin et al., 2011, Wiese et al., 2011, Wiese and Harris, 2012, Bradshaw et al., 2005b). Vianna (2004) showed that maximum recovery of sulphide minerals can be achieved in the absence of a depressant at a collector coverage of about 20%. In this study, the collector was added prior to milling, and the depressant was added to the flotation system post milling. Thus, assuming homogenous collector surface coverage on the surface of the sulphide minerals, interference of the depressant with the hydrophobic sulphide mineral surfaces and collector adsorption would not be expected. However, the findings of this study showed that there was a reduction in sulphide mineral recovery at high depressant dosage (500 g/t). This may be indicative of some CMC adsorption onto the hydrophobic sulphide mineral pyrite, and this affected the floatability of the minerals at high depressant concentrations.

The majority of the Fe reporting to the concentrate was recovered within the first 2 minutes for each pyrite… feed grade as illustrated in Figure 5- 5, thus indicating that the flotation rate of Fe was highest/fastest in the first concentrate (C1) across all feed grades and this was achieved with about 200g utilization of synthetic plant water. The fitted kinetic models as evaluated in section 5.3.1 showed a range of flotation rate constants for each pyrite feed grade, with the lowest flotation rate constant 0.30 min^{-1} corresponding to 3% pyrite feed, and the highest flotation rate constant 1.4 min^{-1} corresponding to 6% pyrite feed grade. The lowest flotation rate constant of Fe was obtained under 3SPW while the highest flotation rate constant of Fe was obtained under 10SPW. Ionic strength of plant of plant water may have also influenced the flotation rate of Fe such that the rate constant increased as the amount of inorganic electrolytes in solution increased.

In an attempt to differentiate the entrained from floating gangue, this study considered the UCT high depressant method. The method assumes that at a high depressant dosage (>300 g/t), all floatable gangue is depressed and any gangue reporting to the concentrate is owing to entrainment (Corin et al., 2011, Wiese and Harris, 2012, Wiese, 2009). Studies have shown that the amount of entrained material reporting to the concentrate is directly proportional to water recoveries (Ekmekçi et al., 2003, Yang and

Aldrich, 2006, Boylu and Laskowski, 2007). As illustrated by Figure 5- 12 and Figure 5- 24, the findings showed that the proposed method could not quantify entrainment for the synthetic ores used in this study. Not all the NFG was completely depressed at dosages higher that 500 g/t. It should be noted that the ores used in this study was synthetic and the minerals were fully liberated, unlike real ores for which the UCT high depressant method was successful in quantifying entrainment. The rate of recovery of the total gangue per unit water generally increased with pyrite feed grade at all synthetic plant water types. Total gangue and water recovery increased with an increase in pyrite feed grade at all synthetic plant water types. Furthermore, an increase in ionic strength of plant water led to an increase in the total amount of gangue reporting to the concentrate as the pyrite feed grade was increased. This can be attributed to the NFG that reported to the concentrate via true flotation even at depressant dosages greater than 500 g/t as shown in Figure 5- 24. Although an entrainment factor could not be obtained in this study, other studies have shown that the amount of NFG was reduced to almost zero when the depressant dosage was increased to 300 g/t (Ekmekçi et al., 2003, Wiese et al., 2007); and increasing the dosage further to 500 g/t ensured that no NFG was recovered, thereby allowing for the determination of an entrainment factor (Corin et al., 2011). These studies, for which the UCT high depressant method was successful in quantifying entrainment, made use of a real ore (e.g. Merensky), whereas the ores in this study were synthetic ore with fully liberated minerals. It thus could be that the UCT high depressant method is ore specific and not necessarily applicable to all ores.

6.1.2 Galena System

The findings of this study showed that as the galena feed grade increased, solids reporting to the concentrate increased at all depressant dosages for each synthetic plant water type, while the opposite was true with water recovery, i.e. water reporting to the concentrate decreased at all depressant dosages for each synthetic plant water type as the galena feed grade was increased. This increase in solids recovery is attributed primarily to the increased hydrophobic component (galena) in the ore as the galena feed grade was increased, while the decrease in water recovery could be owing to; (i) the floatability of the sulphide mineral, galena, being affected by the inorganic electrolytes in solution. (ii) galena being highly hydrophobic (Prestidge and Ralston, 1996, Prestidge and Ralston, 1995, Kocabag et al., 1990), may have destabilised the bubbles and thereby froth stability as indicated by the decrease in water recoveries. Water recovery has been reported to be a good indicator of froth stability as stable froths tend to correspond to an increase in water recovery (Wiese and Harris, 2012). Studies have shown that depending on the type of mineral present and water chemistry, the floatability of sulphide minerals may increase or decrease in the presence of inorganic electrolytes (Slatter et al., 2009), and hence it may have decreased in the case of galena. It could be that there was a destabilisation of the bubbles in the froth phase owing to galena being highly hydrophobic, such that this led to a decrease in water recovery and thus froth stability. Studies have shown that high concentrations of inorganic electrolytes stabilise the froth (Dzingai et al., 2020, Corin and Wiese, 2014, Manono et al., 2012, Corin et al., 2011) and attributed this to bubble size reduction and retardation of bubble coalescence when there are high amounts of dissolved inorganic electrolytes in solution (Manono et al., 2012). Klassen and Mokrousov (1963) attributed this to the fact that inorganic electrolytes reduce the surface hydration of naturally hydrophobic minerals and provide attractive forces between the mineral particles and air bubbles. Dishon et al. (2009) postulated that naturally hydrophobic minerals have specific cation adsorptions at high ionic strength of plant water, which may change the surface charge of the mineral particles and yield strong attractive forces between the mineral particles. As illustrated in Figure 5- 15 and Figure 5- 16, an increase in the ionic strength of plant water led to an increase in the amount of solids and water reporting to the concentrate as the galena feed grade was increased at all depressant dosages. This may be attributed to two factors; (i) increased ionic strength of plant water increases surface tension at the air-liquid interface, generating smaller and more stable bubbles with increased surface area. These

bubbles carry more water and therefore more solids. (ii) the increase in the concentration of the valuable hydrophobic mineral (galena) reporting to the froth phase as galena feed grade was increased.

Changes in ionic strength of plant water and pulp pH have been shown to affect the adsorption strength of polymeric depressants such as CMC (Wang et al., 2005, Khraisheh et al., 2005, Bicak et al., 2007, Parolis et al., 2008). The primary role of a depressant is to prevent the flotation of naturally floatable gangue (NFG) by adsorbing onto the NFG surface and thus rendering the minerals hydrophilic (Bradshaw et al., 2005a, Steenberg and Harris, 1984, Shortridge et al., 1999). The amount of solids and water reporting to the concentrate decreased with an increase in CMC depressant dosage at each galena feed grade and synthetic plant water type. Figure 5- 15 and Figure 5- 16 illustrate that this decrease varied with ionic strength of plant water at each galena feed grade. Furthermore, since the amount of solids reporting to the concentrate was higher for the plant water of higher ionic strength, 10SPW, compared to the plant water of lower ionic strength, 3SPW, the depressant action at 10SPW was not the same as that at 3SPW when the same depressant dosage was used. Studies have shown that the amount of inorganic electrolytes in the flotation system affected the degree to which CMC and guar depressed the floating gangue (Manono, 2012, Corin et al., 2011). The decrease in water recovery with an increase in depressant dosage at each pyrite feed grade indicates a reduction in froth stability. This is owing to the removal of the NFG froth stabilising talc (Wiese et al., 2011, Bradshaw et al., 2005b, Steenberg and Harris, 1984, Shortridge et al., 1999, Corin et al., 2011).

In this study, two-phase foam stability tests were conducted using a laboratory froth column to quantify the effect of ionic strength on foam height and foam stability. Knowledge of two-phase foams can be used to describe three-phase systems (solid, liquid and air bubbles). Corin et al. (2011) showed that the increase in froth stability in the presence of solids (three-phase) can be directly related to the increase in the two-phase foam stability of the frother rather than any changes in the hydrophobicity of the solid particles entering the froth. The two-phase findings of this study were evaluated in Chapter 5 and showed that an increase in ionic strength of synthetic plant water from 3SPW to 10SPW, led to an increase in foam height and foam stability, as illustrated in Figure 5- 10. This indicated that the amount of inorganic electrolytes in solution enhanced the foam stability or foamability of the flotation system. Studies have shown that high concentrations of inorganic electrolytes stabilise the froth (Dzingai et al., 2020, Corin and Wiese, 2014, Manono et al., 2012, Corin et al., 2011) and attributed this to bubble size reduction and retardation of bubble coalescence when there are high amounts of dissolved inorganic electrolytes in solution (Manono et al., 2012). Furthermore, the surfactant used in this study was a polyglycol ether, Dow 200, which is non-ionic, therefore its performance could not have been significantly affected by the changes in inorganic electrolytes in solution when ionic strength of plant water was varied. Section 5.2.6 in Chapter 5 evaluated the froth height and froth stability of the galena-based synthetic ore. The findings showed a concurrent increase in froth height and froth stability as the ionic strength of synthetic plant water was increased at all galena feed grades. This can be attributed to the increased amount of inorganic electrolytes in the solution as the ionic strength of plant water was increased; which increased the surface tension at the air-liquid interface, generating smaller and more stable bubbles with increased surface area. These bubbles carry more water and therefore more solids (Dzingai et al., 2020, Manono et al., 2018, Manono et al., 2012, Corin et al., 2011). The findings of this study on the stability of the froth complemented the 2-phase foam stability findings evaluated in Section 5.1.6, Figure 5- 10. Froth height and froth stability decreased as the galena feed grade was increased at all synthetic plant water types as illustrated in Figure 5- 22. This may be attributed to two factors; (i) galena is a highly hydrophobic mineral and thus may have destabilised the bubbles as the galena concentration was increased, and this in turn led to a decrease in froth stability and froth height. (ii) Galena is known to have a high specific gravity of about 7.4 to 7.6, it could be that this affected the bubbles carrying capacity in the froth phase as the galena mineral particles encapsulated the bubbles;

such that as the concentration of the galena mineral particles increased, the chances of the mineral particles settling and draining through the plateau border was also increased, owing to their density, and this increased bubble rapture and thereby compromised froth stability as the galena feed grade was increased within each synthetic plant water type. Ata et al. (2003) reported that highly hydrophobic particles (Θ = 82°) were more capable of destabilising the froth than particles of moderate or intermediate hydrophobicity (Θ = 66°), and this may be the case with galena. It thus could be that the galena mineral particles may have been too hydrophobic and heavy for the bubbles to carry as the galena feed grade was increased. These findings are also consistent with the 3-phase froth stability results obtained from the batch flotation tests illustrated in Figure 5- 15 and Figure 5- 16.

The final Pb concentrate grades and recoveries were evaluated in Chapter 5 Figure 5- 19. The findings showed that the final Pb recoveries were within similar ranges of about 97 to 98% for all galena feed grades. This indicated that the final Pb recoveries were generally unaffected by varying either the galena feed grade or the ionic strength of plant water or depressant dosage. Pb grades increased at all depressant dosages and synthetic plant water types as the galena feed grade was increased. This may be attributed to the increased galena concentration as the galena feed was increased. As the ionic strength of plant water was increased, final Fe grades increased with galena feed grade at all depressant dosages. This increase can be attributed more to the increased sulphide mineral (galena) concentration as the galena feed grade was increased, and less to do with the increased amount of inorganic electrolytes in the system. The reason for this postulation is since increasing the ionic strength of plant water type at each galena feed grade, led to a decrease in final Pb grades at all depressant dosages as illustrated in Figure 5- 19. Therefore, increasing ionic strength may be having an indirect effect on the final Pb grades in the flotation system.

Final Pb grades increased in conjunction with an increase in depressant dosage at each galena feed grade for both synthetic plant water types. This is owing to the reduction in the amount of NFG reporting to the concentrate (Corin et al., 2011, Wiese et al., 2011, Bradshaw et al., 2005b, Steenberg and Harris, 1984) thus less dilution of the grade. The highest final Pb grade for each galena feed grade was; ~34% for 3%; ~47% for 6%; and ~ 50% for 12%. This showed that the increase in Pb grades was not directly proportional to the galena feed grade. Furthermore, these findings showed the highest Pb grades were obtained at a CMC dosage of 500 g/t, under 3SPW, and this is owing to a reduction in the entrainment of the NFG reporting to the concentrate (which dilutes the grade) and thus results in a reduction in froth stability (Corin et al., 2011, Wiese et al., 2011, Wiese and Harris, 2012, Bradshaw et al., 2005b). It was shown by Vianna (2004) that maximum recovery of sulphide minerals can be achieved in the absence of a depressant at a collector coverage of about 20%. In this study, the collector was added before milling, and the depressant was added to the flotation system post-milling. Thus, assuming homogenous collector surface coverage on the surface of the sulphide minerals, interference of the depressant with the hydrophobic sulphide mineral surfaces and collector adsorption would not be expected. However, the findings of this study showed that there was a reduction in sulphide mineral recovery at high CMC concentrations (500 g/t). This may be indicative of some CMC adsorption onto the hydrophobic sulphide mineral galena, and this affected the floatability of the minerals at high depressant concentrations.

Varying the galena feed grade affected the flotation rate of Pb. The majority of the Pb was recovered within the first 2 minutes of the batch flotation tests for each galena feed grade as illustrated in Figure 5- 17, thus the flotation rate of Pb was highest/fastest in the first concentrate (C1) across all feed grades and this was achieved with about 200 g utilisation of synthetic plant water. The fitted kinetic models as evaluated in Section 5.3.2 showed a range of flotation rate constants for each galena feed grade, with the lowest flotation rate constant of Pb, 0.52 min^{-1} corresponding to 6% galena feed grade while the

highest flotation rate constant of Pb corresponds to 12% galena feed grade. The lowest flotation rate constant of Pb was obtained under 3SPW while the highest flotation rate constant of Pb was obtained under 10SPW. The ionic strength of plant of plant water may have influenced the flotation rate of Pb such that the rate constant increased as the amount of inorganic electrolytes in the solution increased. Furthermore, the findings illustrated in Section 5.3.2 Table 5- 2, generally showed that the flotation rate of Pb increased with galena feed grade, with the highest rate constant for the low galena feed grade (3%) being 0.903 min^{-1} and that of the high galena feed grade (12%) being 1.095 min^{-1}. It could be that as the concentration of the sulphide mineral was increased with galena feed grade, the rate of Pb recovery also increased.

This study considered the UCT high depressant method in an attempt to differentiate the entrained from floating gangue. The method assumes that at a high depressant dosage (>300 g/t), all floatable gangue is depressed and any gangue reporting to the concentrate is owing to entrainment (Corin et al., 2011, Wiese and Harris, 2012, Wiese, 2009). Previous studies have shown that the amount of entrained material reporting to the concentrate is directly proportional to water recoveries (Ekmekçi et al., 2003, Yang and Aldrich, 2006, Boylu and Laskowski, 2007). Figure 5- 23 and Figure 5- 24 showed that the proposed method could not quantify entrainment for the synthetic ores used in this study. Not all the NFG was completely depressed at dosages higher than 500 g/t. It is worth noting that the ores used in this study were synthetic and the minerals were fully liberated, unlike real ores for which the UCT high depressant method was successful in quantifying entrainment. The rate of recovery of the total gangue per unit water generally increased with galena feed grade at all synthetic plant water types. Total gangue increased with an increase in galena feed grade at all synthetic plant water types, while the opposite was true with water recovered decreased, i.e. water reporting to the concentrate decreased with an increase in galena feed grade at all synthetic plant water types. Furthermore, an increase in the ionic strength of plant water led to an increase in the total amount of gangue reporting to the concentrate as the galena feed grade was increased. This could be primarily due to the NFG that reported to the concentrate via true flotation, even at depressant dosages greater than 500 g/t as illustrated in Figure 5- 24.

6.2 How does a simultaneous change in ore feed grade and ionic strength of plant water affect froth stability and flotation performance?

6.2.1 Pyrite System

The interpretation of the flotation response can be complex owing to the interactive effects which may be present in the sub-processes of flotation (Bradshaw et al., 2005b). This study showed that solids and water reporting to the concentrate increased with a simultaneous increase in pyrite feed grade and ionic strength of plant water type at all depressant dosages. The highest solid recovered for each pyrite feed grade was: ~ 75 g for 3%, ~ 100 g for 6%, and ~ 162 g for 12%. This could be attributed to two factors; (i) the increased amount of hydrophobic sulphide mineral, pyrite, as the pyrite feed grade was increased, may have promoted the amount of solids reporting to the froth phase. (ii) increasing the ionic strength of plant water increases the surface tension at the air-liquid interface, generating smaller and more stable bubbles with increased surface area. These bubbles carry more water and therefore more solids. Studies have shown that high concentrations of inorganic electrolytes stabilise the froth (Dzingai et al., 2020, Corin and Wiese, 2014, Manono et al., 2012, Corin et al., 2011) and attributed this to bubble size reduction and retardation of bubble coalescence when there are high amounts of dissolved inorganic electrolytes in solution (Manono et al., 2012). Klassen and Mokrousov (1963) attributed this to the fact that inorganic electrolytes reduce the surface hydration of naturally hydrophobic minerals and provide attractive forces between the mineral particles and air bubbles. The two factors postulated may have

had a direct effect on one another and thereby froth stability and flotation performance, as measured by solids and water recovery. Furthermore, the froth height and froth stability evaluated in Chapter 5, Section 5.1.7, showed that a simultaneous increase in pyrite feed grade and ionic strength of plant water led to an increase in froth height and froth stability. This could also be attributed to two factors; (i) the increased hydrophobic component, pyrite, as the pyrite feed grade was increased. (ii) the increased amount of inorganic electrolytes in solution as the ionic strength of plant water was increased improved froth height and stability with the increase in pyrite feed grade. Dishon et al. (2009) postulated that naturally hydrophobic minerals can adsorb specific cations at high ionic strength of solution, which may change the surface charge of the mineral particles and yield strong attractive forces between the mineral particles. These findings complement the batch flotation froth stability findings and indicate that a simultaneous increase in pyrite feed grade and ionic strength improved froth stability and therefore flotation performance.

The final Fe recoveries were generally within similar ranges for each pyrite feed grade; ~ 80 to 85% for 3%; ~ 86 to 90% for 6%; and ~ 84 to 94% for the 12%. These minimal changes in final Fe recoveries indicated that neither varying pyrite feed grade nor ionic strength of plant water or depressant dosage affected the final Fe recoveries. Therefore, a simultaneous change in pyrite feed grade and ionic strength of plant water also had no effect on the final Fe recoveries, as illustrated by Figure 5- 7 in Chapter 5. A simultaneous increase in pyrite feed grade and ionic strength of plant water led to an increase in final Fe grade at all depressant dosages. This can be attributed primarily to the increased hydrophobic mineral, pyrite, as the pyrite feed grade was increased. It can be postulated that the increased hydrophobic component promoted the recovery of Fe reporting to the concentrate grade and thereby improved flotation performance.

6.2.2 Galena System

The interpretation of the flotation response can be complex owing to the interactive effects which may be present in the sub-processes of flotation (Bradshaw et al., 2005b). As aforementioned, high concentrations of inorganic electrolytes yield strong attractive forces between the mineral particles (Dishon et al., 2009), and high ionic strengths of plant water stabilise the froth (Dzingai et al., 2020, Corin and Wiese, 2014, Manono et al., 2012, Corin et al., 2011). The floatability of sulphide minerals may increase or decrease in the presence of inorganic electrolytes depending on the type of minerals present and water chemistry (Slatter et al., 2009). The findings of this study showed that simultaneously increasing the galena feed grade and ionic strength of plant water type, led to an increase in solids and water reporting to the concentrate at all depressant dosages. This could also be attributed to the two factors as previously mentioned; hydrophobic sulphides and increased carrying capacity of the bubbles. These factors may have had a direct effect on one another and thereby flotation performance and froth stability. Furthermore, the froth column findings evaluated in Chapter 5, Section 5.2.6, showed that a simultaneous increase in galena feed grade and ionic strength of plant water type led to a slight increase in froth height and froth stability. It could be that the increased mineral attachment and accumulation of the highly hydrophobic mineral galena onto the bubbles surface, destabilised the bubbles and thereby led to the slight decrease in froth height and froth stability. These findings complement the batch flotation findings and indicate that a simultaneous increase in galena feed grade and ionic strength of plant water improved froth stability and flotation performance as measured by solids and water recovery.

The findings of this study showed that final Pb recoveries were within similar ranges about 97 to 98% for all galena feed grades and that the ranges were too similar and almost indistinguishable. This indicated that the final Pb recovered was unaffected by changes in neither galena feed grade nor ionic strength of plant water or depressant dosage. Hence, simultaneously varying the galena feed grade and

ionic strength had no effect on froth stability and flotation performance as illustrated by Figure 5- 17 in Chapter 5. The final Pb grades increased with a simultaneous increase in galena feed grade and ionic strength of plant water type at all depressant dosages. This could primarily owing to the increased amount of hydrophobic sulphide mineral, galena, in the froth phase, as the galena feed grade increased. This may have promoted the recovery of Pb reporting into the concentrate grade and thus improved flotation performance.

6.3 How does a combination of varying ore feed grade and ionic strength of plant water affect gangue recovery?

As mentioned previously, this study made use of the UCT high depressant method in an attempt to differentiate entrained gangue from floating gangue (Corin et al., 2011, Wiese and Harris, 2012, Wiese, 2009). Studies have shown a successful reduction in the amount of NFG to almost zero when the depressant dosage was increased to 300 g/t (Ekmekçi et al., 2003, Wiese et al., 2007); while Corin et al. (2011) further showed that increasing the dosage further to 500 g/t, ensured that no NFG was recovered, thereby allowing for the determination of an entrainment factor (Corin et al., 2011). These studies made use of real ores unlike the synthetic ores used in this study, which consisted of fully liberated minerals and only two gangue mineral phases; quartz and talc. Due to the fact that an entrainment factor could not be attained in this study, the effect that a combination of varying ore feed sulphide grade and ionic strength of plant water has on entrainment could not be determined. The UCT high depressant method is therefore shown to be ore specific. This study has shown that not all the NFG was completely depressed at dosages as high as and higher than 500 g/t. The rate of recovery of the total gangue per unit water generally increased with ore sulphide feed grade under all synthetic plant water types. Total gangue and water recovery increased with an increase in ore feed sulphide grade at all synthetic plant water types. Simultaneously increasing the ore feed sulphide grade and ionic strength of plant water generally led to an increase in the total gangue and water reporting to the concentrate at all depressant dosages. This could be owing to; (i) the increase in sulphide mineral concentration as the ore feed sulphide grade was increased, and (ii) the increase in dissolved inorganic electrolytes as the ionic strength of plant water was increased (Dzingai et al., 2020, Manono et al., 2018, Manono et al., 2012, Corin et al., 2011) and entrainment of gangue minerals.

6.4 Effect of varying ore feed grade on pulp chemistry as measured by Eh, pH, DO, EC and TDS?

6.3.1 Pyrite System

The findings of this study showed that there was no significant effect on the pulp chemistry parameters Eh, pH, DO, EC and TDS, when either the pyrite feed grade or depressant dosage was varied. Varying the ionic strength of plant water did however have an effect on the EC and TDS at all pyrite feed grades, which was expected. An increase in the ionic strength of synthetic plant water from 3SPW to 10SPW led to an average EC and TDS increase from 3369.57 mV and 1684.79 ppm to 9681.25 mV and 4841.46 ppm for C1, and from 3523.63 mV and 1761.77 ppm to 10126.01 mV and 5064.31 ppm for the tails, as shown in Appendix D1. This could be owing to the increased amount of dissolved inorganic electrolytes as the ionic strength of plant water was increased from 3SPW to 10SPW. Furthermore, EC and TDS measurements were higher for the tails than those of C1 at all synthetic plant types and pyrite feed grades. This is owing to the difference in residence time for the dissolution of mineral species into

the aqueous phase; C1 was collected after only milling, while tails were collected after milling and 20 minutes of flotation.

6.3.2 Galena System

The batch flotation findings from the galena system showed that there was no significant effect on the pulp chemistry parameters Eh, pH, DO, EC and TDS, when either the galena feed grade or depressant dosage was varied. However, varying the ionic strength of plant water did have an effect on the EC and TDS at all galena feed grades, which was expected. Increasing in the ionic strength of synthetic plant water from 3SPW to 10SPW led to an average EC and TDS increase from 3205.58 mV and 1602.75 ppm to 9514.91 mV and 4757.91 ppm for C1, and from 3355.14 mV and 1677.56 ppm to 9863.82 mV and 4932.66 ppm for the Tails, as shown in Appendix D2. This could be owing to the increased amount of dissolved inorganic electrolytes as the ionic strength of plant water was increased from 3SPW to 10SPW. Furthermore, EC and TDS measurements were higher for the tails than those of C1 at all synthetic plant types and galena feed grades, in the same manner as for the pyrite system.

Chapter 7. Conclusion

The primary objective of this study was to develop a relationship between ore feed grade and flotation performance. In order to establish this relationship, it was considered necessary to investigate the impact of varying ore feed grade on froth stability, entrainment and flotation performance under varying water qualities. The study considered two synthetic ore types; a pyrite-based synthetic ore, whereby pyrite was the valuable mineral, and a galena-based synthetic ore whereby galena was the valuable mineral. The relationship between the key performance indicators and the factors influencing them could then be constructed by focusing on the studies objectives and essentially answering the formulated four key questioned outlined in Chapter 3. It was in answering these key questions that the validity of the postulated hypothesis could then be assessed.

7.1 What effect does varying ore feed grade have on froth stability and flotation performance?

7.1.1Pyrite System

This study showed that increasing the pyrite feed grade led to an increase in the amount of solids and water reporting to the concentrate at all ionic strength of plant water types and depressant dosages. This was attributed to the increased hydrophobic component (pyrite concentration) as the pyrite feed grade was increased. Increasing the ionic strength of synthetic plant water type increased the solids and water reporting to the concentrate as the pyrite feed grade was increased at all depressant dosages, and this was attributed to the increased amount of inorganic electrolytes in solution as ionic strength of plant water was increased. Water recovery is a good indicator of froth stability and the increased water recovery with increase in pyrite feed grade thus indicated stable froths and was further validated by froth height and froth stability results obtained from the froth stability tests conducted. Thus, froth stability and flotation performance was improved when pyrite feed grade was increased as measured by the amount of water and solids recovered.

There was no apparent effect on the final Fe recovery when either pyrite feed grade, ionic strength of plant water type or depressant dosage was varied. Increasing the pyrite feed grade led to an increase in Fe grades at all synthetic plant water types and depressant dosages, and this was attributed to the increase in concentration of the pyrite as the hydrophobic component was increased. However, this increase was not directly proportional to the pyrite feed grade (hydrophobic component). Furthermore, the final Fe grades increased in conjunction with depressant dosage at each pyrite feed grade for all synthetic plant water types, owing to the reduction in NFG reporting to the concentrate, which dilutes the grade. The increased Fe grades as the pyrite feed grade was increased showed an indication of an enhancement in the flotation performance as measured by the grade.

7.1.2 Galena System

An increase in the amount of solids reporting to the concentrate was seen when the galena feed grade was increased at all depressant dosages, while the opposite was true for water recovery, i.e. water reporting to the concentrate decreased as the galena feed grade was increased at all depressant dosages. The increase in solids recovery was attributed to the increased hydrophobic component (galena concentration) as the galena feed grade was increased, while the decrease in water recovery was thought to have been owing to galena being highly hydrophobic such that the mineral destabilised the bubbles once it reached the froth phase, however, was still able to reach the concentrate. Increasing the ionic strength of synthetic plant water type increased the amount of solids and water reporting to the concentrate when the galena feed grade was increased at all depressant dosages, agreeing with the

current literature. This was attributed to smaller bubbles carrying more water and therefore solids as the ionic strength increased, as well as the increased hydrophobic component as the galena feed grade was increased. The dynamic froth stability findings showed that the froth height and froth stability decreased with an increase in galena feed grade and this correlated with the batch flotation water recoveries. It was therefore concluded that although the flotation performance was improved when galena feed grade was increased, froth stability was compromised mainly owing to galena being a highly hydrophobic mineral such that high concentrations of the mineral destabilised the bubbles.

Varying either the galena feed grade, ionic strength of synthetic plant water type or depressant dosage, had no apparent effect on the final Pb recoveries. The final Pb grades increased with galena feed grade at all depressant dosages and synthetic plant water types, and this was owing to an increase in the hydrophobic component in the ore. However, the increase in Pb grades was not directly proportional to the initial hydrophobic component added. An increase in ionic strength of synthetic plant water type led to an increase in final Pb grades as the galena feed grade was increased at all depressant dosages. Furthermore, final Pb grades increased in conjunction with depressant dosage at each galena feed grade for all synthetic plant water types, and this was attributed to the reduction in the amount of NFG reporting to the concentrate, thus less dilution of the grade.

7.2 How does a simultaneous change in ore feed grade and ionic strength of plant water affect froth stability and flotation performance?

7.2.1 Pyrite System

Simultaneously increasing the pyrite feed grade and ionic strength of synthetic plant water led to an increase in the amount of solids and water reporting to the concentrate at all depressant dosages. This was due to the increased amount of inorganic electrolytes in solution and increased hydrophobic component as the pyrite feed grade was increased. Dynamic froth stability and froth height increased with a simultaneous increase in pyrite feed grade and ionic strength of synthetic plant water.

The final Fe recoveries were generally unaffected by a simultaneous change in pyrite feed grade and ionic strength of plant water at all depressant dosages. Final Fe grades increased with a simultaneous increase in pyrite feed grade and ionic strength of synthetic plant water at all depressant dosages, and this led to the postulation that increasing the hydrophobic component and the ionic strength may have both promoted Fe recovery and thereby improved flotation performance.

7.2.2 Galena System

Solids and water recovery reporting to the concentrate increased concurrently when the galena feed grade and ionic strength of synthetic plant water were simultaneously increased at all depressant dosages. Furthermore, simultaneously increasing the galena feed grade and ionic strength of synthetic plant water type led to an increase in the dynamic froth stability and froth height. This was attributed to the increased concentration of the hydrophobic component and amount of inorganic electrolytes in solution when the galena feed grade was increased.

A simultaneous change in galena feed grade and ionic strength of plant water showed no apparent effect on the final Pb recoveries at all depressant dosages. Pb grades increased at all depressant dosages when the galena feed grade and ionic strength of plant water type were simultaneously increased.

7.3 How does a combination of varying ore feed grade and ionic strength of plant water affect gangue recovery?

This study has shown that simultaneously increasing the ore feed sulphide grade (pyrite feed grade or galena feed grade) and ionic strength of synthetic plant water generally led to an increase in the total gangue and water reporting to the concentrate at all depressant dosages. Furthermore, the rate of gangue recovery per unit water generally increased with ore feed sulphide grade at all synthetic plant water types. This agrees well with the current literature.

7.4 What effect does varying the ore feed grade have on pulp chemistry as measured by Eh, pH, DO, EC and TDS?

This study has shown that varying ore feed sulphide grade (pyrite feed grade or galena feed grade) had no significant effect on the pulp chemistry parameters Eh, pH, DO, EC and TDs. However, varying the ionic strength of plant water did have an effect on the EC and TDS at all pyrite feed grades, as expected, owing to the increased amount of inorganic electrolytes in solution as the ionic strength was increased.

7.5 Response to the Hypotheses of this Study

In light of the hypotheses proposed in Chapter 3;

(i) *Froth stability is determined by the hydrophobic components within an ore. A higher feed grade yields a more stable froth when the feed grade is higher owing to a higher proportion of hydrophobic minerals.*

Higher ore feed sulphide grades, corresponding to higher hydrophobic component concentrations, led to higher amount of solid mass and water reporting to the concentrate for the pyrite-based synthetic ore at all depressant dosages. The concentration of the hydrophobic component and type of mineral present in the feed played an important role in the flotation performance and dynamic froth stability of the synthetic ores investigated. The dynamic froth stability findings of the pyrite-based synthetic ore generally showed no apparent variation in froth height and dynamic froth stability when the hydrophobic concentration component was varied. Furthermore, increasing the hydrophobic component's concentration generally had no apparent effect on the Fe recovery whilst increasing the Fe grades at all depressant dosages.

Galena is a highly hydrophobic mineral, and the findings of this study showed that increasing its concentration in the feed destabilised the froth; dynamic froth stability and froth height decreased with an increase in galena feed grade, such that higher concentrations of the hydrophobic component (galena) also reported lower water recovery from the batch flotation tests. The mass of solids reporting to the concentrate did however increase with increased concentration of the hydrophobic component (galena). Higher concentrations of galena in the feed led to higher Pb grades at all depressant dosages but had no apparent effect on the Pb recovery since the Pb recovery remained generally unaffected for all the hydrophobic component concentrations considered in this investigation.

This study has shown that froth stability is determined by the hydrophobic components in the ore. However, higher concentrations of the hydrophobic component do not always yield a more stable froth, it depends on the type of hydrophobic mineral component present. Thus, depending on the mineralogy of the ore, hypothesis one can be true.

(ii) *The ionic strength of plant water is a strong determinant of froth stability due to its effects on the behaviour of hydrophobic and hydrophilic components. A low feed grade at a high ionic strength water causes an increase in water and gangue minerals recovery, which in turn yields a more stable froth.*

Higher amount of inorganic electrolytes in solution and their corresponding ionic strengths of plant water yielded higher water and solids recovery in comparison to lower ionic strengths of plant water, and thereby more stable froths and an enhancement in the flotation performance.

This study has shown that a low feed grade at high ionic strength of synthetic plant water led to an increase water and gangue recovery, which in turn yielded more stable froths and thus proving the second hypothesis to be correct.

7.6 Relevance to Industry

The depletion of high-grade ore deposits to low-grade and more complex ores has posed a serious processing challenge for the mining industry to increase metal production owing to the rising demand for metals to meet the demand for our technologically driven future. As such, the findings of this study may be key for metallurgical operations whereby pyrite is considered to be non-valuable; such operations may need to implement early strategies for managing the recovery of pyrite in future as there is a greater chance that the mineral will report to the concentrate the more ores deplete with time. This work may also be a positive indicator for metallurgical plants which consider pyrite to be valuable, such as in gold processing, this is because the findings of this work have shown that there would still be a greater chance of recovering the pyrite associated with gold even at lower feed grades.

Galena is a major source of commercial lead and as such, metallurgical operations which mine lead may find the findings of this work as a positive for their production; this is because this work has shown that there is still a greater chance of recovering galena even at lower feed grades.

The kind of knowledge contribution of this study may be key for the mining industry and metallurgical plants that have incorporated a closed-circuit water system in their operations. Recycled water may contain deleterious ions and thereby higher ionic strengths, however, this work has shown that higher ionic strengths should not have adverse effects on the overall flotation performance as measured by the Fe and Pb recoveries, as such, metallurgical plants motivated by recovery are encouraged to continue recycling onsite process water. Furthermore, grade was seen to be impacted significantly by changing water quality, and as such, operations that are motivated by grade should consider the recycling of water carefully. Appreciating that this water quality studies have been seen to be ore dependent and so operational response to water quality should be done on an ore – ore basis.

Chapter 8. Recommendations and Future Work

In light of the results and conclusions drawn, the following recommendations are put forward;

- Use alternative entrainment methods such as the use of a tracer to determine an entrainment factor from synthetic ores.
- Floatability tests comparing the minerals pyrite and galena through the use of a polymetallic bearing synthetic ore system could add value to current knowledge and research in sulfide flotation.
- Adsorption tests should be conducted in order to determine the extent to which depressants adsorb onto gangue mineral surfaces for synthetic ore systems with varying sulfide feed grade.
- Investigating the effects of varying ore feed grade and water quality on flotation performance by making use of a collector less system should be conducted to help make an inference on the natural hydrophobicity and floatability of the minerals in the system.
- A study on whether there is a threshold hydrophobic component(s) concentration from which optimum flotation performance can be attained with regards to water quality should be conducted.
- A case study in which the findings obtained from this study are compared to a real ore could help to infer on the differences in the trends obtained.
- Application of machine learning in an attempt to develop a predictive model(s) from which flotation performance when the ore feed and water qualities are known.

References

ACHAYE, I., WIESE, J. & MCFADZEAN, B. 2021. Effect of mineral particle size on froth stability. *Mineral Processing and Extractive Metallurgy,* 130**,** 253-261.

AHMED, S. 1978. Electrochemical studies of sulphides, II. Measurement of the galvanic currents in galena and the general mechanism of oxygen reduction and xanthate adsorption on sulphides in relation to flotation. *International Journal of Mineral Processing,* 5**,** 175-182.

AKTAS, Z., CILLIERS, J. J. & BANFORD, A. W. 2008. Dynamic froth stability: Particle size, airflow rate and conditioning time effects. *International Journal of Mineral Processing,* 87**,** 65-71.

ALLAHKARAMI, E., POOR, A. Z. & REZAI, B. 2017. Pyrite flotation in the presence of galena. Study on galvanic interaction. *Physicochemical Problems of Mineral Processing,* 53**,** 846-858.

ATA, S., AHMED, N. & JAMESON, G. J. 2003. A study of bubble coalescence in flotation froths. *International Journal of Mineral Processing,* 72**,** 255-266.

AVEYARD, R., BINKS, B., FLETCHER, P., PECK, T. & RUTHERFORD, C. 1994. Aspects of aqueous foam stability in the presence of hydrocarbon oils and solid particles. *Advances in colloid and interface science,* 48**,** 93-120.

BABEDI, L., TADIE, M., VON DER HEYDEN, B. P. & CHAREEV, D. A. 2023. A rest potential study of impurity (As, Au, Ni and Co) bearing synthetic pyrite in alkaline flotation conditions. *Minerals Engineering,* 202**,** 108277.

BARBIAN, N., HADLER, K., VENTURA-MEDINA, E. & CILLIERS, J. 2005. The froth stability column: linking froth stability and flotation performance. *Minerals Engineering,* 18**,** 317-324.

BARBIAN, N., VENTURA-MEDINA, E. & CILLIERS, J. 2003. Dynamic froth stability in froth flotation. *Minerals Engineering,* 16**,** 1111-1116.

BARKER, G. J., GERSON, A. R. & MENUGE, J. F. 2014. The impact of iron sulfide on lead recovery at the giant Navan Zn–Pb orebody, Ireland. *International Journal of Mineral Processing,* 128**,** 16-24.

BARKER, L. M. 1983. *The effect of electrolytes on the flotation of pyrite.* University of Cape Town, South Africa.

BESTER, M. & VERMEULEN, P. D. 2010. Investigation of potential water quality and quantity impacts associated with mining of the shallow Waterberg coal reserves, west of the Daarby Fault, Limpopo Province, South Africa. *Water SA,* 36.

BICAK, O., EKMEKCI, Z., BRADSHAW, D. & HARRIS, P. 2007. Adsorption of guar gum and CMC on pyrite. *Minerals engineering,* 20**,** 996-1002.

BIKERMAN, J. 1973. Measurement of foaminess. *Foams.* Springer.

BINKS, B. P. 2002. Particles as surfactants—similarities and differences. *Current opinion in colloid & interface science,* 7**,** 21-41.

BOULTON, A., FORNASIERO, D. & RALSTON, J. 2001. Depression of iron sulphide flotation in zinc roughers. *Minerals Engineering,* 14**,** 1067-1079.

BOYLU, F. & LASKOWSKI, J. S. 2007. Rate of water transfer to flotation froth in the flotation of low-rank coal that also requires the use of oily collector. *International Journal of Mineral Processing,* 83**,** 125-131.

BRADSHAW, D., HARRIS, PJ & O'CONNOR, C. 1998. Synergistic interactions between reagents in sulphide flotation. *Journal of the Southern African Institute of Mining and Metallurgy,* 98**,** 189-193.

BRADSHAW, D., O'CONNOR, C. & HARRIS, P. 2005a. The effect of collectors and their interactions with depressants on the behaviour of the froth phase in flotation. *Australasian Institute of Mining and Metallurgy (AusIMM)*.

BRADSHAW, D., OOSTENDORP, B. & HARRIS, P. 2005b. Development of methodologies to improve the assessment of reagent behaviour in flotation with particular reference to collectors and depressants. *Minerals Engineering,* 18**,** 239-246.

BRADSHAW, D. J. 1997. Synergistic effects between thiol collectors used in the flotation of pyrite.

BROŻEK, M. & MŁYNARCZYKOWSKA, A. 2006. Application of the stochastic model for analysis of flotation kinetics with coal as an example. *Physicochemical Problems of Mineral Processing,* 40**,** 31-44.

BULUT, G. & ATAK, S. 2002. Role of dixanthogen on pyrite flotation: solubility, adsorption studies and Eh, FTIR measurements. *Mining, Metallurgy & Exploration,* 19**,** 81-86.

BULUT, G., YENIAL, Ü., EMIROĞLU, E. & SIRKECI, A. A. 2014. Arsenic removal from aqueous solution using pyrite. *Journal of Cleaner Production,* 84**,** 526-532.

BURDUKOVA, E. 2007. *Surface properties of New York talc as a function of pH, polymer adsorption and electrolyte concentration.* University of Cape Town, South Africa

CASTRO, S., MIRANDA, C., TOLEDO, P. & LASKOWSKI, J. 2013. Effect of frothers on bubble coalescence and foaming in electrolyte solutions and seawater. *International Journal of Mineral Processing,* 124**,** 8-14.

CELIK, M. S. & SOMASUNDARAN, P. Wettability of reservoir minerals by flotation and correlation with surfactant adsorption. SPE International Conference on Oilfield Chemistry, 1980. *SPE*, SPE-9002-MS.

CHANDRA, A. P. & GERSON, A. R. 2009. A review of the fundamental studies of the copper activation mechanisms for selective flotation of the sulfide minerals, sphalerite and pyrite. *Advances in Colloid and Interface Science,* 145**,** 97-110.

CHAU, T. 2009. A review of techniques for measurement of contact angles and their applicability on mineral surfaces. *Minerals engineering,* 22**,** 213-219.

CHEN, J.-H., LI, Y.-Q., LAN, L.-H. & GUO, J. 2014. Interactions of xanthate with pyrite and galena surfaces in the presence and absence of oxygen. *Journal of Industrial and Engineering Chemistry,* 20**,** 268-273.

CHENG, X. & IWASAKI, I. 1992. Pulp potential and its implications to sulfide flotation. *Mineral Processing and Extractive Metullargy Review,* 11**,** 187-210.

CHERNYSHOVA, I. 2003. An in situ FTIR study of galena and pyrite oxidation in aqueous solution. *Journal of Electroanalytical Chemistry,* 558**,** 83-98.

CHO, Y. S. & LASKOWSKI, J. S. 2002. Effect of flotation frothers on bubble size and foam stability. *International Journal of Mineral Processing,* 64**,** 69-80.

CISTERNAS, L. A. & GÁLVEZ, E. D. 2018. The use of seawater in mining. *Mineral Processing and Extractive Metallurgy Review,* 39**,** 18-33.

CORIN, K., MISHRA, J. & O'CONNOR, C. 2013. Investigating the role of pulp chemistry on the floatability of a Cu–Ni sulfide ore. *International Journal of Mineral Processing,* 120**,** 8-14.

CORIN, K. C., REDDY, A., MIYEN, L., WIESE, J. G. & HARRIS, P. J. 2011. The effect of ionic strength of plant water on valuable mineral and gangue recovery in a platinum bearing ore from the Merensky reef. *Minerals Engineering,* 24**,** 131-137.

CORIN, K. C. & WIESE, J. G. 2014. Investigating froth stability: A comparative study of ionic strength and frother dosage. *Minerals Engineering,* 66-68**,** 130-134.

CRAIG, J. R., VAUGHAN, D. J. & HAGNI, R. D. 1981. *Ore microscopy and ore petrography*, Wiley New York.

CROZIER, R. D. 1992. *Flotation: theory, reagents and ore testing. United Kingdom:*, U.S. Department of Energy

Office of Scientific and Technical Information.

DAVIS, F., HYATT, D. & COX, C. 1975. Environmental Problems of Flotation Reagents in Mineral Processing Plant Tailings Water Mineral Processing Plant Tailings Water. *US Department of the Interior: Washington, DC, USA*.

DEAN, A. M., MORRIS, M., STUFKEN, J. & BINGHAM, D. 2015. *Handbook of design and analysis of experiments*, CRC Press Boca Raton.

DENKOV, N. D. & MARINOVA, K. G. 2006. Antifoam effects of solid particles, oil drops and oil-solid compounds in aqueous foams. *Colloidal particles at liquid interfaces***,** 383-444.

DHLIWAYO, E. C. 2005. *The interactive effect of depressant type and dosage with frother dosage in the flotation of a PGE ore.* University of Cape Town, South Africa.
DICHMANN, T. K. & FINCH, J. A. 2001. The role of copper ions in sphalerite-pyrite flotation selectivity. *Minerals Engineering,* 14**,** 217-225.
DIMITRIJEVIC, M., ANTONIJEVIC, M. M. & JANKOVIC, Z. 1996. Kinetics of pyrite dissolution by hydrogen peroxide in perchloric acid. *Hydrometallurgy,* 42**,** 377-386.
DISHON, M., ZOHAR, O. & SIVAN, U. 2009. From repulsion to attraction and back to repulsion: the effect of NaCl, KCl, and CsCl on the force between silica surfaces in aqueous solution. *Langmuir,* 25**,** 2831-2836.
DRZYMAŁA, J. 2007. *Mineral processing: foundations of theory and practice of minerallurgy*, University of Technology, Wroclaw, Poland.
DZINGAI, M., MANONO, M. & CORIN, K. 2020. Simulating the effect of water recirculation on flotation through ion-spiking: effect of Ca2+ and Mg2+. *Minerals,* 10**,** 1033.
EKMEKÇI, Z., BRADSHAW, D., ALLISON, S. & HARRIS, P. 2003. Effects of frother type and froth height on the flotation behaviour of chromite in UG2 ore. *Minerals Engineering,* 16**,** 941-949.
EKMEKÇI, Z. & DEMIREL, H. 1997. Effects of galvanic interaction on collectorless flotation behaviour of chalcopyrite and pyrite. *International journal of mineral processing,* 52**,** 31-48.
ENGELBRECHT, J. & WOODBURN, E. 1975. The effects of froth height, aeration rate, and gas precipitation on flotation. *Journal of the South African Institute of Mining and Metallurgy*.
FARROKHPAY, S., NDLOVU, B. & BRADSHAW, D. 2018. Behavior of talc and mica in copper ore flotation. *Applied Clay Science,* 160**,** 270-275.
FINCH, J., GELINAS, S. & MOYO, P. 2006. Frother-related research at McGill University. *Minerals Engineering,* 19**,** 726-733.
FINCH, J. A., NESSET, J. E. & ACUÑA, C. 2008. Role of frother on bubble production and behaviour in flotation. *Minerals Engineering,* 21**,** 949-957.
FORNASIERO, D., LI, F., RALSTON, J. & SMART, R. S. C. 1994. Oxidation of galena surfaces: I. X-ray photoelectron spectroscopic and dissolution kinetics studies. *Journal of Colloid and Interface Science,* 164**,** 333-344.
FRYE, G. C. & BERG, J. C. 1989. Antifoam action by solid particles. *Journal of colloid and interface science,* 127**,** 222-238.
FUERSTENAU, D. 1982a. Adsorption at Mineral/Water Interfaces. *Principles of flotation***,** 53-71.
FUERSTENAU, D. & MISHRA, R. 1980. On the mechanism of pyrite flotation with xanthate collectors. *Complex Sulphide Ores***,** 271-278.
FUERSTENAU, M. 1982b. Sulphide mineral flotation: in Principles of Flotation. *SAIMM monograph series,* 3**,** 159-182.
FUERSTENAU, M., MISRA, M. & PALMER, B. 1990. Xanthate adsorption on selected sulfides in the virtual absence and presence of oxygen, Part 2. *International Journal of Mineral Processing,* 29**,** 111-119.
FUERSTENAU, M., OLIVAS, S., HERRERA-URBINA, R. & HAN, K. 1987. The surface characteristics and flotation behavior of anglesite and cerussite. *International journal of mineral processing,* 20**,** 73-85.
FUERSTENAU, M. C. & HAN, K. N. 2003. *Principles of mineral processing*, SME.
GARRETT, P. R. 1980. Preliminary considerations concerning the stability of a liquid heterogeneity in a plane-parallel liquid film. *Journal of colloid and interface science,* 76**,** 587-590.
GONG, W. Q. 1999. *Poly (acrylamides) at the Talc-aqueous Solution Interface.* Metallurgical Society of the Canadian Institute of Mining, Metallurgy and Petroleum.
GOODALL, C. M. 1993. *The effects of flotation variables on the bubble size, mixing characteristics and froth behaviour in column flotation cells.* University of Cape Town, South Africa.
GU, G.-H., HU, Y.-H., QIU, G.-Z., WANG, H. & WANG, D.-Z. 2002. Potential control flotation of galena in strong alkaline media. *Journal of Central South University of Technology,* 9**,** 16-20.

GUNSON, A. J., KLEIN, B., VEIGA, M. & DUNBAR, S. 2012. Reducing mine water requirements. *Journal of Cleaner Production,* 21**,** 71-82.
GUO, B., PENG, Y. & ESPINOSA-GOMEZ, R. 2014. Cyanide chemistry and its effect on mineral flotation. *Minerals Engineering,* 66**,** 25-32.
GUY, P. & TRAHAR, W. 1984. The effects of oxidation and mineral interaction on sulphide flotation. *Flotation of sulphide minerals***,** 91-110.
HADLER, K. & CILLIERS, J. 2009. The relationship between the peak in air recovery and flotation bank performance. *Minerals Engineering,* 22**,** 451-455.
HAGGARD, E., SHERIDAN, C. & HARDING, K. 2015. Quantification of water usage at a South African platinum processing plant. *Water SA,* 41**,** 279-286.
HAMPTON, M. A., PLACKOWSKI, C. & NGUYEN, A. V. 2011. Physical and chemical analysis of elemental sulfur formation during galena surface oxidation. *Langmuir,* 27**,** 4190-4201.
HARRIS, P. 1982. Frothing phenomena and frothers. *South African Institute of Mining and Metallurgy, Principles of Flotation***,** 237-250.
HAUNG, H. & MILLER, J. 1978. Kinetics and thermochemistry of amyl xanthate adsorption by pyrite and marcasite. *International Journal of Mineral Processing,* 5**,** 241-266.
HAYES, R. A. & RALSTON, J. 1988. The collectorless flotation and separation of sulphide minerals by Eh control. *International journal of mineral processing,* 23**,** 55-84.
HE, S., FORNASIERO, D. & SKINNER, W. 2005. Correlation between copper-activated pyrite flotation and surface species: Effect of pulp oxidation potential. *Minerals Engineering,* 18**,** 1208-1213.
HERNÁINZ, F. & CALERO, M. 2001. Froth flotation: kinetic models based on chemical analogy. *Chemical Engineering and Processing: Process Intensification,* 40**,** 269-275.
HERRERA-URBINA, R., SOTILLO, F. & FUERSTENAU, D. 1999. Effect of sodium sulfide additions on the pulp potential and amyl xanthate flotation of cerussite and galena. *International Journal of Mineral Processing,* 55**,** 157-170.
HOROZOV, T. S. 2008. Foams and foam films stabilised by solid particles. *Current Opinion in Colloid & Interface Science,* 13**,** 134-140.
HSIEH, Y. & HUANG, C. 1989. The dissolution of PbS (s) in dilute aqueous solutions. *Journal of colloid and interface science,* 131**,** 537-549.
HUANG, P., CAO, M. & LIU, Q. 2013. Selective depression of pyrite with chitosan in Pb–Fe sulfide flotation. *Minerals Engineering,* 46-47**,** 45-51.
HUNTER, T. N., PUGH, R. J., FRANKS, G. V. & JAMESON, G. J. 2008. The role of particles in stabilising foams and emulsions. *Advances in colloid and interface science,* 137**,** 57-81.
IGLESIAS, E., ANDEREZ, J., FORGIARINI, A. & SALAGER, J.-L. 1995. A new method to estimate the stability of short-life foams. *Colloids and Surfaces A: Physicochemical and Engineering Aspects,* 98**,** 167-174.
JANETSKI, N., WOODBURN, S. & WOODS, R. 1977. An electrochemical investigation of pyrite flotation and depression. *International Journal of Mineral Processing,* 4**,** 227-239.
JENKINS, P. & RALSTON, J. 1998. The adsorption of a polysaccharide at the talc–aqueous solution interface. *Colloids and Surfaces A: Physicochemical and Engineering Aspects,* 139**,** 27-40.
JIANG, C., WANG, X., PAREKH, B. & LEONARD, J. 1998. The surface and solution chemistry of pyrite flotation with xanthate in the presence of iron ions. *Colloids and Surfaces A: Physicochemical and Engineering Aspects,* 136**,** 51-62.
JOHANSSON, G. & PUGH, R. 1992. The influence of particle size and hydrophobicity on the stability of mineralized froths. *International Journal of Mineral Processing,* 34**,** 1-21.
KARTIO, I., LAAJALEHTO, K., KAURILA, T. & SUONINEN, E. 1996. A study of galena (PbS) surfaces under controlled potential in pH 4.6 solution by synchrotron radiation excited photoelectron spectroscopy. *Applied surface science,* 93**,** 167-177.
KARTIO, I., WITTSTOCK, G., LAAJALEHTO, K., HIRSCH, D., SIMOLA, J., LAIHO, T., SZARGAN, R. & SUONINEN, E. 1997. Detection of elemental sulphur on galena oxidized in acidic solution. *International journal of mineral processing,* 51**,** 293-301.

KHRAISHEH, M., HOLLAND, C., CREANY, C., HARRIS, P. & PAROLIS, L. 2005. Effect of molecular weight and concentration on the adsorption of CMC onto talc at different ionic strengths. *International Journal of Mineral Processing,* 75**,** 197-206.

KING, R. 1982. Principles of flotation. *South African Institute of Mining and Metallurgy, Kelvin House, 2 Holland St, Johannesburg, South Africa, 1982. 268*.

KLASSEN, V. I. & MOKROUSOV, V. A. 1963. An introduction to the theory of flotation. *Butterworths*.

KLIMPEL, R. Froth Flotation: the Kinetic Approach.(Retroactive Coverage). MINTEK 50: International Conference on Mineral Science and Technology., 1984. 385-392.

KLIMPEL, R. & ISHERWOOD, S. 1991. Some industrial implications of changing frother chemical structure. *International journal of mineral processing,* 33**,** 369-381.

KLIMPEL, R. R. 1980. Selection of chemical reagents for flotation. *Mineral processing plant design,* 2**,** 907-934.

KOCABAG, D., KELSALL, G. & SHERGOLD, H. 1990. Natural oleophilicity/hydrophobicity of sulphide minerals, I. Galena. *International Journal of Mineral Processing,* 29**,** 195-210.

KOWALCZUK, P. B. 2013. Determination of critical coalescence concentration and bubble size for surfactants used as flotation frothers. *Industrial & Engineering Chemistry Research,* 52**,** 11752-11757.

KUOPANPORTTI, H., SUORSA, T., DAHL, O. & NIINIMÄKI, J. 2000. A model of conditioning in the flotation of a mixture of pyrite and chalcopyrite ores. *International journal of mineral processing,* 59**,** 327-338.

LASKOWSKI, J. & LIU, Q. 1999. On the adsorption mechanism of carboxymethyl cellulose. *Polymers Mineral Processing. MetSoc of CIM***,** 357-373.

LASKOWSKI, J., LIU, Q. & O'CONNOR, C. 2007. Current understanding of the mechanism of polysaccharide adsorption at the mineral/aqueous solution interface. *International Journal of Mineral Processing,* 84**,** 59-68.

LASKOWSKI, J., TLHONE, T., WILLIAMS, P. & DING, K. 2003. Fundamental properties of the polyoxypropylene alkyl ether flotation frothers. *International Journal of Mineral Processing,* 72**,** 289-299.

LASKOWSKI, J. & WOODBURN, E. T. 1998. *Frothing in flotation ii: Recent advances in coal processing*, Gordon and Breach Science Publishers

LI, Y., QUANJUN, L., SHIMEI, L., CHAO, S., YANG, G. & JIANWEN, S. 2019. The synergetic depression effect of KMnO4 and CMC on the depression of galena flotation. *Chemical Engineering Communications,* 206**,** 581-591.

LOVELL, V. 1982. Industrial flotation reagents. *South African Institute of Mining and Metallurgy, Principles of Flotation***,** 73-89.

MANOCHA, A. & PARK, R. L. 1977. Flotation related ESCA studies on PbS surfaces. *Applications of Surface Science,* 1**,** 129-141.

MANONO, M., CORIN, K. & WIESE, J. 2018. Water quality effects on a sulfidic PGM ore: Implications for froth stability and gangue management. *Physicochemical Problems of Mineral Processing,* 54**,** 1253-1265.

MANONO, M. S. 2012. *An investigation into the effect of ionic strength of plant water on valuable mineral and gangue recovery of a platinum bearing ore from the Merensky reef.* University of Cape Town, South Africa

MANONO, M. S., CORIN, K. C. & WIESE, J. G. 2012. An investigation into the effect of various ions and their ionic strength on the flotation performance of a platinum bearing ore from the Merensky reef. *Minerals Engineering,* 36-38**,** 231-236.

MARTINOVIC, J. 2005. *Investigation of the surface properties of gangue minerals in PGM bearing ores.* University of Cape Town, South Africa.

MELO, F. & LASKOWSKI, J. S. 2006. Fundamental properties of flotation frothers and their effect on flotation. *Minerals Engineering,* 19**,** 766-773.

MHLONGO, S. P., MATIVENGA, P. T. & MARNEWICK, A. 2018. Water quality in a mining and water-stressed region. *Journal of Cleaner Production,* 171**,** 446-456.

MILLER, J., DU PLESSIS, R., KOTYLAR, D., ZHU, X. & SIMMONS, G. 2002. The low-potential hydrophobic state of pyrite in amyl xanthate flotation with nitrogen. *International Journal of Mineral Processing,* 67**,** 1-15.

MOORUTH, N. & BOOLEY, D. 2009. *Effect of ionic strength on gangue recovery in a platinum bearing ore. BSc. Eng thesis.*, University of Cape Town, South Africa

MORAR, S. H., BRADSHAW, D. J. & HARRIS, M. C. 2012. The use of the froth surface lamellae burst rate as a flotation froth stability measurement. *Minerals Engineering,* 36**,** 152-159.

MORRIS, G., PURSELL, M., NEETHLING, S. & CILLIERS, J. 2008. The effect of particle hydrophobicity, separation distance and packing patterns on the stability of a thin film. *Journal of colloid and interface science,* 327**,** 138-144.

MOSLEMI, H. & GHARABAGHI, M. 2017. A review on electrochemical behavior of pyrite in the froth flotation process. *Journal of Industrial and Engineering Chemistry,* 47**,** 1-18.

MOSLEMI, H., SHAMSI, P. & HABASHI, F. 2011. Pyrite and pyrrhotite open circuit potentials study: Effects on flotation. *Minerals Engineering,* 24**,** 1038-1045.

MUZENDA, E. 2010. An investigation into the effect of water quality on flotation performance. *World Academy of Science, Engineering and Technology,* 69**,** 237-241.

MUZINDA, I. & SCHREITHOFER, N. 2018. Water quality effects on flotation: Impacts and control of residual xanthates. *Minerals Engineering,* 125**,** 34-41.

NAICKER, K., CUKROWSKA, E. & MCCARTHY, T. 2003. Acid mine drainage arising from gold mining activity in Johannesburg, South Africa and environs. *Environmental pollution,* 122**,** 29-40.

NANTHAKUMAR, B. & KELEBEK, S. 2007. Stagewise analysis of flotation by factorial design approach with an application to the flotation of oxidized pentlandite and pyrrhotite. *International Journal of Mineral Processing,* 84**,** 192-206.

NEETHLING, S. J. & CILLIERS, J. J. 2002. The entrainment of gangue into a flotation froth. *International Journal of Mineral Processing,* 64**,** 123-134.

NEETHLING, S. J. & CILLIERS, J. J. 2009. The entrainment factor in froth flotation: Model for particle size and other operating parameter effects. *International Journal of Mineral Processing,* 93**,** 141-148.

NODA, Y., MASUMOTO, K., OHBA, S., SAITO, Y., TORIUMI, K., IWATA, Y. & SHIBUYA, I. 1987. Temperature dependence of atomic thermal parameters of lead chalcogenides, PbS, PbSeand PbTe. *Acta Crystallographica Section C: Crystal Structure Communications,* 43**,** 1443-1445.

NORTHEY, S. A., MUDD, G. M., SAARIVUORI, E., WESSMAN-JÄÄSKELÄINEN, H. & HAQUE, N. 2016. Water footprinting and mining: Where are the limitations and opportunities? *Journal of Cleaner Production,* 135**,** 1098-1116.

NOWAK, P. & LAAJALEHTO, K. 2000. Oxidation of galena surface–an XPS study of the formation of sulfoxy species. *Applied Surface Science,* 157**,** 101-111.

NOWAK, P., LAAJALEHTO, K. & KARTIO, I. 2000. A flotation related X-ray photoelectron spectroscopy study of the oxidation of galena surface. *Colloids and Surfaces A: Physicochemical and Engineering Aspects,* 161**,** 447-460.

OCTOBER, L., MANONO, M., WIESE, J., SCHREITHOFER, N. & CORIN, K. 2021. Fundamental and flotation techniques assessing the effect of water quality on bubble-particle attachment of chalcopyrite and galena. *Minerals Engineering,* 167**,** 106880.

OERTEL, J., ELLMER, K., BOHNE, W., RÖHRICH, J. & TRIBUTSCH, H. 1999. Growth of n-type polycrystalline pyrite (FeS2) films by metalorganic chemical vapour deposition and their electrical characterization. *Journal of Crystal Growth,* 198**,** 1205-1210.

OWUSU, C., BRITO E ABREU, S., SKINNER, W., ADDAI-MENSAH, J. & ZANIN, M. 2014. The influence of pyrite content on the flotation of chalcopyrite/pyrite mixtures. *Minerals Engineering,* 55**,** 87-95.

OZUN, S., HASSAS, B. V. & MILLER, J. D. 2019. Collectorless flotation of oxidized pyrite. *Colloids and Surfaces A: Physicochemical and Engineering Aspects,* 561**,** 349-356.

PAROLIS, L. A., VAN DER MERWE, R., GROENMEYER, G. V. & HARRIS, P. J. 2008. The influence of metal cations on the behaviour of carboxymethyl celluloses as talc depressants. *Colloids and Surfaces A: Physicochemical and Engineering Aspects,* 317**,** 109-115.

PECINA-TREVINO, E., URIBE-SALAS, A. & NAVA-ALONSO, F. 2003. Effect of dissolved oxygen and galvanic contact on the floatability of galena and pyrite with Aerophine 3418A. *Minerals engineering,* 16**,** 359-367.

PECINA, E. T., URIBE, A., NAVA, F. & FINCH, J. A. 2006. The role of copper and lead in the activation of pyrite in xanthate and non-xanthate systems. *Minerals Engineering,* 19**,** 172-179.

POLAT, M. & CHANDER, S. 2000. First-order flotation kinetics models and methods for estimation of the true distribution of flotation rate constants. *International Journal of Mineral Processing,* 58**,** 145-166.

POLING, G. 1976. Reactions between thiol reagents and sulphide minerals. *The American Institute of Mining, Metallurgical, and Petroleum Engineers*.

PRESTIDGE, C. & RALSTON, J. 1996. Contact angle studies of particulate sulphide minerals. *Minerals Engineering,* 9**,** 85-102.

PRESTIDGE, C. A. & RALSTON, J. 1995. Contact angle studies of galena particles. *Journal of colloid and interface science,* 172**,** 302-310.

PUGH, R. 2005. Experimental techniques for studying the structure of foams and froths. *Advances in colloid and interface science,* 114**,** 239-251.

QIN, W., WANG, X., MA, L., JIAO, F., LIU, R., YANG, C. & GAO, K. 2015. Electrochemical characteristics and collectorless flotation behavior of galena: With and without the presence of pyrite. *Minerals Engineering,* 74**,** 99-104.

RAICHUR, A., WANG, X. & PAREKH, B. 2000. Quantifying pyrite surface oxidation kinetics by contact angle measurements. *Colloids and Surfaces A: Physicochemical and Engineering Aspects,* 167**,** 245-251.

RALSTON, J. 1991. Eh and its consequences in sulphide mineral flotation. *Minerals Engineering,* 4**,** 859-878.

RALSTON, J. 1994. The chemistry of galena flotation: Principles & practice. *Minerals engineering,* 7**,** 715-735.

RAO, S. R. 2013. *Surface chemistry of froth flotation: Volume 1: Fundamentals*, Springer Science & Business Media.

RAO, S. R. & FINCH, J. 1988. Galvanic interaction studies on sulphide minerals. *Canadian Metallurgical Quarterly,* 27**,** 253-259.

RAO, S. R. & LEJA, J. 2004. *Surface chemistry of froth flotation: reagents and mechanisms*, Kluwer Academic/Plenum Publishers.

RASHCHI, F., DASHTI, A., ARABPOUR-YAZDI, M. & ABDIZADEH, H. 2005. Anglesite flotation: a study for lead recovery from zinc leach residue. *Minerals Engineering,* 18**,** 205-212.

ROSSEN, W., PRUD'HOMME, R. & KHAN, S. 1996. Foams: theory, measurements and applications. *Foams in Enhanced Oil Recovery***,** 413-464.

SAVASSI, O., ALEXANDER, D., FRANZIDIS, J. & MANLAPIG, E. 1998. An empirical model for entrainment in industrial flotation plants. *Minerals Engineering,* 11**,** 243-256.

SCHWARZ, S. & GRANO, S. 2005. Effect of particle hydrophobicity on particle and water transport across a flotation froth. *Colloids and Surfaces A: Physicochemical and Engineering Aspects,* 256**,** 157-164.

SHACKLETON, N., MALYSIAK, V. & O'CONNOR, C. 2007a. Surface characteristics and flotation behaviour of platinum and palladium arsenides. *International Journal of Mineral Processing,* 85**,** 25-40.

SHACKLETON, N., MALYSIAK, V. & O'CONNOR, C. 2007b. Surface characteristics and flotation behaviour of platinum and palladium tellurides. *Minerals Engineering,* 20**,** 1232-1245.

SHAMAILA, S. & O'CONNOR, C. T. 2008. The role of synthetic minerals in determining the relative flotation behaviour of Platreef PGE tellurides and arsenides. *Minerals Engineering,* 21**,** 899-904.

SHORTRIDGE, P., HARRIS, P. & BRADSHAW, D. 1999. The influence of ions on the effectiveness of polysaccharide depressants in the flotation of talc. *Canadian Institute of Mining, Metallurgy and Petroleum*.

SLATTER, K., PLINT, N., COLE, M., DILSOOK, V., DE VAUX, D., PALM, N. & OOSTENDORP, B. Water management in Anglo Platinum process operations: effects of water quality on process operations. International Mine Water Conference, Pretoria, South Africa, 2009. 19-23.

SMITH, P. & WARREN, L. 1989. Entrainment of particles into flotation froths. *Mineral Procesing and Extractive Metallurgy Review,* 5**,** 123-145.

STEENBERG, E. & HARRIS, P. J. 1984. Adsorption of carboxymethylcellulose, guar gum, and starch onto talc, sulphides, oxides, and salt-type minerals. *South African Journal of Chemistry,* 37**,** 85-90.

SUBRAHMANYAM, T. & FORSSBERG, E. 1988. Froth stability, particle entrainment and drainage in flotation—a review. *International Journal of Mineral Processing,* 23**,** 33-53.

SUBRAHMANYAM, T. & FORSSBERG, K. 1993. Mineral solution-interface chemistry in minerals engineering. *Minerals Engineering,* 6**,** 439-454.

SWEET, C., VAN HOOGSTRATEN, J., HARRIS, M. & LASKOWSKI, J. The effect of frothers on bubble size and frothability of aqueous solutions. Processing of Complex Ores–Proc. 2nd UBC-Mc Gill Int. Symp. Metallurgical Society of CIM, Montreal, 1997. 235-245.

TAGUTA, J., O'CONNOR, C. & MCFADZEAN, B. 2017. The effect of the alkyl chain length and ligand type of thiol collectors on the heat of adsorption and floatability of sulphide minerals. *Minerals Engineering,* 110**,** 145-152.

TAO, D., LUTTRELL, G. & YOON, R.-H. 2000. A parametric study of froth stability and its effect on column flotation of fine particles. *International Journal of Mineral Processing,* 59**,** 25-43.

TOLLEY, W., KOTLYAR, D. & VAN WAGONER, R. 1996. Fundamental electrochemical studies of sulfide mineral flotation. *Minerals Engineering,* 9**,** 603-637.

TRAHAR, W. 1984a. The influence of pulp potential in sulphide flotation. *Principles of mineral flotation*.

TRAHAR, W. 1984b. The influence of pulp potential in sulphide flotation. *Principles of mineral flotation,* 40**,** 117-135.

TRAHAR, W., SENIOR, G. & SHANNON, L. 1994. Interactions between sulphide minerals—the collectorless flotation of pyrite. *International Journal of Mineral Processing,* 40**,** 287-321.

TU, Z., WAN, J., GUO, C., FAN, C., ZHANG, T., LU, G., REINFELDER, J. R. & DANG, Z. 2017. Electrochemical oxidation of pyrite in pH 2 electrolyte. *Electrochimica acta,* 239**,** 25-35.

VENTURA-MEDINA, E. & CILLIERS, J. 2002. A model to describe flotation performance based on physics of foams and froth image analysis. *International Journal of Mineral Processing,* 67**,** 79-99.

VIANNA, S. M. S. 2004. *The effect of particle size collector coverage and liberation on the floatability of galena particles in an ore.* The University of Queensland, Australia.

WANG, J., SOMASUNDARAN, P. & NAGARAJ, D. 2005. Adsorption mechanism of guar gum at solid–liquid interfaces. *Minerals Engineering,* 18**,** 77-81.

WANG, L., PENG, Y. & RUNGE, K. 2016. Entrainment in froth flotation: The degree of entrainment and its contributing factors. *Powder Technology,* 288**,** 202-211.

WANG, L., PENG, Y., RUNGE, K. & BRADSHAW, D. 2015. A review of entrainment: Mechanisms, contributing factors and modelling in flotation. *Minerals Engineering,* 70**,** 77-91.

WANG, X.-H. 1995. Interfacial Electrochemistry of Pyrite Oxidation and Flotation: II. FTIR Studies of Xanthate Adsorption on Pyrite Surfaces in Neutral pH Solutions. *Journal of Colloid and Interface Science,* 171**,** 413-428.

WANG, X.-H. & FORSSBERG, K. E. 1991. Mechanisms of pyrite flotation with xanthates. *International journal of mineral processing,* 33**,** 275-290.

WANG, X. & FORSSBERG, E. 1990. EDTA-induced flotation of sulfide minerals. *Journal of colloid and interface science,* 140**,** 217-226.

WHELAN, P. & BROWN, D. 1956. Particle-bubble attachment in froth flotation. *Transactions of the Institute of Mining and Metallurgy,* 65**,** 181-192.
WIESE, J. & HARRIS, P. 2012. The effect of frother type and dosage on flotation performance in the presence of high depressant concentrations. *Minerals Engineering,* 36**,** 204-210.
WIESE, J., HARRIS, P. & BRADSHAW, D. 2005. The influence of the reagent suite on the flotation of ores from the Merensky reef. *Minerals Engineering,* 18**,** 189-198.
WIESE, J., HARRIS, P. & BRADSHAW, D. 2007. The response of sulphide and gangue minerals in selected Merensky ores to increased depressant dosages. *Minerals Engineering,* 20**,** 986-995.
WIESE, J., HARRIS, P. & BRADSHAW, D. 2008. The use of very low molecular weight polysaccharides as depressants in PGM flotation. *Minerals Engineering,* 21**,** 471-482.
WIESE, J., HARRIS, P. & BRADSHAW, D. 2011. The effect of the reagent suite on froth stability in laboratory scale batch flotation tests. *Minerals Engineering,* 24**,** 995-1003.
WIESE, J. G. 2009. *Investigating depressant behaviour in the flotation of selected Merensky ores.* University of Cape Town, South Africa.
WILLS, B. A. & FINCH, J. 2015. *Wills' mineral processing technology: an introduction to the practical aspects of ore treatment and mineral recovery*, Butterworth-Heinemann.
WILLS, B. A. & NAPIER-MUNN, T. 2005. 12 - Froth flotation. *In:* WILLS, B. A. & NAPIER-MUNN, T. (eds.) *Wills' Mineral Processing Technology (Seventh Edition).* Oxford: Butterworth-Heinemann.
WILLS, B. A. & NAPIER-MUNN, T. J. 2006. *Wills' mineral processing technology: an introduction to the practical aspects of ore treatment and mineral recovery*, Elsevier Ltd.
WITNEY, J. & YAN, D. 1997. Reduction of magnesia in nickel concentrates by modification of the froth zone in column flotation. *Minerals engineering,* 10**,** 139-154.
WOODBURN, E. & LOVEDAY, B. 1965. The effect of variable residence time on the performance of a flotation system. *Journal of the Southern African Institute of Mining and Metallurgy,* 65**,** 612-628.
XU, Z. 2000. FLOTATION | Historical Development. *In:* WILSON, I. D. (ed.) *Encyclopedia of Separation Science.* Oxford: Academic Press.
YANG, X.-S. & ALDRICH, C. 2006. Effects of impeller speed and aeration rate on flotation performance of sulphide ore. *Transactions of Nonferrous Metals Society of China,* 16**,** 185-190.
YANG, X., ALBIJANIC, B., LIU, G. & ZHOU, Y. 2018. Structure–activity relationship of xanthates with different hydrophobic groups in the flotation of pyrite. *Minerals Engineering,* 125**,** 155-164.
YIANATOS, J., BERGH, L., VINNETT, L., CONTRERAS, F. & DÍAZ, F. 2010. Flotation rate distribution in the collection zone of industrial cells. *Minerals Engineering,* 23**,** 1030-1035.
YIANATOS, J., FINCH, J. & LAPLANTE, A. 1988. Selectivity in column flotation froths. *International Journal of Mineral Processing,* 23**,** 279-292.
ZÁRATE-GUTIÉRREZ, R., LAPIDUS, G. & MORALES, R. 2012. Aqueous oxidation of galena and pyrite with nitric acid at moderate temperatures. *Hydrometallurgy,* 115**,** 57-63.
ZHANG, Q., XU, Z., BOZKURT, V. & FINCH, J. A. 1997. Pyrite flotation in the presence of metal ions and sphalerite. *International Journal of Mineral Processing,* 52**,** 187-201.
ZHENG, X., JOHNSON, N. W. & FRANZIDIS, J. P. 2006. Modelling of entrainment in industrial flotation cells: Water recovery and degree of entrainment. *Minerals Engineering,* 19**,** 1191-1203.

Appendices

Appendix A: Flotation Data

A.1. pyrite system:

i) final solids and water recovery.

The solid/water recovery shows that the solids per unit water reporting to the concentrate were not directly proportional to the feed grade.

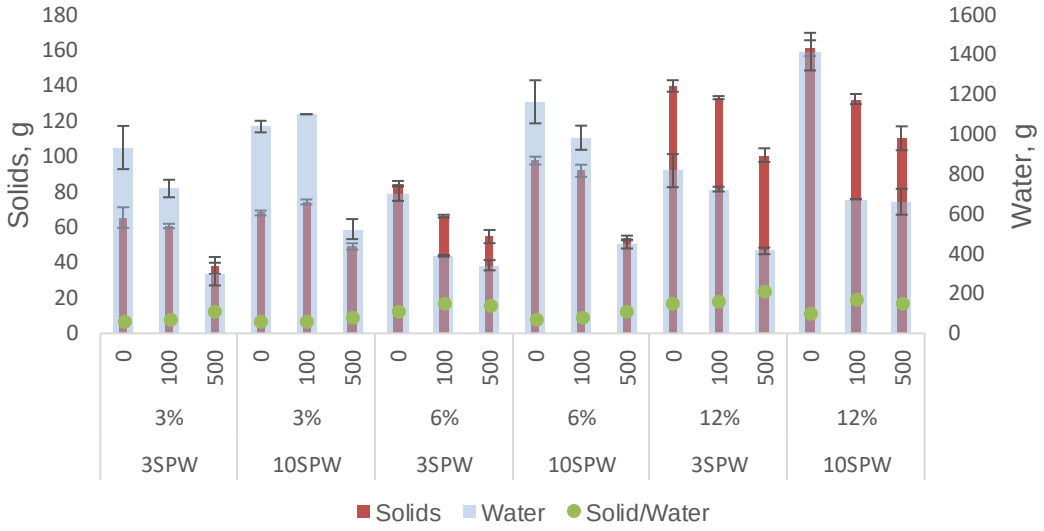

ii) Cumulative Water vs. Time

Figure a, b and c illustrates the cumulative water recovered vs. time for each respective pyrite feed grade under the tested conditions. Water recovered per unit time generally increased with increasing pyrite feed grade, with water recoveries increasing in the order 3% (blue) > 6% (orange) > 12% (grey), i.e., cumulative water recovered per unit time in Figure a > b > c.

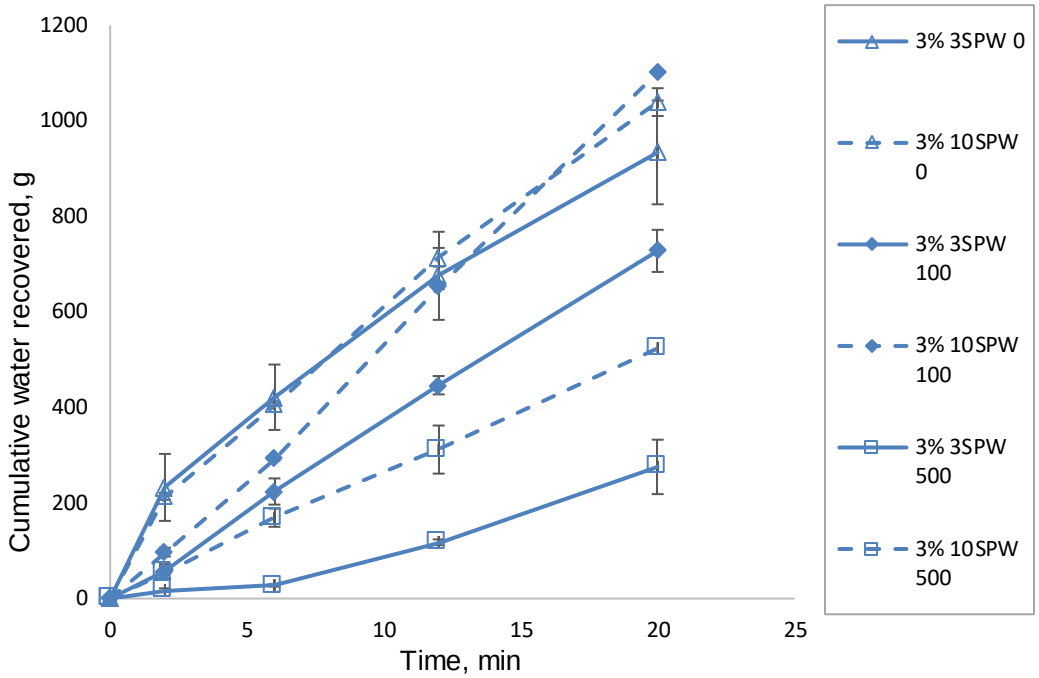

Figure a: Cumulative water recovered Vs. Time for the 3% pyrite feed grade under the tested.

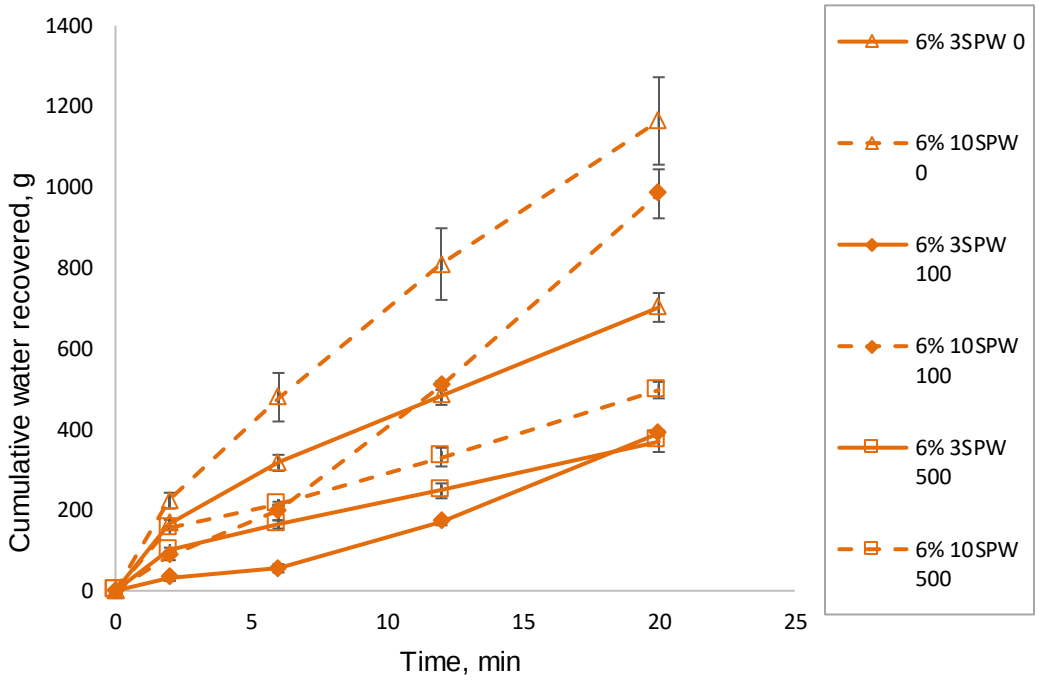

Figure b: Cumulative water recovered Vs. Time for the 6% pyrite feed grade under the tested.

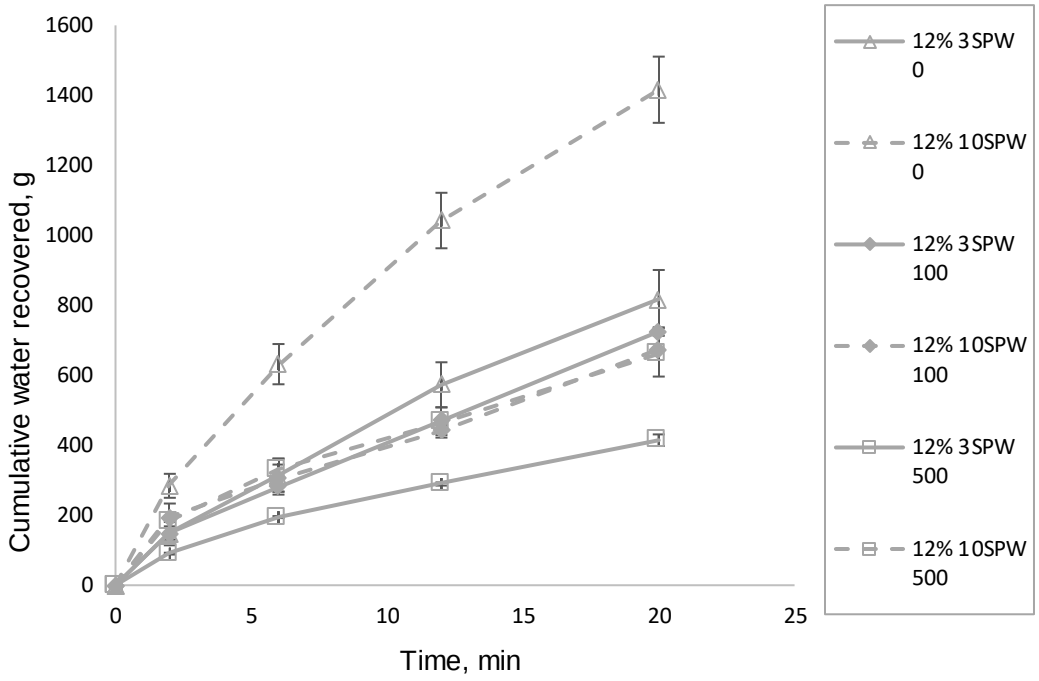

Figure c: Cumulative water recovered Vs. Time for the 12% pyrite feed grade under the tested.

A.2. galena system:

i) final solids and water

The solid/water recovery shows that the solids per unit water reporting to the concentrate were not directly proportional to the feed grade.

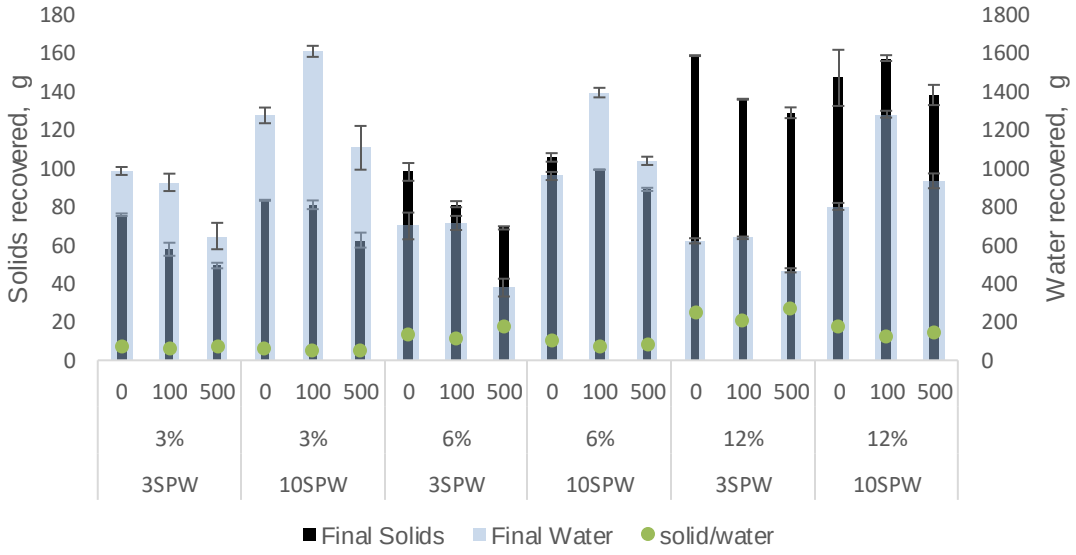

ii) Cumulative Water vs. Time

Figure d, e and f illustrates the cumulative water recovered vs. time for each respective galena feed grade under the tested conditions. Water recovered per unit time generally decreased with increasing galena feed grade, with water recoveries decreasing in the order 3% (blue) > 6% (orange) > 12% (grey), i.e., cumulative water recovered per unit time in Figure d > e > f.

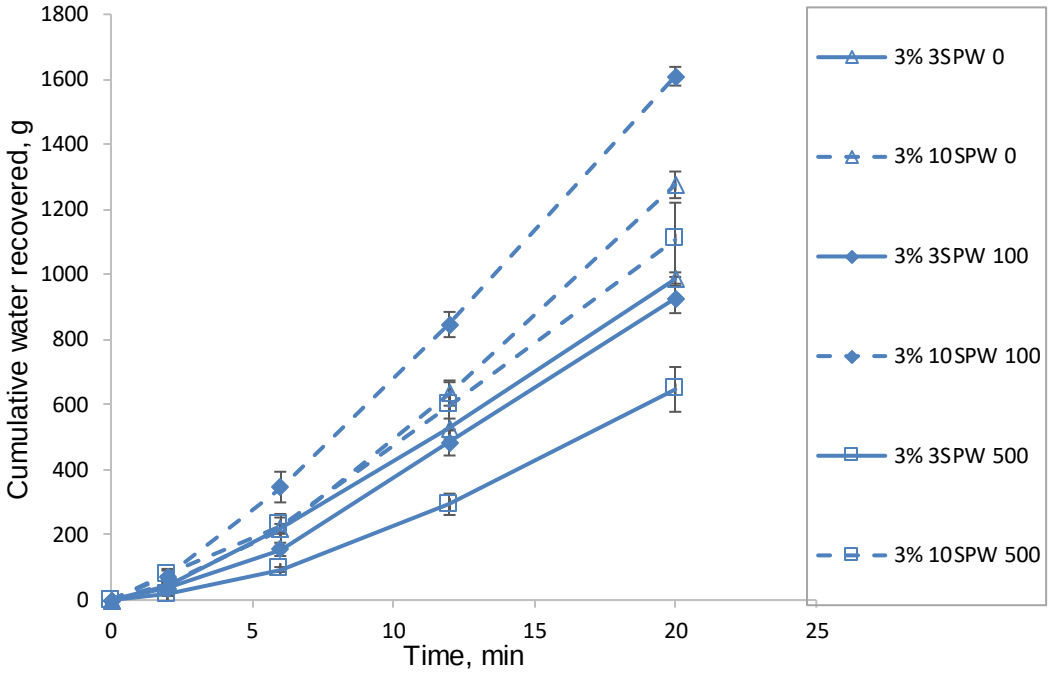

Figure d: Cumulative water recovered Vs. Time for the 3% galena grade under the tested conditions.

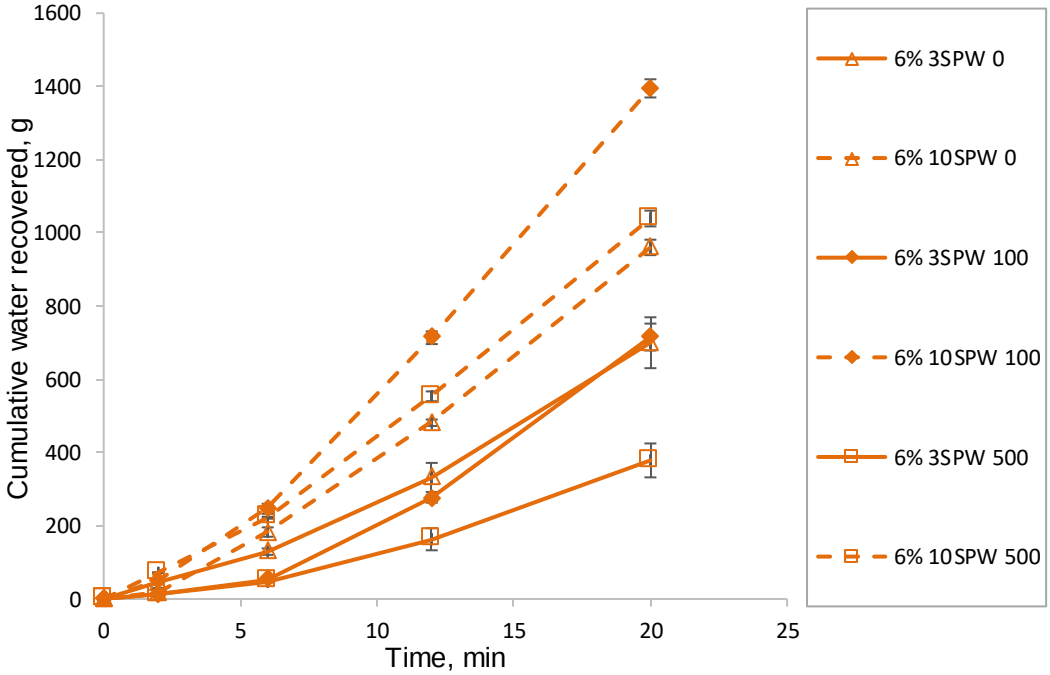

Figure e: Cumulative water recovered Vs. Time for the 6% galena feed under the tested conditions.

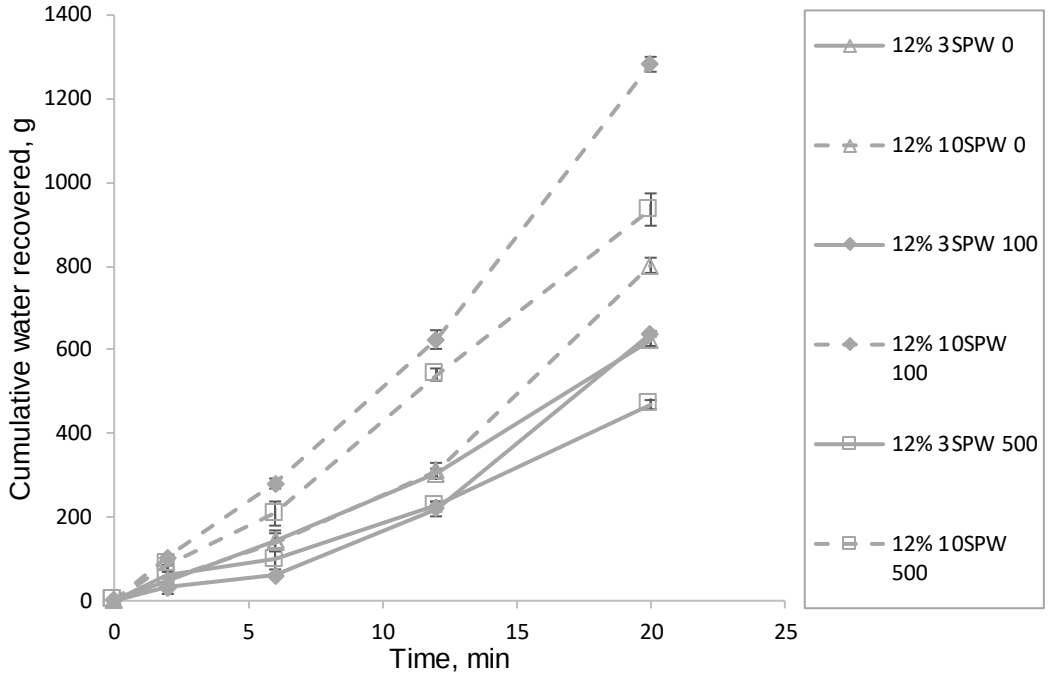

Figure f: Cumulative water recovered Vs. Time for the 12% galena feed under the tested conditions.

Appendix B: Concentrate grades

B.1. pyrite system

i) Cumulative Fe recovery vs. Time

Figures g, h and i illustrates for each respective pyrite feed grade, the decrease in Fe recovery per unit time with increasing depressant dosage. This effect is shown by the markers generally arranged in the order triangle (0 g/t) > diamond (100 g/t) > square (500 g/t).

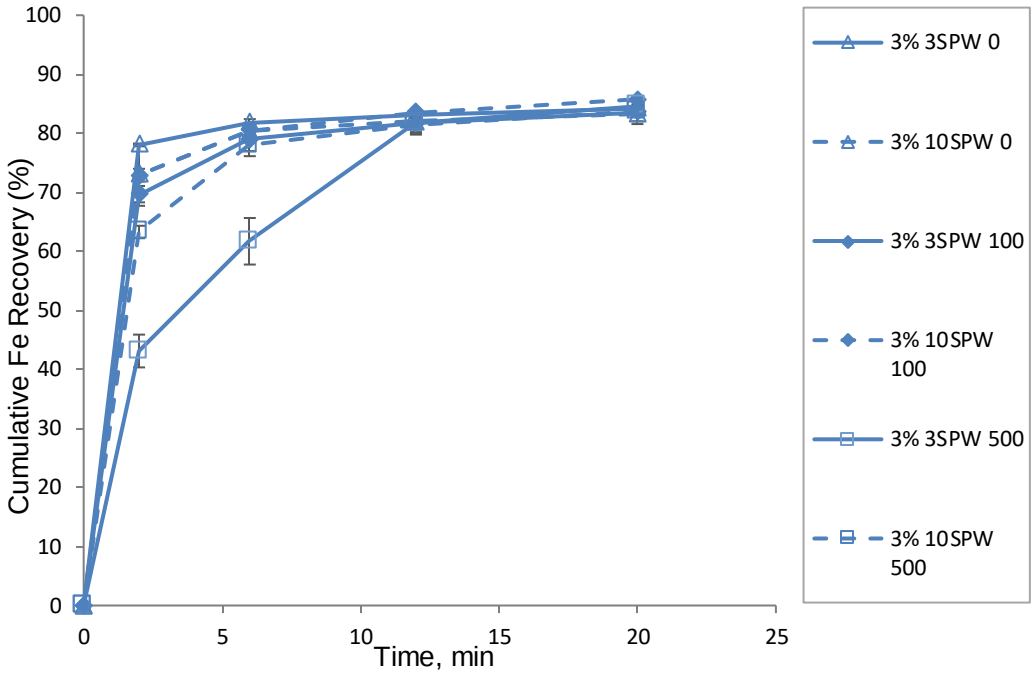

Figure g: Cumulative Fe recovery Vs. cumulative time for the 3% pyrite feed under the tested conditions.

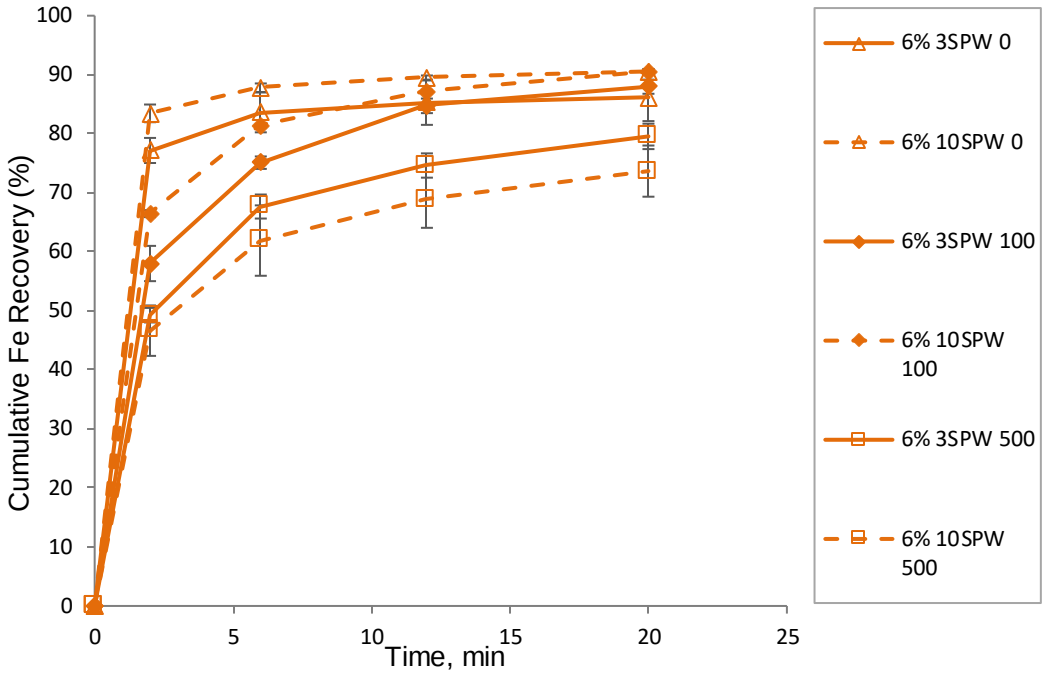

Figure h: Cumulative Fe recovery Vs. cumulative time for the 6% pyrite feed under the tested conditions.

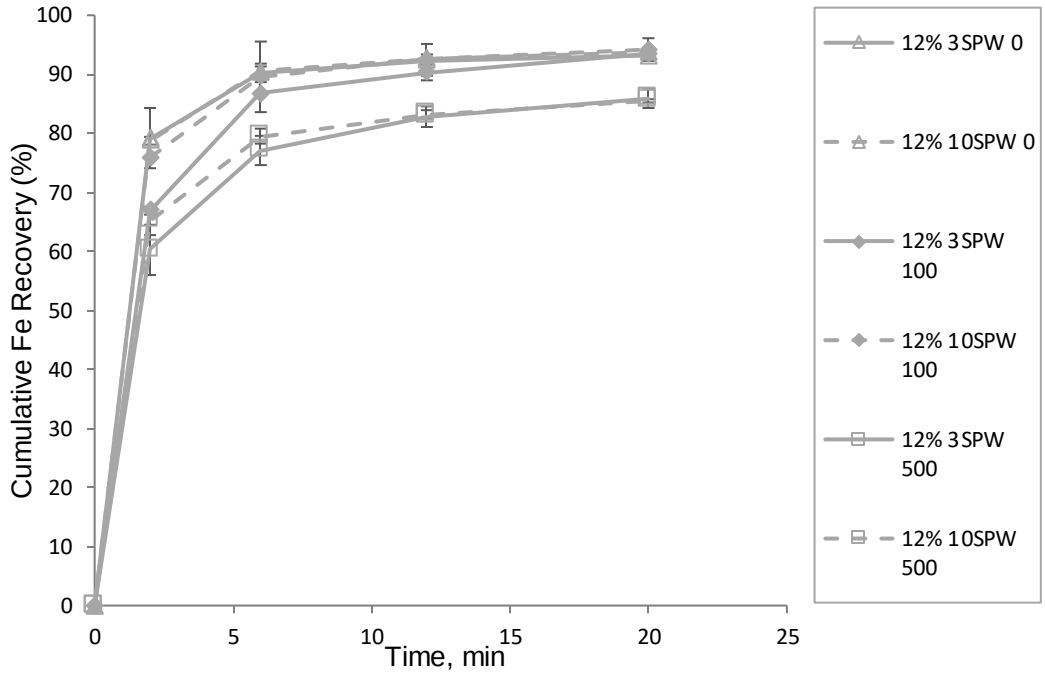

Figure i: Cumulative Fe recovery Vs. cumulative time for the 12% pyrite feed under the tested conditions.

ii) Cumulative Fe recovery vs. Water

Figure j, k and l illustrates the cumulative Fe recovered vs. water for each respective pyrite feed grade under the tested conditions. Cumulative Fe and water increased with an increase in pyrite feed, with Fe recovery and water recovery increasing in the order 3% (blue) < 6% (orange) < 12% (grey).

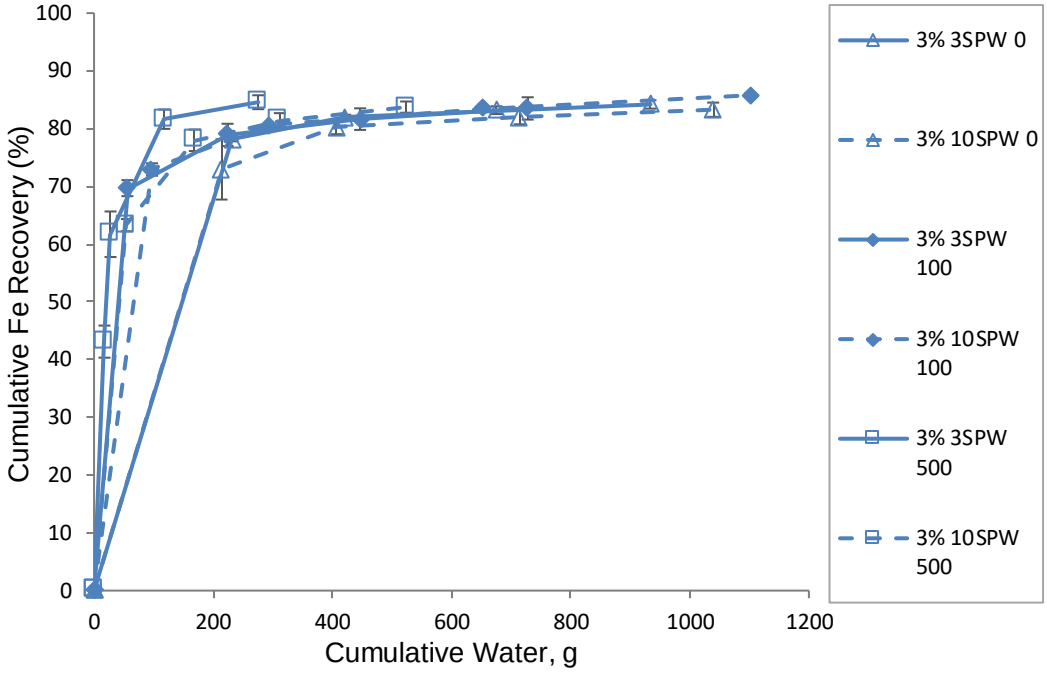

Figure j: Cumulative Fe recovery Vs. cumulative water recovered for the 3% pyrite feed under the tested conditions.

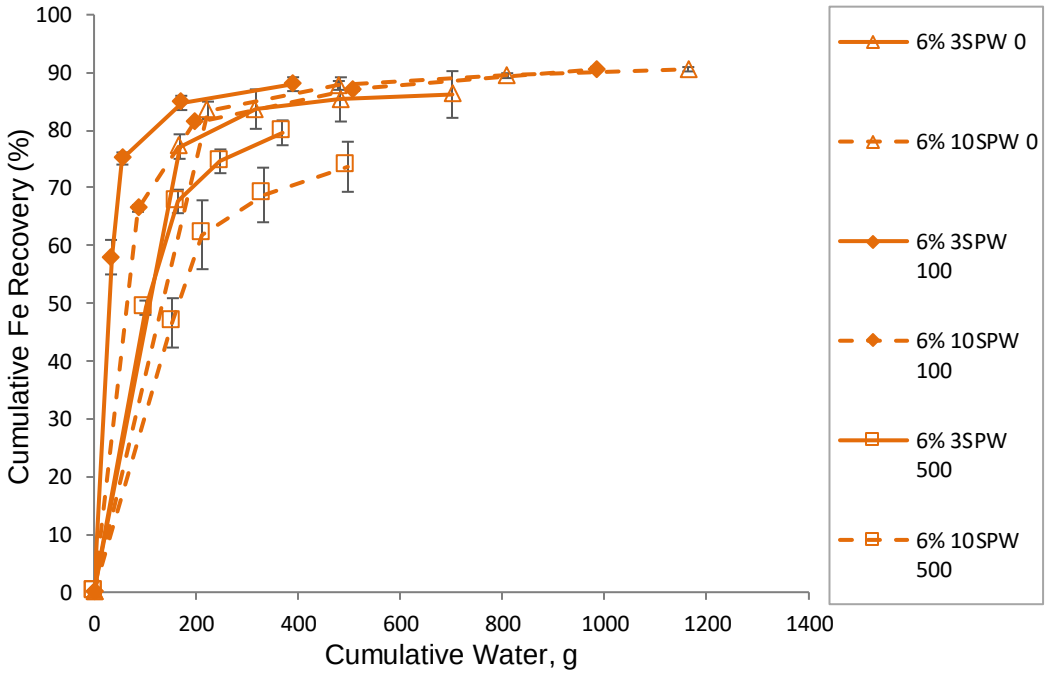

Figure k: Cumulative Fe recovery Vs. cumulative water recovered for the 6% pyrite feed under the tested conditions.

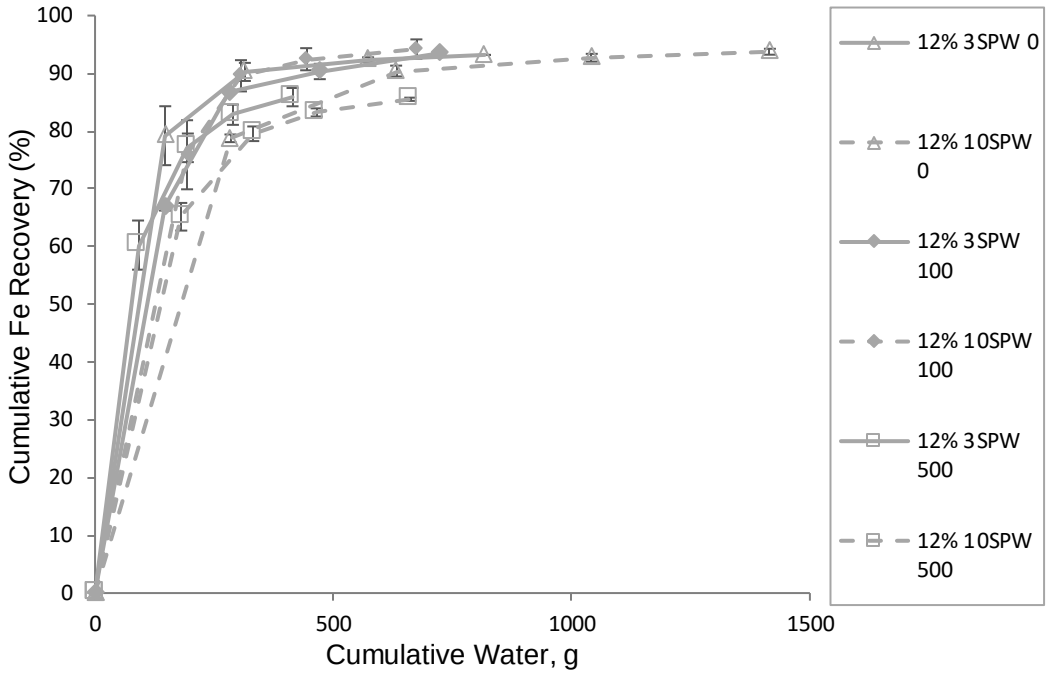

Figure l: Cumulative Fe recovery Vs. cumulative water recovered for the 12% pyrite feed under the tested conditions.

B.2. galena system

i) Cumulative Pb Recovery vs. Time

Figures m, n and o illustrates for each respective galena feed grade, the decrease in Pb recovery per unit time with increasing depressant dosage. This effect is shown by the markers generally arranged in the order triangle (0 g/t) > diamond (100 g/t) > square (500 g/t).

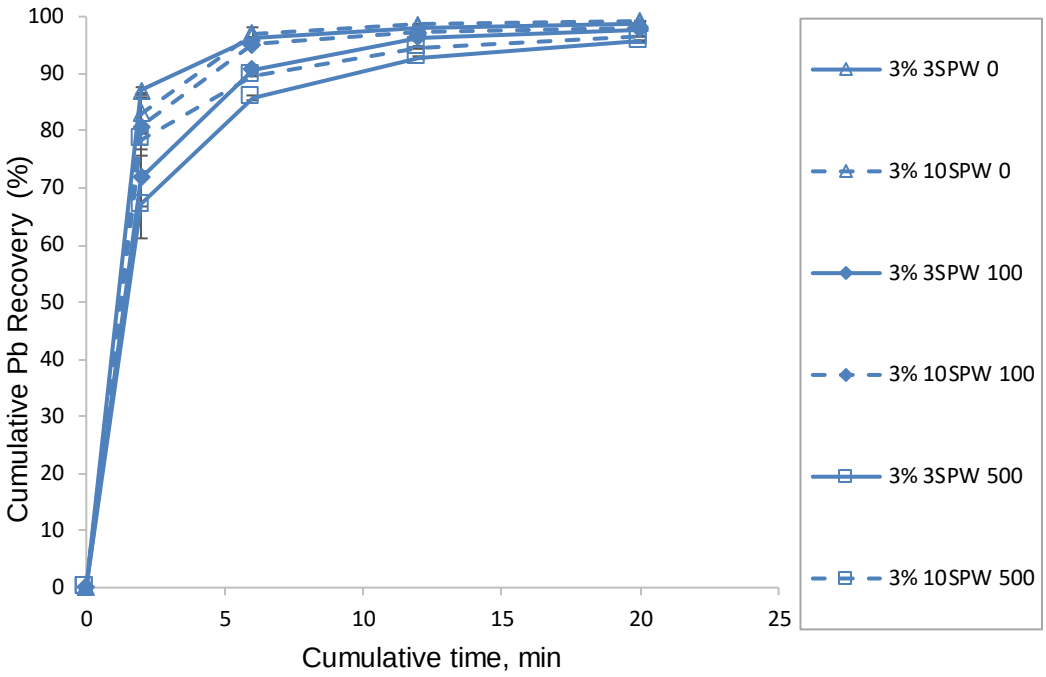

Figure m: Cumulative Pb recovery Vs. cumulative time for the 3% galena feed under the tested conditions.

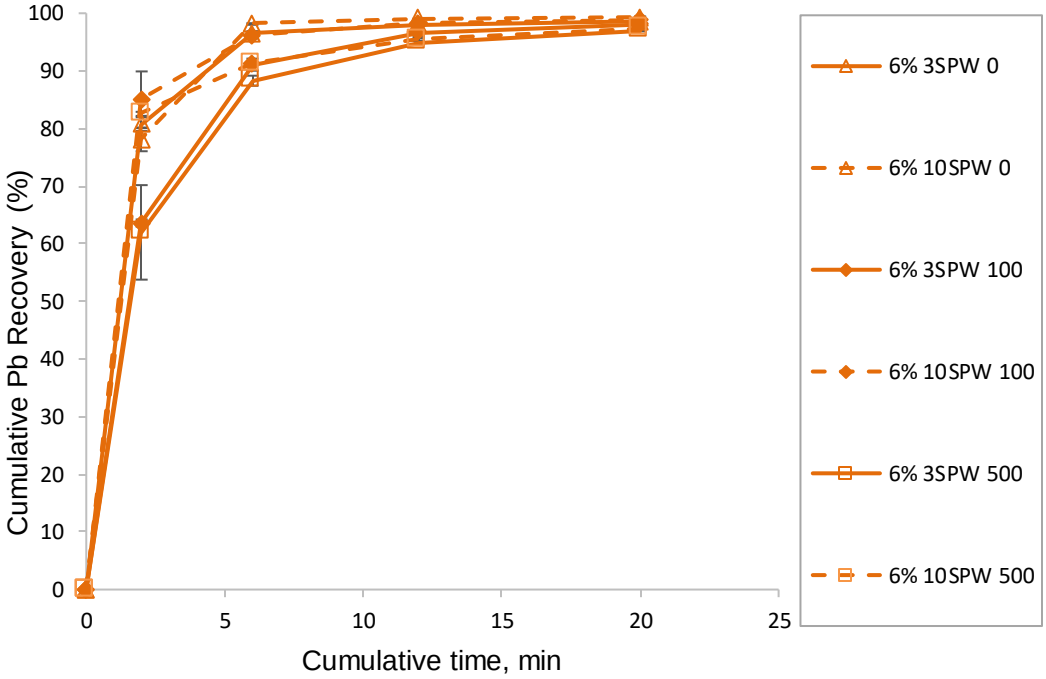

Figure n: Cumulative Pb recovery Vs. cumulative time for the 6% galena feed under the tested conditions.

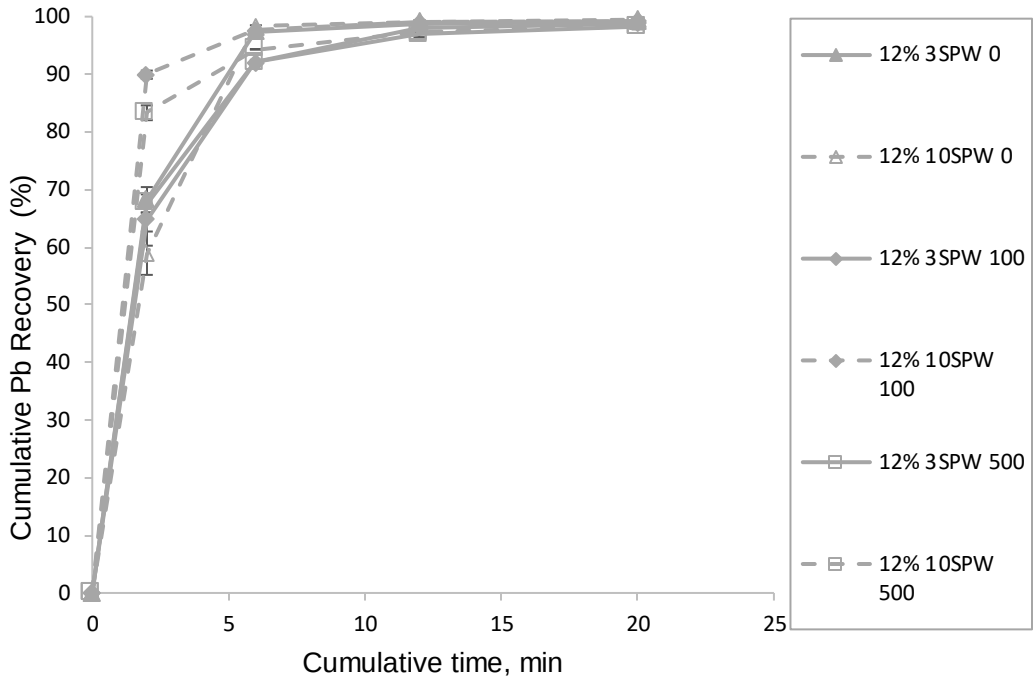

Figure o: Cumulative Pb recovery Vs. cumulative time for the 12% galena feed under the tested conditions.

ii) Cumulative Pb recovery vs. Water

Figures p, q and r illustrates for each respective galena feed grade, the decrease in Pb recovery per unit water with increasing depressant dosage. This effect is shown by the markers generally arranged in the order triangle (0 g/t) > diamond (100 g/t) > square (500 g/t).

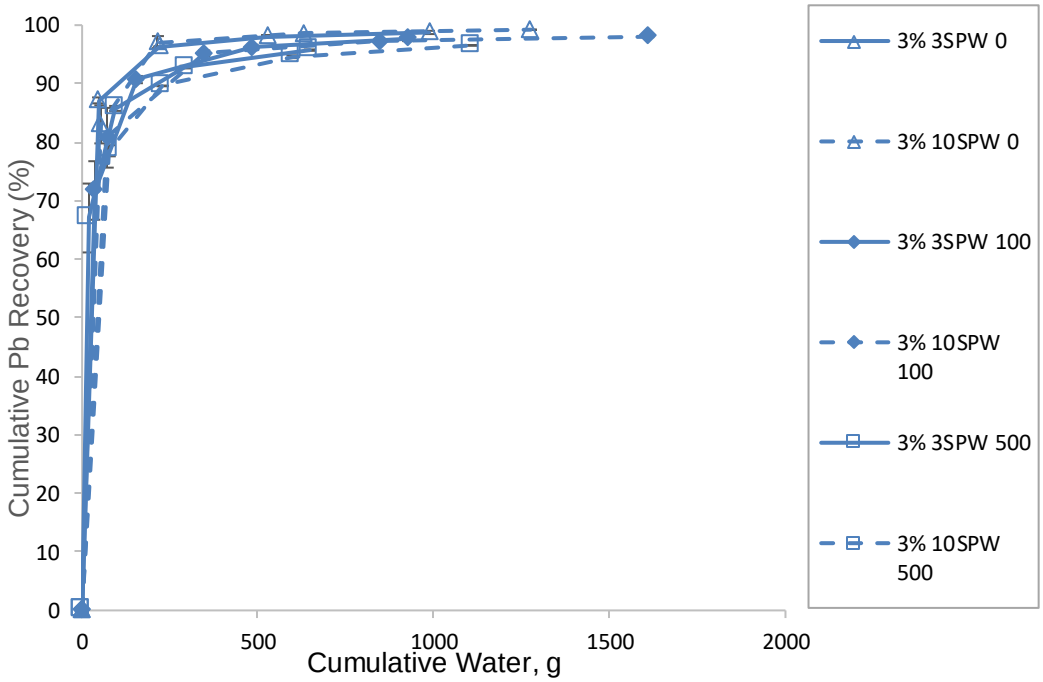

Figure p: Cumulative Pb recovery Vs. cumulative water recovered for the 3% galena feed under the tested conditions.

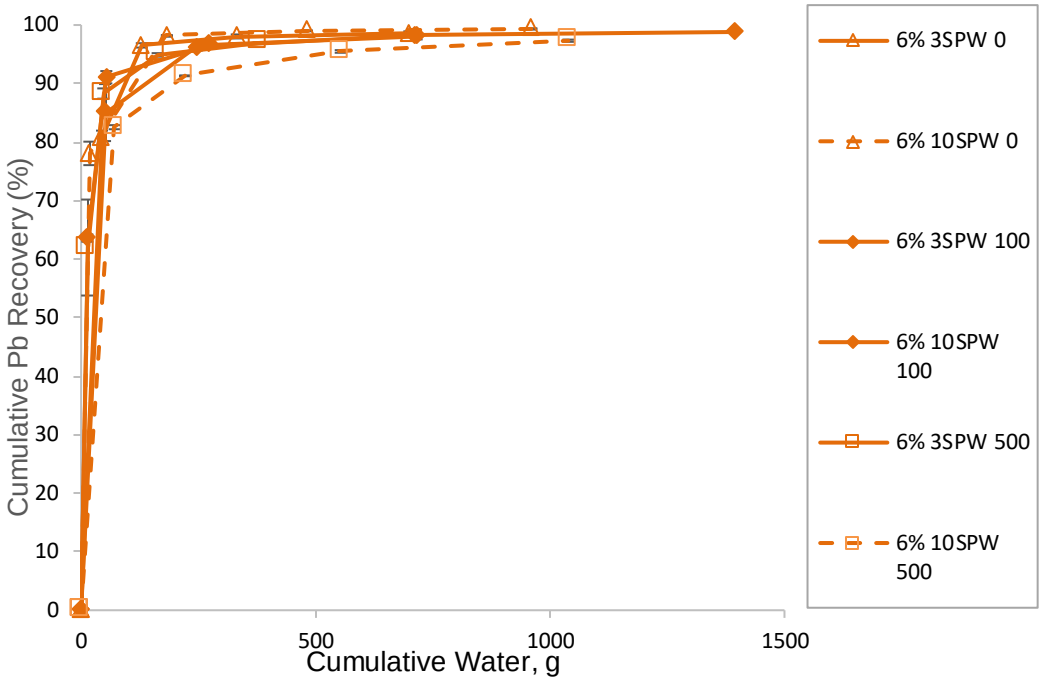

Figure q: Cumulative Pb recovery Vs. cumulative water recovered for the 6% galena feed under the tested conditions.

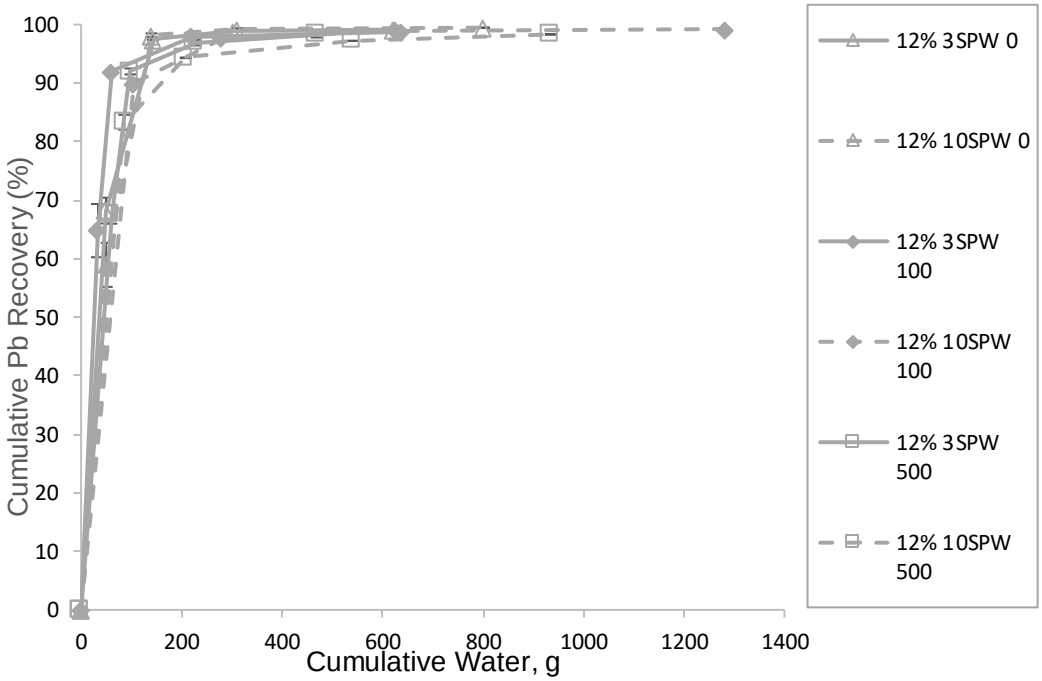

Figure r: Cumulative Pb recovery Vs. cumulative water recovered for the 12% galena feed under the tested conditions.

Appendix C: Total Gangue Recovery

C.1. pyrite system:

The total gangue recovery for the pyrite-based synthetic ore at 0 and 100 g/t CMC depressant dosage, under 3 and 10SPW, respectively.

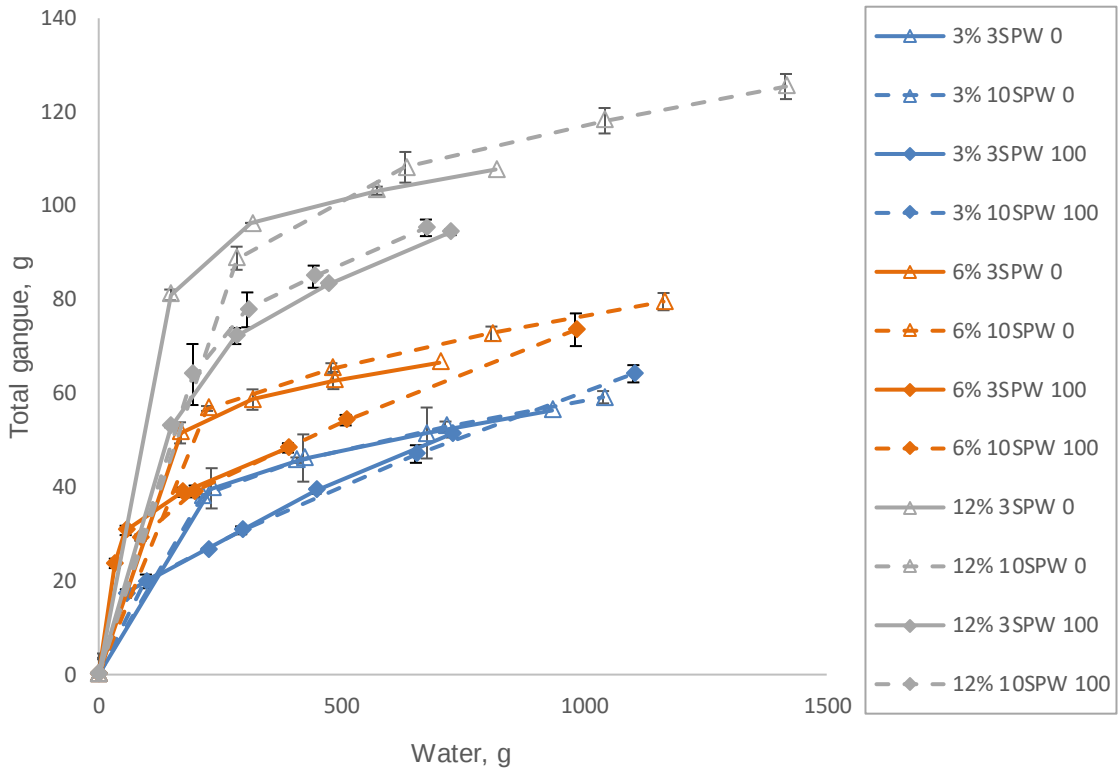

C.2. galena system:

The total gangue recovery for the galena-based synthetic ore at 0 and 100 g/t CMC depressant dosage, under 3 and 10SPW, respectively.

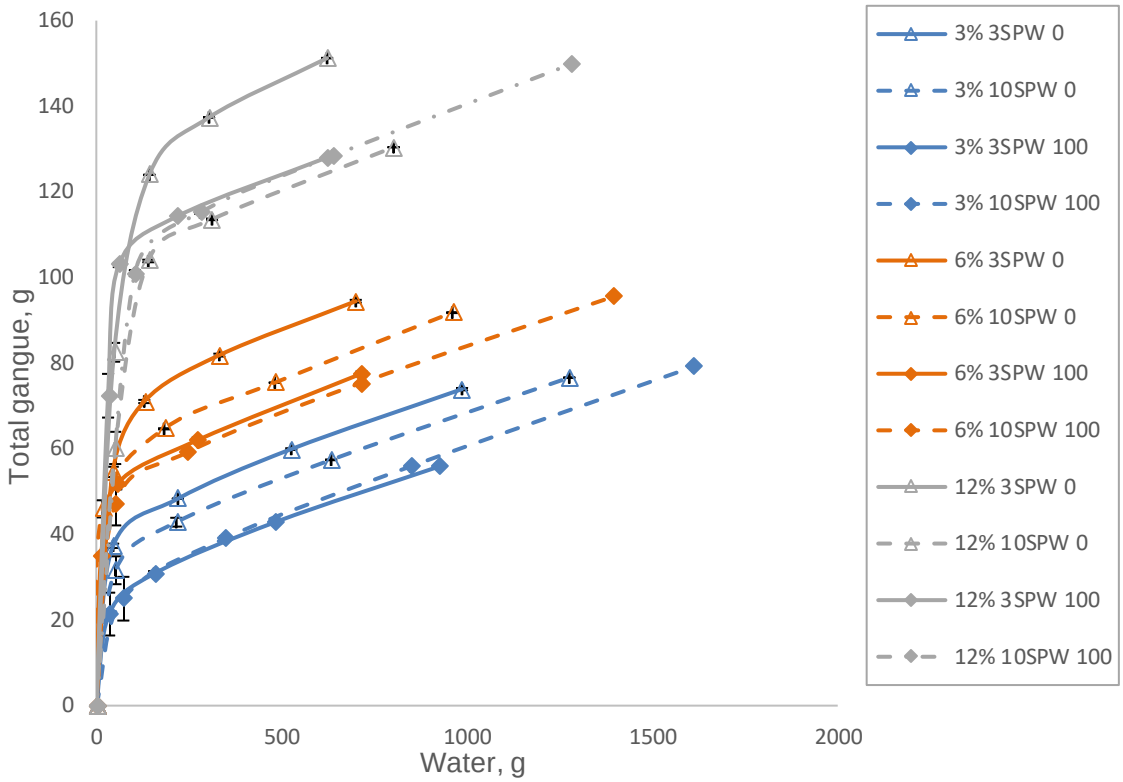
Total gangue, g
Water, g
0
20
40
60
80
100
120
140
160
0
500
1000
1500
2000
3% 3SPW 0
3% 10SPW 0
3% 3SPW 100
3% 10SPW 100
6% 3SPW 0
6% 10SPW 0
6% 3SPW 100
6% 10SPW 100
12% 3SPW 0
12% 10SPW 0
12% 3SPW 100
12% 10SPW 100

Appendix D: Pulp Chemistry Data

D.1. Pyrite system:

PYRITE PULP CHEMISTRY

D.2. Galena system:

GALENA PULP CHEMISTRY

Appendix E: Experimental Data

E.1. Online Files:

All the data regarding this study has been compiled and made available online as outlined:

1. All batch flotation data and calculations, as well as mineral assays for the pyrite system: PYRITE SYSTEM

2. All batch flotation data and calculations, as well as mineral assays for the galena system: GALENA SYSTEM

3. All dynamic foam/froth stability data and calculations for the 2-phase system as well as the 3-phase pyrite system: PYRITE COLUMN

4. All dynamic froth stability data and calculations for the galena system: GALENA COLUMN